DOE Contract DE-AC26-99BC15222

Development of Improved Oil Field Waste Injection Disposal Techniques

Final Report
March 31, 2002

Prepared by:

Terralog Technologies USA, Inc.
332 E. Foothill Blvd, Arcadia, CA 91006
(626) 305-8460
www.terralog.com

Disclaimer

This report was prepared as an account of work sponsored by an agency of the United States Government. Neither the United States Government nor any agency thereof, nor any of their employees, makes any warranty, express or implied, or assumes any legal liability or responsibility for the accuracy, completeness, or usefulness of any information, apparatus, product, or process disclosed, or represents that its use would not infringe privately owned rights. Reference herein to any specific commercial product, process, or service by trade name, trademark, manufacturer, or otherwise does not necessarily constitute or imply its endorsement, recommendation, or favoring by the United States Government or any agency thereof. The views and opinions of authors expressed herein do not necessarily state or reflect those of the United States Government or any agency thereof.

ABSTRACT

This Final Report summarizes Terralog's efforts and results for the project "Development of Improved Fracture Injection Disposal Techniques for Oilfield Waste", completed under DOE Contract DE-AC26-99BC15222. The goals of this project have been to: 1) assemble and analyze a comprehensive database of past waste injection operations; 2) develop improved diagnostic techniques for monitoring fracture growth and formation changes; 3) develop operating guidelines to optimize daily operations and ultimate storage capacity of the target formation; and 4) to apply these improved models and guidelines in the field.

Terralog Technologies first assembled a Slurry Fracture Injection (SFI) database template, and populated it with the monitoring data collected from eight oil field waste injection projects, comprising a total of more than 700 injection episodes. Pressure and rate data was analyzed using fracture models and well test analysis to determine the characteristics of fractures, the permeability of the surrounding formation, and the changing in-situ stress conditions. The database is created in Microsoft ACCESS format. Terralog also created two plotting programs within Access in order to graphically view the data for visual interpretation. The power of the SFI database is that different variables can be plotted easily using the Microsoft Access program. Data from different projects can be compared directly. Cross plots of various injection parameters and observations can be made, with filtering on a third variable. The database and query tools were applied to investigate a number of correlations between operating parameters and formation response, providing insight and useful information for optimizing future injection operations.

Terralog next investigated the use of two dimensional analytical models (Perkins-Kern-Nordgren) and pseudo three-dimensional models (FRACPRO) to simulate slurry fracture injection. These were modified to allow variations in shear modulus, leakoff coefficients, and closure stress with repeated injection episodes in order to capture observed formation behavior. Varying these parameters provides improvement over typical constant value assumptions. Terralog also investigated the use of coupled fluid flow and particle flow models to simulate fracture and dilation processes during waste injection. These studies lead us to conclude that when formations are weakly cemented with limited shear strength, there is a transition from brittle, discrete fracture extension, to more widescale dilation and inelastic parting. We successfully developed a coupling process between a continuum flow model and a discrete particle model, allowing simulation of slurry particle injection and resulting fracture and dilation. The method shows good potential for better simulating waste injection, and warrants additional investigation and development effort.

Using insights and observations from the database analysis and modeling efforts, Terralog next developed design and operating guidelines for fracture injection projects. Some of these recommendations were incorporated into new fracture injection regulations established by the Louisiana Department of Natural Resources, and approved by the US EPA. Some recommendations have also been informally accepted as "best-practices" in the State of California by the California Division of Oil and Gas. Terralog applied these guidelines to design and submit permit applications for three new injection projects in California.

Finally, Terralog applied some of the modeling techniques developed through this project to a Slurry Fracture Injection project in Long Beach, California. In February, 2002, Terralog collaborated with THUMS Long Beach Company to review and analyze waste injection into a new interval of the Lower Terminal formation in the Wilmington Oilfield. We evaluated operations over a two-week period from February 18 to February 29, 2002, during which about 6000 bbls of waste slurry was injected, and successfully model injection behavior by taking into account changing formation properties.

TABLE OF CONTENTS

ABSTRACT ..... **III**

EXECUTIVE SUMMARY **1**

DATABASE ASSEMBLY 1
EMPIRICAL CORRELATIONS 1
IMPROVED FRACTURE MODELING TECHNIQUES 2
OPERATING GUIDELINES 3
FIELD APPLICATIONS 4

INTRODUCTION **5**

DATABASE ASSEMBLY **6**

DATABASE SUMMARY 6
PROJECT INFORMATION TABLE 6
PRESSURE AND RATE TABLE 7
DAILY SUMMARY TABLE 8
General Project Information *10*
Independent Measurements *12*
Dependent Values *12*
Interpreted Values: Determining ISIP and Closure *13*
PRESSURE INJECTION AND PRESSURE FALL-OFF ANALYSIS 16
Pressure Falloff Analysis *16*
Log-Log Plot *16*
Horner Plot *18*
Pressure Injection Analysis *19*
PKNLL Fracture Growth Rate *19*
PKNLL Shear Modulus *21*
DATABASE QUERY TOOLS 21
BHP Plotter *21*
SFI Daily Plotter *22*
Access Query Tools *24*

EMPIRICAL CORRELATIONS **26**

DATA CORRELATIONS 26
EFFECT OF CUMULATIVE WASTES ON CLOSURE GRADIENT 26
IMPACT OF SLURRY COMPONENT PERCENTAGES ON CLOSURE GRADIENT 28
EFFECT OF CUMULATIVE SLURRY VOLUME ON INJECTIVITY 30
EFFECT OF SLURRY COMPONENTS PERCENTAGES ON INJECTIVITY 31
EFFECT OF VISCOSITY ON INJECTIVITY AND PERMEABILITY 34
EFFECT OF SFI OPERATIONS ON FORMATION PERMEABILITY 36
RELATIONSHIP BETWEEN PERMEABILITY AND WASTE MATERIAL PERCENTAGE 37
RELATIONSHIP BETWEEN INJECTIVITY AND NEAR WELLBORE PERMEABILITY 38
EFFECT OF INJECTIVITY, VISCOSITY, AND CUM. MATERIAL ON GROWTH RATE 39
EFFECT OF CUM. MATERIAL, GROWTH RATE, AND CLOSURE ON SHEAR MODULUS 41
SUMMARY OF CORRELATIONS 43

FIELD OBSERVATIONS **45**

FRACTURE MODELING CONSIDERATIONS **48**

STATE OF THE ART OF FRACTURE MODELS AND THEIR LIMITATIONS 48
Intrinsic Fracture Resistance *48*
Shearing Resistance, Dilation *49*

Pore Pressure and Bleed-Off ... *51*
Natural Stress and Properties Differences ... *51*
Pressure, Stress Gradients and Fracture Rise ... *51*
Changes in Fracture Direction ... *52*
STATUS AND FUTURE OF FRACTURE SIMULATIONS ... 52

MODELING AND DIAGNOSTIC INVESTIGATIONS ... 54

TWO DIMENSIONAL ANALYTICAL MODELS WITH HISTORY MATCHING ... 56
The Perkins-Kern-Nordgren (PKN) Model ... *56*
Regression Analysis ... *58*
PKN-Large Leakoff Analysis: Case Study ... *59*
PKN-Zero Leakoff Analysis: Case Study ... *64*
Analytic Modeling Discussion ... *65*
PSEUDO-3D NUMERICAL MODELS WITH HISTORY MATCHING ... 66
Introduction ... *66*
Case Study ... *67*
FRACPRO Modeling Discussion ... *68*
DISCRETE ELEMENT MODELING ... 71
Background ... *71*
Cementation Influence on Brittle Fracture and Dilation ... *71*
Coupled Fluid Flow and Particle Flow Simulation ... *75*
Simulation Results and Discussion ... *78*

MODEL INVESTIGATION SUMMARY ... 81

GUIDELINES FOR SLURRY FRACTURE INJECTION ... 82

GEOLOGIC & WELL LOCATION GUIDELINES ... 82
Target Formation ... *82*
Containment Zone ... *82*
Confining Zone ... *83*
Well Site Considerations ... *83*
WELL COMPLETION GUIDELINES ... 86
Well Cementing ... *86*
Well Completion ... *87*
OPERATING GUIDELINES ... 87
MONITORING AND ANALYSIS GUIDELINES ... 88
Well Logging ... *88*
Injection Parameters ... *89*
Bottomhole Pressure ... *89*
Formation Tests ... *89*
Observation Wells ... *91*
Tiltmeter Systems ... *91*
Microseismic Systems ... *92*
GUIDELINES SUMMARY ... 92

FIELD APPLICATIONS: PROJECT DESIGN AND PERMITTING ... 93

GUADALUPE FIELD SLURRY FRACTURE INJECTION ... 93
SOUTH ELLWOOD FIELD SLURRY FRACTURE INJECTION ... 97
ALISO CANYON FIELD SLURRY FRACTURE INJECTION ... 101

THUMS LONG BEACH SFI OPERATIONS AND ANALYSIS ... 104

FIELD OVERVIEW ... 104
Local Geology and Reservoir Characterization ... *105*
Local Stress Analysis ... *107*
SLURRY FRACTURE INJECTION HISTORY ... 108
DOE RESEARCH PROJECT DESCRIPTION ... 110

C-822I Well Completion *110*
AA Sand SFI Operations *112*
Determining fracture closure stress *114*
Fracture growth behavior *114*
Injection Analysis Summary *122*

CONCLUSIONS **123**

REFERENCES **124**

LIST OF FIGURES

Figure 1: Determining ISIP and Closure Pressure from pressure derivative plot 14
Figure 2: Determining ISIP from well test analysis 15
Figure 3: Determining Closure from well test analysis 15
Figure 4: Example of a log-log plot, showing 3 different flow regimes 17
Figure 5: Horner plot corresponding to Figure 4 log-log plot 18
Figure 6: Geometry of PKN Fracture 20
Figure 7: Interface of BHP Plotter 22
Figure 8: User interface of the SFI Daily Plotter. 23
Figure 9: Example of correlation plot 24
Figure 10: Example of Access Query 25
Figure 11: Table resulting from query in Figure 10 25
Figure 12: Closure Gradient vs. Cumulative Materials 26
Figure 13: Closure Gradient vs. Cumulative Sand 27
Figure 14: Closure Gradient vs. Cumulative Mud 27
Figure 15: Closure Gradient vs. Percent Materials 28
Figure 16: Closure Gradient vs. Percent Materials for Project TTI6 29
Figure 17: Closure Gradient vs. Percent Material for Project TTI7 29
Figure 18: Closure Gradient vs. Percent Mud 30
Figure 19: Injectivity vs. Cumulative Material Volume 31
Figure 20: Injectivity vs. Percent Materials 32
Figure 21: Injectivity vs. Percent Mud in Slurry 32
Figure 22: Injectivity vs. Percent Sand in Slurry 33
Figure 23: Injectivity vs. Percent Slop in Slurry 34
Figure 24: Slurry Viscosity vs. Percent Materials 35
Figure 25: Injectivity vs. Slurry Viscosity 35
Figure 26: Near-Well Permeability vs. Slurry Viscosity 36
Figure 27: Near-Well Permeability vs. Time for TTI6 37
Figure 28: Near Wellbore Permeability vs. Percent Waste Materials 38
Figure 29: Near Wellbore Permeability vs. Injectivity 38
Figure 30: PKN Growth Rate vs. Injectivity 39
Figure 31: PKN Growth Rate vs. Slurry Viscosity 40
Figure 32: PKN Growth Rate vs. Cumulative Materials Injected 40
Figure 33: PKN Shear Modulus vs. Cumulative Materials Injected 41
Figure 34: PKN Shear Modulus vs. Percent Sand in Slurry 42
Figure 35: Closure Gradient vs. PKN Shear Modulus 42
Figure 36: Varying net injection and shut-in pressures for sequential injection episodes. 45
Figure 37: Fracture re-orientation during sequential injection episodes at project TTI 4 46
Figure 38: Closure Stress and Azimuth vs. Time for Project TTI 4 47
Figure 39: Injection scheme can be modified to maintain injectivity and improve pressure decline after shut-in 47
Figure 40: Mode II fracturing in SWR (soft weak rocks) and UCSS (unconsol. sandstones) 49
Figure 41: The poroelastic effect 50
Figure 42: Fracture re-orientation due to stressing of waste pod 54
Figure 43: Fracture re-orientation vs. cumulative injected volume 56
Figure 44: PKN Fracture Geometry 57
Figure 45: Log-log plot of measured net normalized pressures and best-fit PKN model line 58
Figure 46: Injection and shut-in pressure data for October 18 to 22, 1999 (TTI 11) 59
Figure 47: Injection and shut-in pressure data for October 25 to 29, 1999 (TTI 11) 60

Figure 48: Closure pressures determined by best-fit methods to analyzed injection periods 62
Figure 49: Stiffness/leakoff ratios ($G/C^{1/3}$) determined for best-fit daily closures..... 62
Figure 50: Stiffness/leakoff ratio ($G/C^{1/3}$) determined for three fixed closure values..... 64
Figure 51: Fit of PKN-Large Leakoff and PKN-Zero Leakoff models to October 20, 1999..... 65
Figure 52: Net pressure match for injection 4-6 using scenario 2. 69
Figure 53: Net pressure match for injection 4-6 using scenario 2. 69
Figure 54. FRACPRO variables required to match pressure behavior for scenarios 1 and 2. 70
Figure 55: Transition from discrete brittle fracture to process zone dilation by decreasing bond strength. 72
Figure 56: Dilation behavior is caused by decrease in shear bond strength alone. 73
Figure 57: Decrease in normal bond strength does not lead to dilation. 74
Figure 58: Schematic representation of the iterative coupling process 75
Figure 59: Windows interface developed to couple fluid flow and particle models 75
Figure 60: Initial particle assembly and fluid flow mesh to simulate slurry injection 76
Figure 61: Pore pressure distribution in model after a few iterations 77
Figure 62: Discrete particle model showing fracture initiation and slurry particle injection..... 78
Figure 63: Closeup view of fracture initiation and slurry injection in porous media..... 79
Figure 64. Typical pressure behavior for repeated injection cycles with particle flow model..... 80
Figure 65: Suggested well construction guidelines 84
Figure 66: Fracture height growth into the Containment Zone, Project TTI 11. 85
Figure 67: Techniques used to monitor the SFI process 88
Figure 68: Example of a typical step rate test 90
Figure 69: Example of a step rate test where fracture height growth is occurring..... 91
Figure 70. Type stratigraphy, cross section, and structure map for Guadalupe Field 94
Figure 71. Geologic Map – Top Monterey Formation, Cross Section and Composite Electric Log for South Ellwood Field 98
Figure 72. Type stratigraphic section and type log for South Ellwood Block 3120..... 99
Figure 73. Geologic structure map and cross section of the Aliso Canyon Field 102
Figure 74. Offshore Island in Long Beach Harbor includes production wells and slurry injection operations. 104
Figure 75. Top of Ranger zone structure map 105
Figure 76. Stratigraphic Column of the Long Beach Unit, Wilmington Oil Field..... 106
Figure 77. Drilling rigs on Island Chafee produce cuttings and mud waste requiring disposal. 109
Figure 78. Slurry processing system includes two 50 barrel tanks for shearing and slurrification. 109
Figure 79. 200 barrel holding tank for final mixing prior to injection. 110
Figure 80. C-822I Well Completion Diagram..... 111
Figure 82: Treatment Data for February 18, 19 and 21, 2002. 113
Figure 83: Treatment Data February 23, 25 and 26, 2002. 113
Figure 84: Closure stress measurements using different techniques for each injection. 114
Figure 85: Fracture dimensions at the end of each injection for pressure matching scenario 1. 116
Figure 86. Net Pressure Match for Wilmington Field - C822I - 2/18/2002 117
Figure 87. Net Pressure Match for Wilmington Field - C822I - 2/19/2002 117
Figure 88. Net Pressure Match for Wilmington Field - C822I - 2/21/2002 118
Figure 89. Net Pressure Match for Wilmington Field - C822I - 2/23/2002 118
Figure 90. Net Pressure Match - Injection #5 for Wilmington Field - C822I - 2/25/2002..... 119
Figure 91. Net Pressure Match for Wilmington Field - C822I - 2/26/2002 119
Figure 92: Fracture dimensions at the end of each injection for pressure matching scenario 2. 120
Figure 93: Fracture dimensions at the end of each injection for pressure matching scenario 3. 121

LIST OF TABLES

Table 1: Description of Pressure and Rate Table Parameters 7
Table 2: Sample of Pressure and Rate Data from Project TTI6 7
Table 3: Description of Daily Summary Table Parameters 8
Table 4: A Portion of the Daily Summary Table 10
Table 5: SFI Operational Status Codes 11
Table 6: SFI Monitoring Status Codes 12
Table 7. Summary of Correlations Investigated 43
Table 8: PKN-Large Leakoff analysis summary table (TTI 11) 61
Table 9: Fracture growth scenarios 67
Table 10. Sisquoc Formation Volumetrics at the Guadalupe Field 95
Table 11. Reservoir and fluid properties 107
Table 12. Total Volume Injected and Waste Composition 108
Table 13. C-822I Well and Slurry Specifications 108
Table 14: THUMS SFI Fracture growth scenarios 115

EXECUTIVE SUMMARY

Slurry Fracture Injection (SFI) is a waste disposal technology in which petroleum exploration and production wastes, such as produced sand, drill cuttings, tank bottoms, and pit sludge are mixed with water into a slurry and injected into deep unconsolidated sandstone formations above fracturing pressure. The solids are permanently emplaced within hydraulic fractures generated during the pumping process, and the carrying fluid subsequently drains into the high permeability formation. The mechanics governing the fracturing of unconsolidated sandstone formations remain poorly understood, and as a result there are few guidelines available to optimize the SFI process.

This Final Report summarizes Terralog's efforts and results for the project "Development of Improved Fracture Injection Disposal Techniques for Oilfield Waste", completed under DOE Contract DE-AC26-99BC15222. The goals of this project have been to: 1) assemble and analyze a comprehensive database of past waste injection operations; 2) develop improved diagnostic techniques for monitoring fracture growth and formation changes; 3) develop operating guidelines to optimize daily operations and ultimate storage capacity of the target formation; and 4) to apply these improved models and guidelines in the field.

Database Assembly

Terralog Technologies has assembled an SFI database template, and has populated it with the monitoring data collected from eight oil field waste injection projects, comprising a total of more than 700 injection episodes in Canada and the United States. The measured data consists of slurry and material volumes, wellhead and bottomhole pressures, pumping rates, slurry densities, and other relevant information collected continuously at intervals from 5 seconds to 5 minutes.

The database is created in Microsoft ACCESS format. It includes three tables: a Project Information Table, a Pressure and Rate Table, and a Daily Summary Table. Terralog has also created two plotting programs within Access in order to graphically view the data provided in the Pressure and Rate Table and Daily Summary Table. These can be used to rapidly view data for visual interpretation. The query tools built into Access can also be used to create custom datasets for specialized interpretation. The power of the Terralog database is that different variables can be plotted easily using the Microsoft Access program. Data from different projects can be compared directly. Cross plots of various injection parameters and observations can be made, with filtering on a third variable. For example, injectivity vs. viscosity can be plotted for all days in which sand percentage exceeds a certain value.

Empirical Correlations

This database has been used to evaluate influences of operational changes on injection and formation response in order to optimize operations and to provide insight into large-scale slurry injection in high porosity media. Some of the observed trends are consistent with expectations; however, some are not. For example, closure gradient does increase with accumulation, but is not particularly sensitive to daily changes in slurry composition. Injectivity appears to be more sensitive to sand concentration then to slop concentration. These types of observations are useful to guide future operations.

In addition to providing insight on basic operating strategies, the database is also useful to evaluate existing and new fracture modeling and diagnostic techniques. In the current work, for example, we have

modeled fracture propagation with a traditional Perkins-Kern-Nordgren analytic approach. With this model neither fracture growth nor shear modulus appear to correlate well with cumulative waste injection or slurry concentration. Closure gradient seems to actually decrease with shear modulus. These observations are not consistent with physical expectations, suggesting that linear elastic fracture models cannot adequately explain the behavior of large-scale waste injection in very soft, porous media. Improved model and diagnostic techniques are therefore required.

Improved Fracture Modeling Techniques

Our observations of fracturing and formation behavior during large-volume waste injection operations suggest a new physical model for episodic injection. When a vertical fracture is first induced in a virgin reservoir, its tendency will be to open against the least regional principal stress, σ_3, and extend in length parallel to this direction. During slurry fracture injection, the stream of waste slurry being pumped into the formation causes a fracture to open and material to dilate around the fracture, or within a "process zone". The waste becomes trapped in the formation when pumping stops and the fracture and dilation zone closes. The fluid component of the slurry will bleed off. The solid component of the slurry is left behind.

This large amount of solids packing the fracture and dilation zone alters formation properties and behavior. The stresses within the process zone increase and the permeability within the process zone decreases. Subsequent injection episodes will then cause fractures to break through the waste pod, in a direction still parallel to σ_3, but with increasing difficulty. This is indicated by increased net pressure and less rapid pressure decline after shut-in. The minimum stress within the waste pod increases and, eventually, fracture re-orientation away from the σ_3 direction occurs. In this project we have proposed a relatively simple analytic model to account for this "packing effect" as the waste pod grows with sequential injection, which allows prediction of fracture re-orientation as a function of injected volume. Model results are consistent with field observations, indicating that fracture re-orientation over a range of 30 to 60 degrees in azimuth can occur due to injection volumes on the order of 5000 cubic meters.

We also investigated the use of two dimensional analytical models (Perkins-Kern-Nordgren) and pseudo three dimensional models (FRACPRO) to simulate slurry fracture injection. These were modified to allow variations in shear modulus, leakoff coefficients, and closure stress with repeated injection episodes in order to capture observed formation behavior. Varying these parameters provides some improvement over typical constant value assumptions, but it is still difficult to capture many of the fundamental observations related to large-volume waste injection into high porosity formations.

Finally we investigated the use of coupled fluid flow and particle flow models to simulate fracture and dilation processes during waste injection. These studies lead us to conclude that when formations are weakly cemented with limited shear strenght, there is a transition from brittle, discrete fracture extension, to more widescale dilation and inelastic parting. We were successful in developing a coupling process between a continuum flow model and a discrete particle model, allowing simulation of slurry particle injection and resulting fracture and dilation. These simulation results, although preliminary, appear to capture the physical processes involved in solids injection into weakly cemented media. This method shows good potential for better simulating waste injection, and warrants additional investigation and development effort.

Operating Guidelines

A successful SFI project requires cooperation between regulatory agencies, the project operator and engineer, drilling and completions companies, and the site operators. Good communications need to be established between each of these groups: the success of an SFI project is sensitive to understanding and applying the guidelines by each project member.

The SFI well should be located in a formation and area that is sufficient to contain the hydraulic fracture process in a suitable permeable zone. The formation properties should include high permeability (1 Darcy or more), high porosity (25% or more), moderate to large thickness (20m or more), and lateral continuity. Special care should be taken to evaluate the mechanical condition and cement coverage for any offset wells within about a kilometer of the proposed injection well. Ideally, the target formation should be overlain by multiple low permeability shale intervals (to provide flow barriers) and high permeability sand formations (to provide a flow sink, or buffer zone, in case of breach).
A typical SFI injection well should include surface casing to below the base of fresh water, and production casing cemented to surface. Injection should take place through a tubing and packer system. Good well drilling and cementing practices are critical in providing a good cement bond along the well for the SFI injection well. If a good cement bond exists, particularly in the 60 to 100 m above the target injection zone, the volume of slurry which infiltrates upwards is very small and the volume of waste which can be placed into the target formation can be very large relative to poorly cemented wells.

SFI is best performed as a cyclic injection process, with daily periods of injection and shut-in. This permits dissipation of pressures and stresses into the formation during shut-in periods. The pressure data collected during these cycles indicates the formation injectivity and stress conditions and can be used to predict future behavior. Continuous slurry injection does not permit dissipation processes to occur and little information is available to determine injectivity and stress states.

Well logging, bottomhole pressure recording and other monitoring and analysis techniques are crucial in determining the behavior of the SFI process. Monitoring and analysis provides information about the growth of hydraulic fractures and the waste pod, and confirms the containment of the injected wastes in the target formation. This feedback loop of information can then be used to direct future injection operations.

During the course of this project, Terralog participated on a committee formed by the Louisiana Department of Natural Resources to help draft new rules for "Disposal of E&P Wastes by Slurry Fracture Injection". Some of the insights gained and guidelines developed through this DOE sponsored project were recommended and accepted for inclusion in new Louisiana regulations as an "Amendment to Statewide Order No. 29-B", which was subsequently approved by the US EPA and has now been implemented in the State of Louisiana. Specific items from the DOE project included:

1) Recommended geologic criteria, such as establishment of a containment zone that can include both impermeable barrier zones and permeable buffer zones;
2) Recommended operating criteria, such as the requirement for cyclic injection, allowing formation pressure to recover at the end of each day; and
3) Recommended monitoring, such as continuous down-hole pressure monitoring and daily shut-in pressure analysis, quarterly step-rate and extended falloff tests, and quarterly tracer and temperature logs.

Some of these recommendations have also been informally accepted as "best-practices" in the State of California by the California Division of Oil and Gas.

Field Applications

Applying the insights gained from the database assembly and review, the modeling efforts, and the establishment of "best practices" guidelines, Terralog next completed feasibility studies and prepared injection permit applications for three new potential injection sites in California. These three sites are:

1. The Guadalupe Dunes former oilfield owned by Unocal Corporation;
2. The South Elwood field operated by Venoco Inc; and,
3. The Aliso Canyon field operated by Southern California Gas Company.

The feasibility studies for each sited included geologic reviews to evaluate the availability of appropriate injection formations, detailed well reviews to confirm cement coverage and recommend the appropriate use of existing wells or new wells, and economic reviews to estimate capital and operating costs for waste injection at each site. Appropriate formations were identified at all three sites, and recommendations were provided on appropriate completion designs, operating plans, and monitoring strategies. These were incorporated into permit applications for submission to the California Department of Oil and Gas.

Finally, Terralog applied some of the modeling techniques developed through this project to a Slurry Fracture Injection project in Long Beach, California. In February, 2002, Terralog collaborated with THUMS Long Beach Company to review and analyze waste injection into a new interval of the Lower Terminal formation in the Wilmington Oilfield. We evaluated operations over a two-week period from February 18 to February 29, 2002, during which about 6000 bbls of waste slurry was injected. We were able to successfully model injection behavior by taking into account changing formation properties.

In summary, all of the research objectives of this DOE sponsored project have been achieved. Successful project completion has provided a number of significant benefits to the oil and gas industry. Some of these benefits include:

1. Establishment and documentation of a comprehensive database of slurry fracture injection operations, and associated database query tools;
2. Identification of empirical trends (or lack thereof) between various operating parameters and formation response, for comparison with future injection operations;
3. Investigation, development, and documentation of improved slurry injection modeling techniques; and,
4. Establishment of design and operating guidelines to maintain waste containment in the target interval (environmental management), help control formation response and optimize operating parameters (operating cost management), and reduce risks for well damage or loss of long-term injectivity (asset management).

INTRODUCTION

More than 100 years of extensive oil production in North America has generated and continues to generate large volumes of oilfield waste, including produced oily sands and tank bottoms, drilling muds and cuttings, crude contaminated surface soils, and produced naturally occurring radioactive materials (NORM). Ongoing exploration and production activity, combined with increased regulatory requirements, are increasing the volume and costs associated with disposal of this waste. A cost-effective and environmentally sound disposal option is to re-inject produced oilfield waste material back into the subsurface into non-productive and/or depleted zones under controlled fracture conditions.

Slurry Fracture Injection (SFI) is a waste disposal technology developed and applied by Terralog Technologies in which petroleum exploration and production wastes, such as produced sand, drilling muds, tank bottoms, and pit sludge are mixed with water into a slurry and injected into deep unconsolidated sandstone formations above fracturing pressure. The solids are permanently emplaced within hydraulic fractures generated during the pumping process, and the carrying fluid subsequently drains into the high permeability formation.

The mechanics governing the fracturing of unconsolidated sandstone formations remain poorly understood, and as a result there are few guidelines available to optimize the injection process.
To improve and optimize industry waste injection practices, two key technical advances are required. These are: 1) prediction and control of fracture or "deformation zone" containment in unconsolidated media; and 2) prediction and optimization of formation storage capacity for large volumes of waste. Terralog Technologies was awarded DOE Contract DE-AC26-99BC15222 to advance the state-of-the-art in these areas through a combined effort of field data assembly and review, improved model development, and establishment and field application of improved operating guidelines.

The specific tasks for this research project have been to:

1. Organize a extensive database of waste injection operations and formation response;
2. Evaluate correlations between waste types, injection pressure, pumping rate, etc…;
3. Investigate improved techniques for modelling fracture growth and formation response for waste injection in high permeability granular formations; and
4. Develop and apply operating guidelines to improve containment and optimize storage capacity.

This Final Report summarizes Terralog's efforts and results for the project "Development of Improved Fracture Injection Disposal Techniques for Oilfield Waste", completed under DOE Contract DE-AC26-99BC15222.

DATABASE ASSEMBLY

Database Summary

Terralog Technologies Inc. has assembled an SFI database template, and has populated it with the monitoring data collected from eight oilfield waste injection projects, comprising a total of more than 500 injection episodes. Each waste disposal project performed by Terralog is monitored extensively. The measured data consists of slurry and material volumes, wellhead and bottomhole pressures, pumping rates, slurry densities, and other relevant information collected continuously at intervals from 5 seconds to 5 minutes. Pressure and rate data is analyzed using fracture models and well test analysis to determine the characteristics of fractures, the permeability of the surrounding formation, and the changing in-situ stress conditions.

The database is created in Microsoft ACCESS format. It includes three tables: a Project Information Table, a Pressure and Rate Table, and a Daily Summary Table. The Project Information Table contains basic information on the injection formation and well completion. The Pressure and Rate Table contains key injection parameters (pressure, rate, density) which were recorded continuously at high frequency (from 5 second to 5 minute sampling frequency) at each of the projects. The Daily Summary Table provides a "snapshot" of information for each day of slurry fracture injection, summarizing information such as the total volumes of the slurry components, average injection rates and pressures, and the associated values of injectivity and pressure gradients. Also included in the database are the analyses of injection pressure and pressure fall-off which are used to determine the state of the formation. Examples of each of these three database components are provided in the following sections.

Project Information Table

To properly assess the data from each project, formation and well parameters are required. The information in this table are summarized below.

- Project Code
- Well Completion
- Well Direction
- Perforation Top (tvd)
- Perforation Bottom (tvd)
- Formation Name
- Geological Formation Top
- Geological Formation Bottom
- Formation Description
- Initial Permeability
- Initial Pressure (MPa)
- Overlying confining geological formation
- Underlying confining geological formation
-

Pressure and Rate Table

The Pressure and Rate Table contains the variables which were monitored continuously at each injection site. At each Terralog project the well pressures, slurry flow rate and density were measured every five minutes throughout the life of the project. In addition, bottomhole pressures were measured at high resolution sample rates of 5 s to 30 s in the period immediately following shut-in for improved well-test analysis. Table 1 lists the parameters which have been stored in the Pressure and Rate Table. Table 2 shows an example of actual data. For each injection episode, this raw data is analyzed and summarized in the Daily Summary Table.

Table 1: Description of Pressure and Rate Table Parameters

Value Description	**Variable Name and Units**
Project Code	Project_Code
Date and Time	Date_Time
Bottomhole Pressure	BHP_kPa
Wellhead Pressure	WHP_kPa
Slurry Flow Rate	Qslurry_m3_per_min
Density	Density_kg_per_m3

Table 2: Sample of Pressure and Rate Data from Project TTI6

Date_Time	BHP_kPa	WHP_kPa	Density_SGU	Qslurry_m3_per_min
06/07/97 7:20:00 AM	5049	57	0.6998	0
06/07/97 7:25:00 AM	5035	28	0.6998	0
06/07/97 7:30:00 AM	5035	69	0.6998	0
06/07/97 7:35:00 AM	5035	75	0.6998	0
06/07/97 7:40:00 AM	6017	161	1.0966	0
06/07/97 7:45:00 AM	11768	6235	1.1000	0.5348
06/07/97 7:50:01 AM	15886	11726	1.0255	1.5934
06/07/97 7:55:00 AM	14275	10154	1.1018	1.5928
06/07/97 8:00:01 AM	13870	9570	1.1082	1.5934
06/07/97 8:05:01 AM	13682	9385	1.1073	1.5947
06/07/97 8:10:01 AM	13502	9177	1.1061	1.5934
06/07/97 8:15:01 AM	13459	8981	1.1781	1.5921
06/07/97 8:20:01 AM	13611	8779	1.2289	1.5941

Daily Summary Table

The Daily Summary Table is the key repository of information and most useful component of the database. This contains a summary of critical injection parameters and interpreted formation response for all injection episodes for all projects. Table 3 presents a summary of the Daily Summary Table parameters. Each row of data in the Daily Summary Table consists of one injection episode, showing all data collected for that time period. In total, there are 68 variables contained in the columns of the Daily Summary Table. Most of these parameters are numeric values, but some are descriptive text variables. The parameters in the database have been chosen to best represent the characteristics of the injection period operations and formation response.

There are 790 daily entries in the database, of which 518 are injection episodes, and 272 are days that operations were suspended due to days off, well workovers, or maintenance issues. The variables can be grouped into those parameters that were directly measured (independent measurements), dependent values calculated directly from the measurements, and interpreted values determined from data analysis. A sample portion of this database Table for one project is presented in Table 4.

Table 3: Description of Daily Summary Table Parameters

Value Description	**Variable Name and Units**
General Project Information:	
Project Code	Project_Code
Project Name	Project_Name
Well Name	Well Name
Formation Name	Formation Name
Perforation Top (tvd)	Perf Top_tvd
Perforation Bottom (tvd)	Perf Bottom tvd
Formation Top (tvd)	Fmn Top tvd
Formation Bottom (tvd)	Fmn Bottom tvd
Date	Date
Operational Status	Operational_Status
Operational Status Code	Operational_Status_Code
Monitoring Status	Monitoring_Status
Monitoring Status Code	Monitoring_Status_Code
Shut-in Analysis(type of analysis performed)	Shut-in Analysis
Flow Regime	Flow_Regime
Shut-in Analysis Confidence	Shut_In_Analysis_Confidence
Injection Behavior	Injection_Behavior
Independent Measurements:	
Pumping Time	Pumping_Time_hr
Shut-in Time	Shut_in_Time_hr
Water Volume	Water_m3
Total Materials Volume	Material_m3
Sand	Sand_m3
Drilling Mud	Drilling_Mud_m3

Slop	Slop_m3
Soil/Pit Material	Soil_Pit_material_m3
Total Slurry Volume	Slurry_m3
Cumulative Water Volume	Cum_Water_m3
Cumulative Materials Volume	Cum_Material_m3
Cumulative Sand Volume	Cum_Sand_m3
Cumulative Slop Volume	Cum_Slop_m3
Cumulative Mud Volume	Cum_Mud_m3
Cumulative Soil/Pit Material Volume	Cum_Soil_Pit_Material
Cumulative Slurry Volume	Cum_Slurry_m3
Average Injection Rate	Avg_Inj_Rate_m3_per_d
Average Slurry Density	Density_kg_m3
Average Injection Bottomhole Pressure	Avg_Inj_BHP_MPa
Average Injection Wellhead Pressure	Avg_Inj_WHP_MPa
Minimum Shut-in Pressure	Simin_BHP_MPa
Dependent Values:	
Injectivity	Injectivity_m3_per_d_per_MPa
Estimated Slurry Viscosity	Est_Slurry_Viscosity_cP
Average Injection BHP Gradient	BHPinj_Grad_kPa_per_m
Minimum Shut-in Pressure Gradient	Simin_Grad_kPa_per_m
% Total Materials in Slurry	PercentMaterials
% Sand	PercentSand
% Mud	PercentMud
% Slop	PercentSlop
% Soil/Pit Material	PercentSoil_Pit_Material
Interpreted Values:	
Instantaneous Shut-in Pressure	ISIP_MPa
Closure Bottomhole Pressure	BHP_Closure_MPa
Closure Bottomhole Pressure Gradient	Closure_Grad_kPa_per_m
Permeability (Zone 1)	Zone_1_Perm_mD
Skin (Zone 1)	Zone_1_Skin
Permeability (Zone 2)	Zone_2_Perm_mD
Skin (Zone 2)	Zone_2_Skin
Wellbore Storage	Wellbore_Storage_m3_per_Kpa
P* (Estimated Reservoir Pressure)	P_Est_Res_Pressure_MPa
Fracture ½ length	Linear_xf_m
PKN_LL Closure (kPa)	PKN_LL_Closure_MPa
PKN_LL Length Growth	PKN_LL_Length_Growth_m_s_e05
PKN_LL Shear Modulus	PKN_LL_Shear_Modulus_GPa
PKN_LL r^2 Value	PKN_LL_R_Squared
PKN_LL % Volume Difference	PKN_PercentVolume_Diff
PKN Injection Time (hrs)	PKN_Injection_Time_hrs

Table 4: A Portion of the Daily Summary Table

Project Code	Date	Pumping Time (hr)	Water Volume (m^3)	Slop Volume (m^3)	Sand Volume (m^3)	Avg. Inj. Rate (m^3/min)	Avg. Inj. BHP (kPa)
TTI 6	10-Aug-97	6.3	641	8	47	1.99	13.5
TTI 6	11-Aug-97	8.7	503	9	135	1.54	14.0
TTI 6	12-Aug-97	8.0	614	17	117	1.65	13.5
TTI 6	13-Aug-97	6.5	445	20	65	1.66	14.0
TTI 6	14-Aug-97	5.9	446	17	0	1.58	13.0
TTI 6	15-Aug-97	3.0	301	0	0	1.67	13.6
TTI 6	16-Aug-97	9.3	518	164	159	1.54	12.5
TTI 6	17-Aug-97	8.8	653	8	104	1.65	12.5
TTI 6	18-Aug-97	3.5	380	0	0	1.81	13.7
TTI 6	19-Aug-97	4.5	543	0	0	2.01	13.5
TTI 6	20-Aug-97	9.3	685	16	124	1.68	13.0
TTI 6	21-Aug-97	9.8	499	0	83	1.23	13.0
TTI 6	22-Aug-97	9.0	553	8	116	1.52	13.5
TTI 6	23-Aug-97	8.5	495	0	154	1.58	13.7
TTI 6	24-Aug-97	8.8	347	0	94	1.16	13.7
TTI 6	25-Aug-97	9.0	669	0	127	1.59	13.7
TTI 6	26-Aug-97	7.3	526	0	72	1.60	13.8
TTI 6	27-Aug-97	7.3	724	0	0	1.88	
TTI 6	28-Aug-97	8.3	735	0	45	1.76	
TTI 6	29-Aug-97	6.3	508	0	13	1.63	13.5
TTI 6	30-Aug-97	9.0	654	0	81	1.58	13.5
TTI 6	31-Aug-97	9.0	642	0	91	1.57	14.0
TTI 6	01-Sep-97	9.5	656	0	65	1.46	13.8

General Project Information

This area provides the basic information about each project. The Operational Status column represents the pumping status of the injection period. Each Operational Status has a numerical code that has been assigned to it (Table 5). The Operational Status Codes are grouped as follows: 10 to 17 are injection days, 20 to 26 indicate well testing operations, 30 and above are for suspended operations and the associated reasons. The status code can be used with the SFI database plotter to screen out specific data points such as injection episodes in which only water was injected.

The Monitoring Status column reflects the status of the monitoring equipment for each injection period. Again, a code has been assigned to each type of status (Table 6). These codes are grouped as follows: 110 to 112 for fully operational data collection system, 120 to 124 for broad monitoring system failures, and 130 and above for specific sensor failures. These codes can be used to assess the quality of specific data in the Daily Summary Table.

Table 5: SFI Operational Status Codes

Operational_Status_Code	Operational_Status
10	Slurry Injection
11	Water Injection by TTI
12	Water Injection by Client
13	Wellbore Failure during injection
14	Communication with offset wells during injection
15	Step Rate Test and Slurry Injection
16	Waste Injection by Client
17	Communication with injection well annulus
20	Step Rate Test
21	Pressure Fall-off Test
22	Step Rate Test and Pressure Fall-off tests
23	Tracer Log Test
24	Tracer Log and Step Rate Tests
25	Dye Injection Tests
26	Testing Well Integrity
30	Operations Suspended - Days off
31	Operations Suspended - Extended Pressure Fall-off Test
32	Operations Suspended - no water/waste available
33	Operations Suspended - no service equipment available
34	Operations Suspended - awaiting client/TTI decision
35	Operations Suspended - blocked well perforations
36	Operations Suspended - well cleanout
37	Operations Suspended - pumping equipment repairs
38	Operations Suspended - well repairs/workover
39	Operations Suspended - Well Clean out and Tracer Log
40	Operations Suspended - frozen equipment or water line
41	Operations Suspended - Rig in/Rig out
42	Well Cleanout and Step Rate Test

Table 6: SFI Monitoring Status Codes

Monitoring_Status_Code	Monitoring_Status
110	Fully Operational
111	Fully Operational, density measured by mud scales
112	Fully Operational, behavior too erratic to obtain averages
120	No data collected - Download Failure
121	No data collected - Power Failure
122	Injection data collected but no fall-off data -Power Supply
123	BHP Data okay, WHP,Density and Rate calculated from pump
124	WHP, Flow Rate and Density okay, BHP calculated from pump
130	BHP Sensor Failure, all other sensors ok
131	WHP, Flow Rate and Density Unit Failure, BHP sensor ok
132	Density Sensor Failure, all other sensors ok
133	Slurry Volumes not correct, all other sensors ok
134	WHP Sensor failure, all other sensors ok
135	BHP Sensor out of well, all other sensors ok
140	Cannot Access Archive

Independent Measurements

Time measurements and material volumes are taken from the daily pump reports. All volumes are reported in units of m^3. As each project dealt with different waste streams, some entries will be blank (for example, some projects did not inject Mud as part of the slurry; therefore, these cells will be blank).

Cumulative values are the running totals for each project to the end of the pumping day in question; values reported in m^3.

The injection rate, Average BHP, Average WHP, Density and Min. Shut-in pressure are measured with a bottomhole sensor (except wellhead pressure) and collected by dataloggers at each project.

Dependent Values

Injectivity is equal to the average pumping rate divided by net pressure (average injection pressure – virgin reservoir pressure), and gives an indication of how well the formation is accepting fluid during a given injection episode.

Viscosity was calculated using an equation based on the turbulent flow equations. This equation is a rearrangement of work developed by Swamee and Jain (1976). Viscosity (μ) is calculated as follows:

$$\mu = 560\sqrt{\frac{1000\rho\, p_f D^3}{L}}\left[\exp\left(-1.0365\frac{Q}{60D^2}\sqrt{\frac{\rho L}{p_f D}}\right)-\frac{\varepsilon}{3.7D}\right] \qquad [1]$$

Where μ is fluid viscosity (cP), ρ is fluid density (kg/m^3), p_f is pressure drop due to friction (kPa), D is pipe diameter (m), L is pipe length (m), Q is flow rate (m^3/min), ε is pipe roughness (m).

Gradients: as each project was conducted in different formations, pressure values are divided by bottomhole sensor depth to provide easy comparison between projects. By doing this, the pressure data can be readily compared across a project by project basis. All values are in reported in kPa/m.

% Total Materials in Slurry: For each injection period, the volume of each component is divided by total slurry volume to obtain volumetric composition of the slurry.

Consistency of the slurry was not the same each day due to different volumes of slop, sand, mud and water. The different flow characteristics of each component contained in the slurry can be best described in terms of viscosity. Direct measurements of slurry viscosity with a viscosity meter were never attempted, so viscosity had to be calculated based on the pressure drop in the pipeline leading to the wellhead and in the well tubing.

Interpreted Values: Determining ISIP and Closure

Instantaneous shut-in pressure (ISIP) corresponds to the bottom hole wellbore pressure just as shut-in occurs (i.e., just when the fracture begins to close). Closure pressure refers to the bottom hole wellbore pressure just as the fracture closes completely; this is identical to the pressure required to open the fracture, and is theoretically equal to the minimum principal stress of the formation (known as σ_3). ISIP is especially important for the purposes of well test analysis; closure is necessary to perform PKN analysis, as Δp in equation [7] is equal to bottom hole wellbore pressure – closure pressure (described in a later section).

Two methods have been used to determine ISIP and closure pressure: the derivative plot method and well test analysis. In the derivative plot method the rate of pressure decline (dP/dt) is plotted against bottomhole pressure (Figure 1). In this plot ISIP occurs at the pressure where the most negative dP/dt occurs. Closure is determined at the point where the dP/dt points deviate from a straight line as shown.

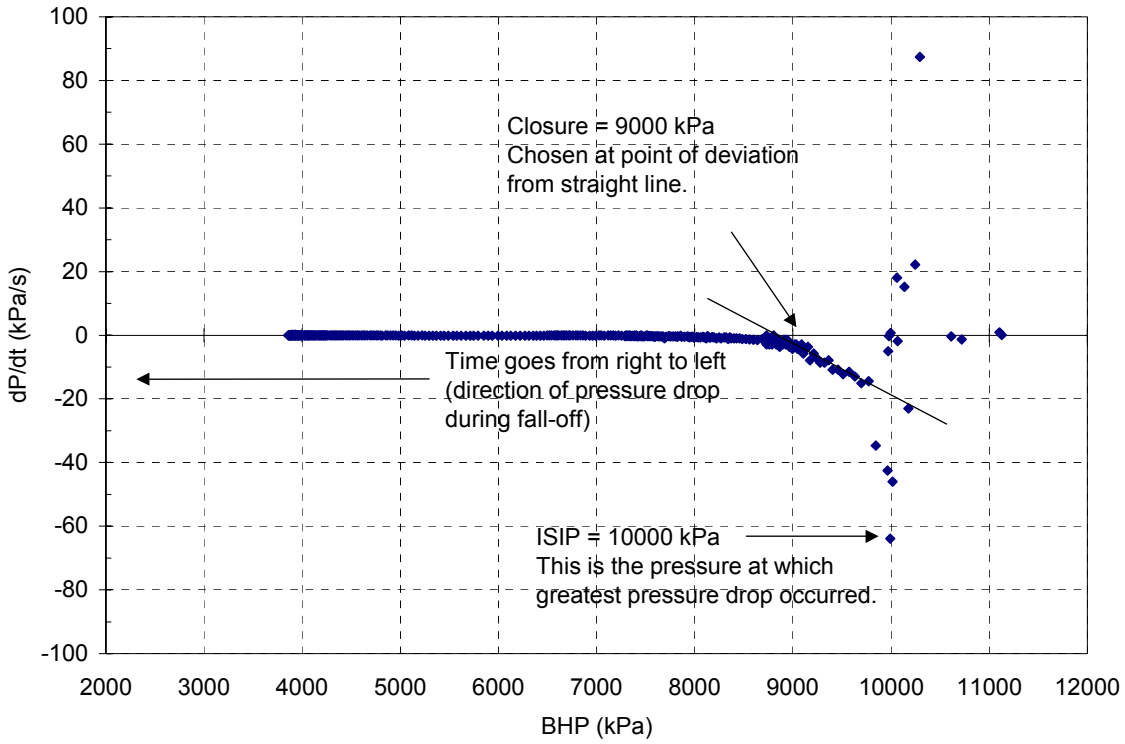

Figure 1: Determining ISIP and Closure Pressure from pressure derivative plot

The other technique for determining ISIP and Closure pressure is from well test analysis. ISIP in this case is defined as the first point at which wellbore storage is observed, as shown in Figure 2 (Horne, 1995). Closure pressure is determined from the point at which linear flow from the fracture into the formation ceases (Figure 3).

The data shown in Figures1, 2 and 3 comes from project TTI5, May 17, 1997. It can be seen that there is some discrepancy in the values returned by both techniques (300 to 500 kPa). The ISIP and closure values in the database were determined by both methods, with probably two-thirds of the values determined by the derivative plot technique. However, the well-test methods are more reliable with complicated fall-off behaviors and will be used primarily in the future.

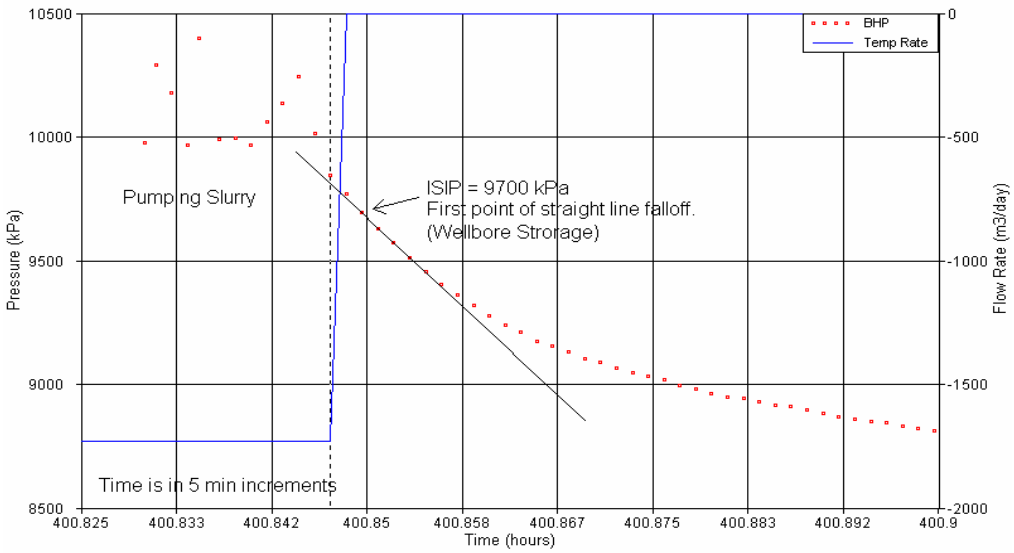

Figure 2: Determining ISIP from well test analysis

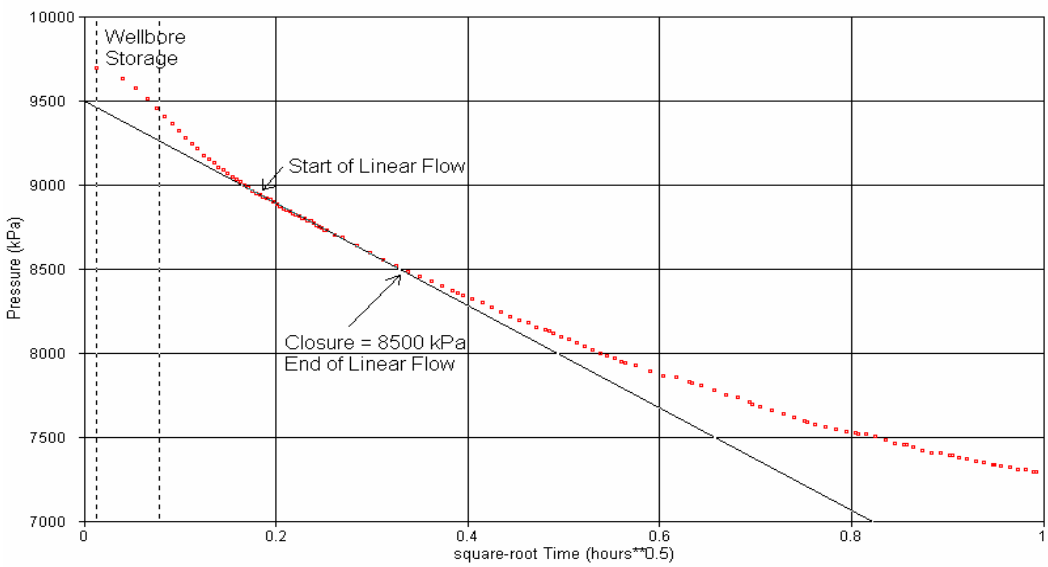

Figure 3: Determining Closure from well test analysis

Pressure Injection and Pressure Fall-Off Analysis

Pressure data during injection is analyzed by statistically curve fitting theoretical pressure response with actual pressure data. Parameters obtained during this procedure include near-well shear modulus, fracture length growth, and closure pressure. Pressure data during fall off is analyzed using conventional radial / linear flow well testing. Parameters obtained here include near-well (zone 1) permeability, far-well (zone 2) permeability, and wellbore storage. Fracture length is determined on days where linear flow is observed during early fall off. This section also explains the method we have used to determine average slurry viscosity for each injection cycle, and describes how we determine ISIP (instantaneous shut-in pressure) and closure pressure.

Pressure Falloff Analysis

Well test analysis is performed on pressure fall-off data in order to determine flow regimes and various reservoir parameters. The most significant is permeability. Due to the relatively short fall-off periods between injection cycles during SFI operations, typically only the near-well reservoir is 'seen' by the bottom hole pressure sensors; the radius of investigation does not extend far into the reservoir before the next injection cycle occurs. Therefore, the permeability obtained from the analysis is the near-well permeability, or the permeability of the waste-pod. Ideally, this is the part of the reservoir we're interested in characterizing, especially as it changes during time (the properties of the virgin reservoir are typically known beforehand).

There are two valuable plots used to characterize flow regimes and determine reservoir parameters; these are the semi-log plot, and the Horner plot. All well test analysis is performed on PAN software.

Log-Log Plot

A log-log plot of net pressure and pressure derivative vs. time is useful in distinguishing flow regimes that are occurring after shut-in. Pressure derivative is calculated by the following finite-difference type equation: $PD = \Delta t \cdot d(\Delta P)/d(\Delta t)$, where PD is pressure derivative (psi), Δt is time elapsed since shut-in (hr), and ΔP is net pressure (pressure – initial pressure, psi). Typically, when shut-in commences, a period of wellbore storage occurs, followed by a transition phase between storage and radial flow, followed by pure radial flow. (Note: sometimes, a period of linear flow can be observed between the transition phase and pure radial flow, denoted by a slope of exactly ½ on both PD and net pressure data series. Linear flow corresponds to fracture flow, and on days in which linear flow is observed, the fracture is still opened for a short time after shut-in occurs. Linear flow is not considered in this report, although it has been seen to occur during some SFI operations).

Wellbore storage is seen as a straight line of unit slope on both the net pressure series and the PD series on the log-log plot. The transition phase occurs from the point at which the data drifts from the unit slope, to the point 1.5 log cycles afterwards. Radial flow is seen as a horizontal line on the PD data series (not the net pressure series).

Using a log-log plot, wellbore storage can also be calculated from the net pressure series, by choosing any point along the unit slope (Δt, Δp) and using the following equation (Lee, 1982):

$$C_s = \frac{qB}{24}\left(\frac{\Delta t}{\Delta p}\right) \qquad [2]$$

Where C_s is wellbore storage (m^3/kPa), q is average slurry injection rate (m^3/d), B is slurry shrinkage factor (bbl/STB), Δp is any y-value falling along the unit slope line (kPa), and Δt is its corresponding x-value (hr).

Wellbore storage reflects how much fluid is present in the wellbore after pumping stops. The higher the wellbore storage, the longer the wellbore storage period lasts, as a result of a large wellbore effect on fluid flow. A large wellbore storage coefficient indicates an effective, open fracture, whereas a small wellbore storage coefficient could indicate perfs plugging off or some other flow restriction that is preventing fluid from filling the wellbore after injection ceases.

Figure 4 gives an example of a log-log plot, showing the wellbore storage regime, transition phase, and the radial flow regime. Note that the red data series is the net pressure, and the blue data series is the PD. Figure 3 shows the corresponding Horner plot for the same injection cycle (Horner plots are explained in the next section).

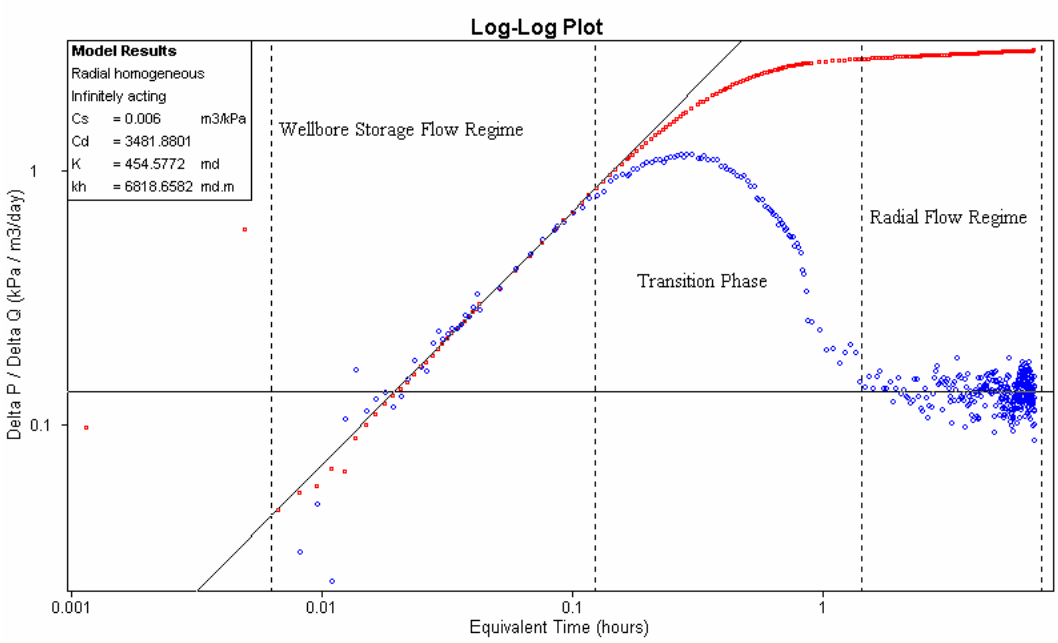

Figure 4: Example of a log-log plot, showing 3 different flow regimes

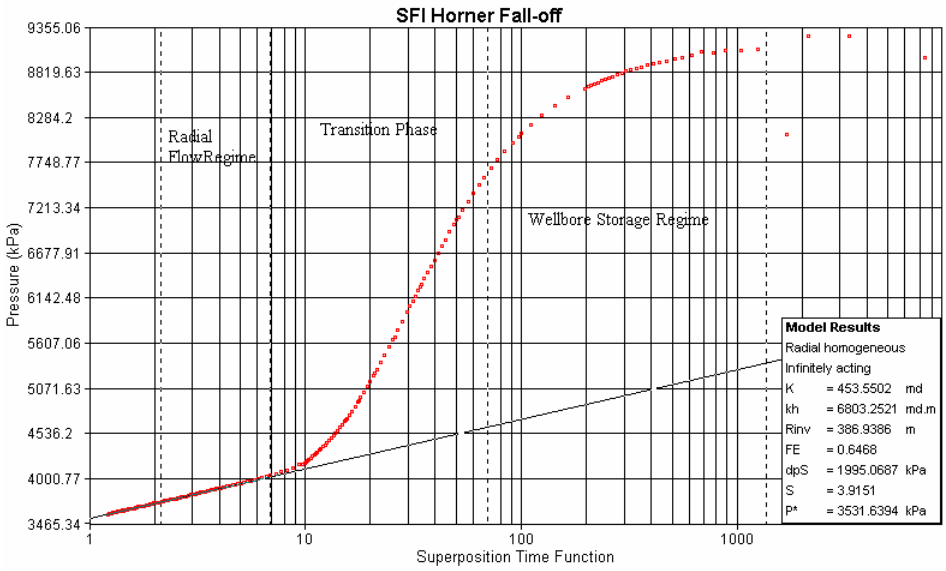

Figure 5: Horner plot corresponding to Figure 4 log-log plot

Horner Plot

The permeability is determined from the Horner plot (Figure 5), a log-log plot of bottom hole pressure vs. Horner time (Horner time is $(t_p+\Delta t)/\Delta t$, where t_p is the time that fall-off starts, and Δt is the elapsed time since t_p). Horner time effectively goes from "right to left" on a Horner plot, i.e., large Horner time corresponds to small real time, and small Horner time corresponds to large real time. A Horner time of 1 indicates a real time of ∞. Horner time is dimensionless.

On the Horner plot, linear flow cannot be seen, however radial flow can be identified as a straight line (over the time period that corresponds to the horizontal line on the log-log plot). Permeability is calculated from the slope of this line, using the following equation (Lee, 1982):

$$k = 2149\left[\frac{qB\mu}{mh}\right] \qquad [3]$$

Where k is permeability (mD), q is the average injection flow rate before shut-in (m^3/d), h is the thickness of the disposal formation (m), B is the slurry shrinkage factor (bbl/STB), μ is the viscosity of the injected fluid (cP), and m is the slope of the line on the Horner plot (kPa/log cycle).

<u>Waste-Pod and Virgin Reservoir Permeabilities</u>

During extended shut-in periods (of several days, for example), the radius of investigation gets large enough to extend past the waste pod and 'see' the virgin reservoir. If there is significant contrast in permeabilities between virgin reservoir and the waste pod, then two distinct slopes on the Horner plot will be seen. These will correspond to two distinct horizontal lines on the semi-log plot. In the case of SFI,

the virgin reservoir, if seen, will have much greater permeability than the near-well waste pod zone, and this will be represented by a steeper slope on the Horner plot and a lower horizontal line on the semi-log plot. Typically, however, shut-in is rarely long enough to see past the waste pod zone, so that the permeability obtained from equation [3] represents the near-well permeability.

Pressure Injection Analysis

Injection pressure analysis allows for fracture parameters to be obtained by analyzing the injection portion of the data. Two types of fracture models, PKN (Perkins-Kern-Nordgren) and GDK (Geertsma-deKlerk) were tested on all injection data, but for the correlations presented this report, the PKN parameters are used, as most pressure responses during SFI typically reflect PKN behavior. There are two types of PKN fractures, large leak-off (LL) and zero leak-off (ZL); the former is more applicable to the mechanics of SFI, and was used in the correlation work to the exclusion of the latter. Analyzing the data using the PKNLL model yields several parameters, the most important being fracture growth rate, or extension rate, and shear modulus of the near-well formation (effectively, of the waste pod). A value for closure is also determined as part of the linear regression data matching technique used in the analysis.

PKNLL Fracture Growth Rate

The PKNLL fracture geometry is shown in Figure 6. The underlying principles behind the PKNLL fracture model are the following (Nordgren, 1972):

- large rate of fluid leak off into fracture walls dominates fracture compressibility
- vertical extent of fracture is constant
- fracture elliptical in both horizontal and vertical cross sections
- wellbore pressure increases with $t^{1/8}$ during fracture propagation
- fracture length as a function of time is given by the following equation (Nordgren, 1972):

$$L = \frac{(q_{inj}/2)t^{1/2}}{\pi C h} \qquad [4]$$

where L is fracture length (m), q_{inj} is the average injection rate (m^3/s), t is time (s), C is fluid leak-off rate ($m/s^{1/2}$), and h is fracture height (m). Based on equation [4], the PKNLL fracture growth rate can be expressed as follows:

$$PKNLLgrowthrate = \frac{(q_{inj}/2)}{\pi C h} \qquad [5]$$

where PKNLL growth rate has units $m/s^{1/2}$. Normalizing PKN length with respect to time is necessary so that injection episodes with different injection times can be compared on the same level. Note that the right hand side of equation [5] is independent of time; effectively, the growth rate is $L/t^{1/2}$, from equation [4].

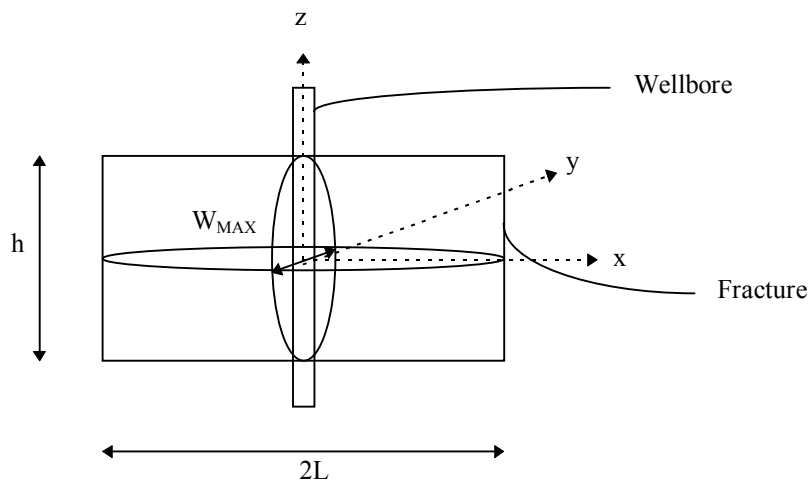

Figure 6: Geometry of PKN Fracture

The leak-off coefficient, C, is given by the following equations (Appendix by R.D. Carter in Howard and Fast, 1957):

$$1/C = 1/C_I + 1/C_{II}; \quad C_I = 0.0469\sqrt{\frac{k\Delta P\phi}{\mu_{ff}}}; \quad C_{II} = 0.0374\sqrt{\frac{k\phi c_f}{\mu_{rf}}} \qquad [6]$$

Where k is permeability (D), ΔP is the difference between fluid pressure at the fracture face and virgin reservoir pressure (psi), ϕ is reservoir porosity, μ_{ff} is the viscosity of the fracturing fluid (cP), μ_{rf} is the viscosity of the reservoir fluid (cP), and c_f is the compressibility of the reservoir fluid (psi^{-1}). C_I corresponds leak-off strongly controlled by the fracturing fluid, and C_{II} corresponds to leak-off that occurs when fracturing fluid is very similar to reservoir fluid. Composite leak-off in SFI environment can be controlled by both, so C in equation [6] is known as the composite leak-off coefficient.

For each data point recorded during an injection cycle, C can be determined from equation [6], and growth rate from equation [5]. An average growth rate is then calculated for each injection cycle, and entered into the daily averages part of the database.

The meaning of PKNLL growth rate is simply how quickly the fracture is propagating during injection. The higher the number, the more efficient the propagation of the fracture and the more effective the SFI treatment is for the particular injection cycle. If the number is becoming anomalously high over the course of a project, however, this could be a problem; the fracture could be extending laterally outside of the specified reservoir, which could have regulatory consequences. A low growth rate indicates that the fracture is having difficulty propagating, and this could be a result of several things: faulty casing that is

allowing slurry to escape, injecting highly viscous slurry that can block out perfs and cause wellbore problems, pressure communication with another formation so that fluid energy is unavailable to extend the fracture into the disposal formation, etc.

PKNLL Shear Modulus

Another parameter that can be obtained from PKNLL analysis is the average shear modulus of the near-well zone during an injection cycle. It is calculated for each data point (see C, above) using the following equation from PKN theory (Nordgren, 1972):

$$\Delta p = 4\left[\frac{2G^3\mu\left(q_{inj}/2\right)^2}{\pi^3\left(1-\nu\right)^3 Ch^5}\right]t^{1/8} \qquad [7]$$

Where Δp is the net pressure (bottom-hole pressure recorded by sensor – closure pressure, kPa), G is shear modulus (kPa – standard treatment is GPa but kPa used for unit consistency), μ is slurry viscosity (kPa·s), q_{inj} is injection rate (m^3/s), ν is Poisson's ratio, C is leak-off coefficient from equation [6], h is reservoir thickness (m), and t is time since pumping begins (s). All of the parameters from equation [7] are known except G; thus G can be calculated for each data point (Flaman, 1998), and a daily average can be computed and entered into the daily averages portion of the database.

PKNLL modulus can give an idea as to whether or not the formation is becoming stiffer (higher G) as the waste pod is becoming more and more packed with slurry.

Database Query Tools

Terralog has created two plotting programs within Access in order to graphically view the data provided in the Pressure and Rate Table and Daily Summary Table. These can be used to rapidly view data for visual interpretation. The query tools built into Access can also be used to create custom datasets for specialized interpretation. The power of the Terralog database is that different variables can be plotted easily using the Microsoft Access program. Data from different projects can be compared directly. Cross plots of various injection parameters and observations can be made, with filtering on a third variable. For example, injectivity vs. viscosity can be plotted for all days in which sand percentage exceeds a certain value.

BHP Plotter

The BHP Plotter is used to view data within the Pressure and Rate Table. The data from any time period can be viewed and then exported to an Excel or ASCII text file if desired.

The BHP Plotter interface is shown in Figure 7. Bottomhole pressures (BHP) and slurry injection rates (Qslurry) are plotted, each with its own axis. The tabs in the upper right corner are used to pick the start

and finish times of the data to be plotted. The BHP axes settings are available to zoom in on the pressure data. The name of the source data table can also be entered.

The bottom section of the plotter interface contains the options for exporting data. The displayed range of data as set by the start and finish times can be exported to either Excel or ASCII text formats. The file name and directory are entered in the two text boxes provided. One limitation of this plotter is that it can display no more than 4096 points, which is an internal Access setting. This does not affect the number of records which can be exported, which can be up to 65535 records.

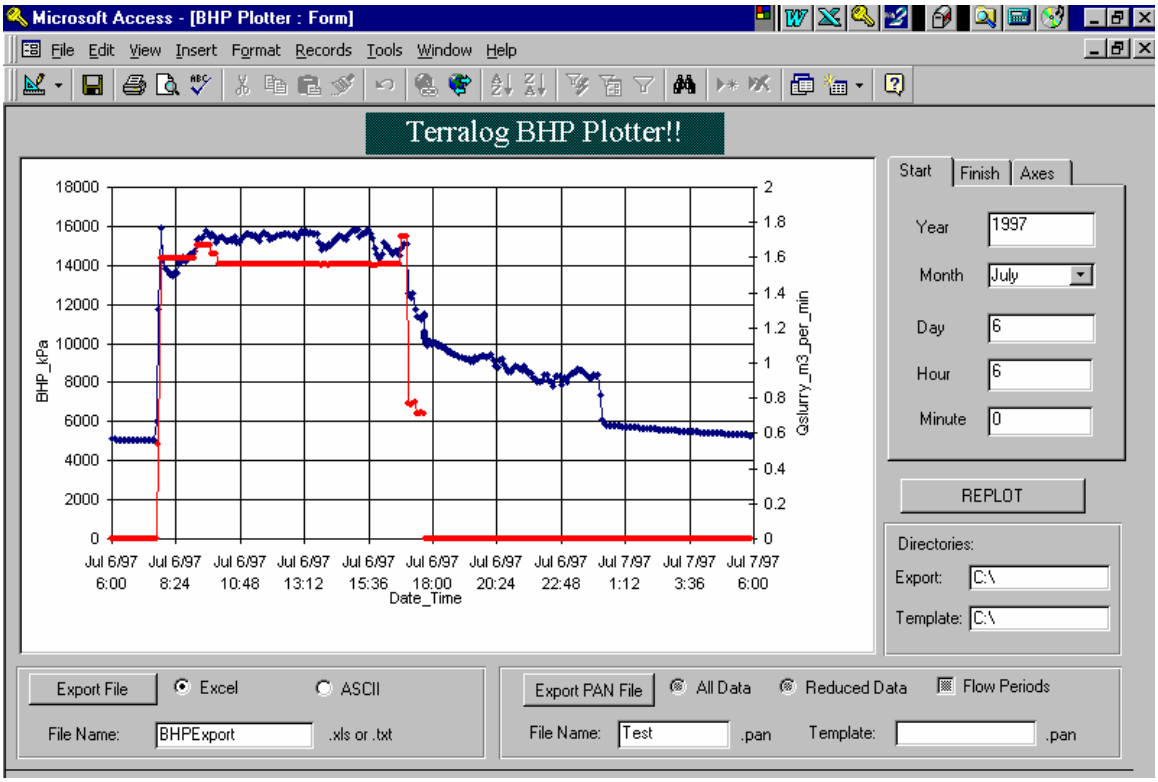

Figure 7: Interface of BHP Plotter

SFI Daily Plotter

The SFI Daily Plotter is used to view data in the Daily Summary Table. This plotter can be used for two purposes: to observe the development of a parameter over the course of a project, and to create cross-plots to determine the correlation between two separate parameters.

Figure 8 shows the user interface of the SFI Daily Plotter. The drop-down boxes in the upper right are used to pick the two parameters to be plotted on the horizontal and vertical axes. Each box contains a list of all the parameters in the Daily Summary Table. The section in the lower right is used to filter the

plotted data based on any parameter, such as Project Code or %Sand. The filter is governed by the "=", "<" and ">" operators. The buttons at the left side of the screen are used to zoom in on the plotted data.

An example of a correlation plot of two parameters is shown in Figure 9. This plot shows the initial shut-in pressure (ISIP_MPa) versus average injection pressure (Avg_Inj_BHP_Mpa), filtered to display all injection episodes in which the percent of injected sand (PercentSand) is less than 20%. Such a plot for example, could be used to compare the influence of injectate on injectivity and shut-in pressure across a range of projects.

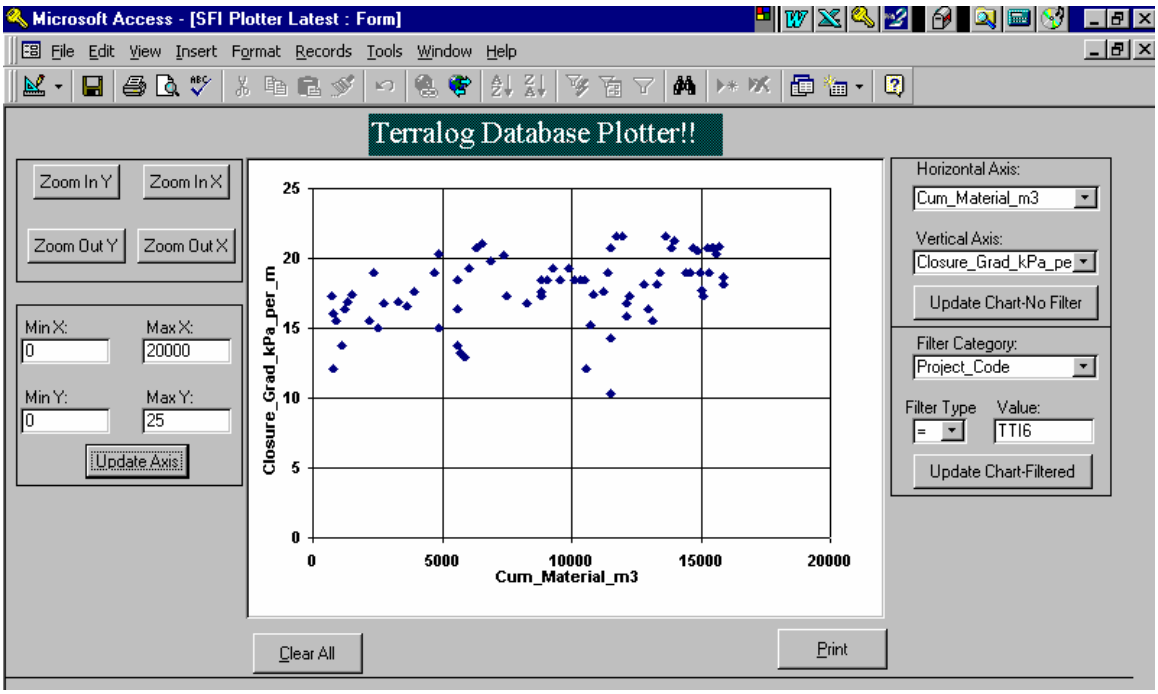

Figure 8: User interface of the SFI Daily Plotter.

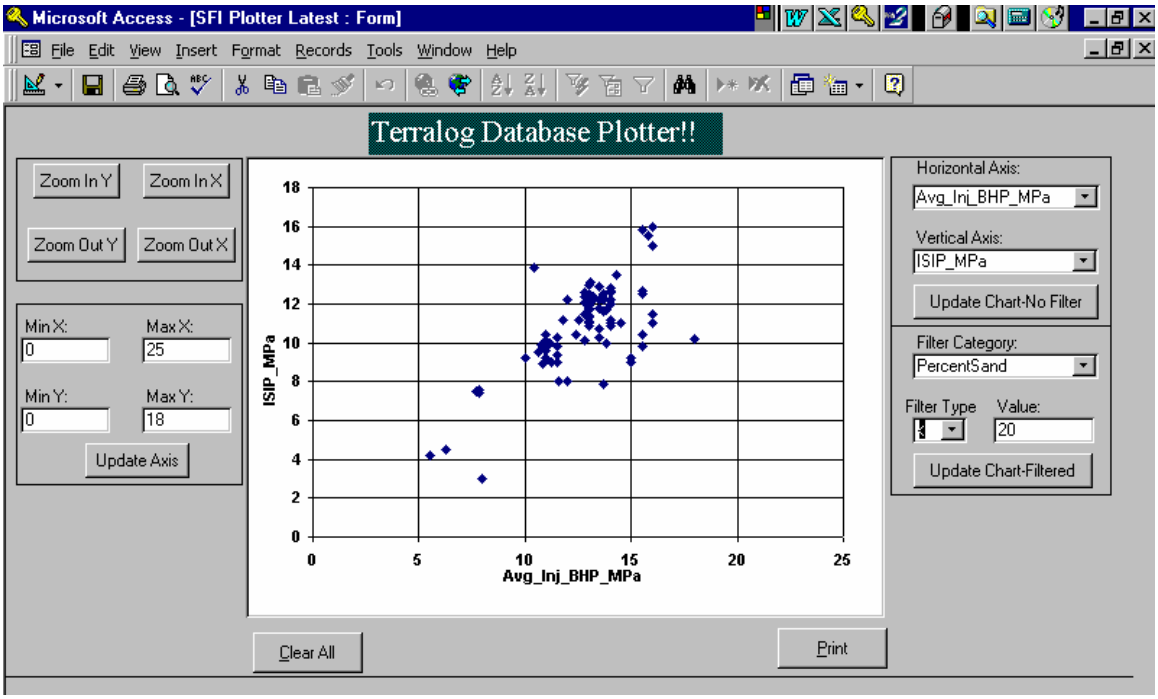

Figure 9: Example of correlation plot

Access Query Tools

In addition to the plotters created by Terralog, Microsoft Access also provides the ability to perform specialized queries of the database. An example query is shown in Figure 10, which then produces a table as shown in Figure 11. Such tables can then be printed or exported to any spreadsheet.

An example use of this tool is generate the list of days injection well tests were performed, such as step rate tests or radioactive tracer tests (as shown in Figures 10 and 11). Another example is creating a list of reservoir permeabilities (generated from well test analysis) when the slurry was composed of certain types of material (e.g., >10% Mud).

Ultimately, other users of the SFI database do not have to rely on Terralog's interpretations; they can develop their own using the plotter and query tools.

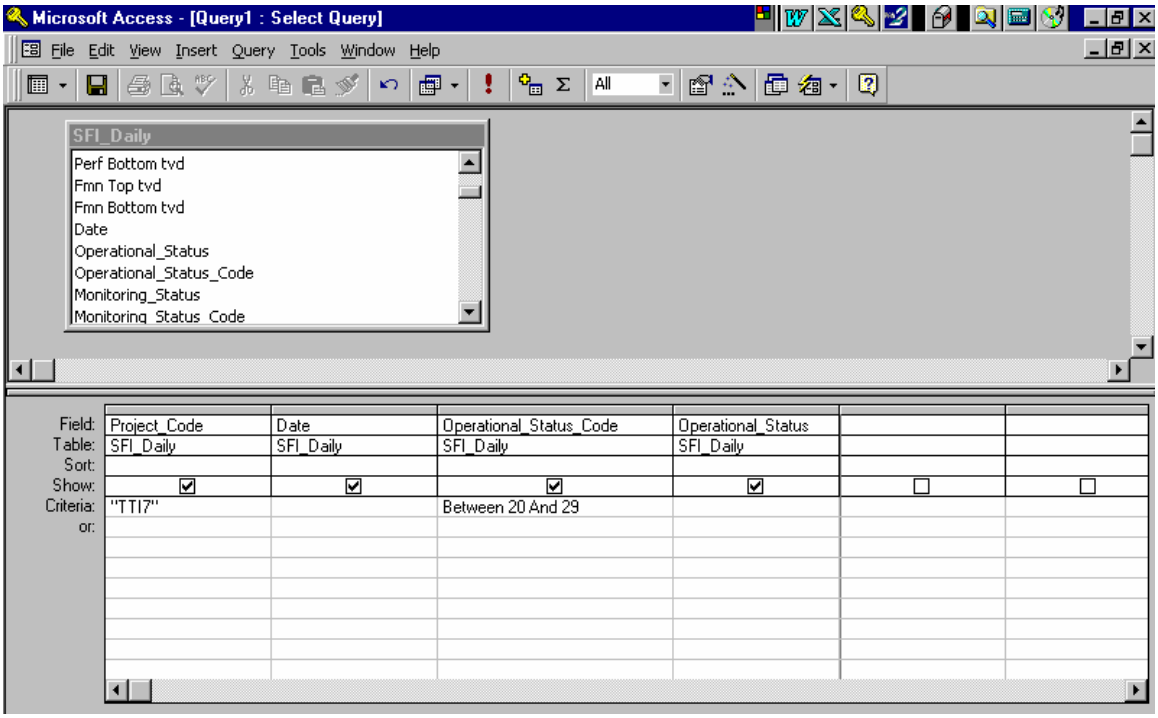

Figure 10: Example of Access Query

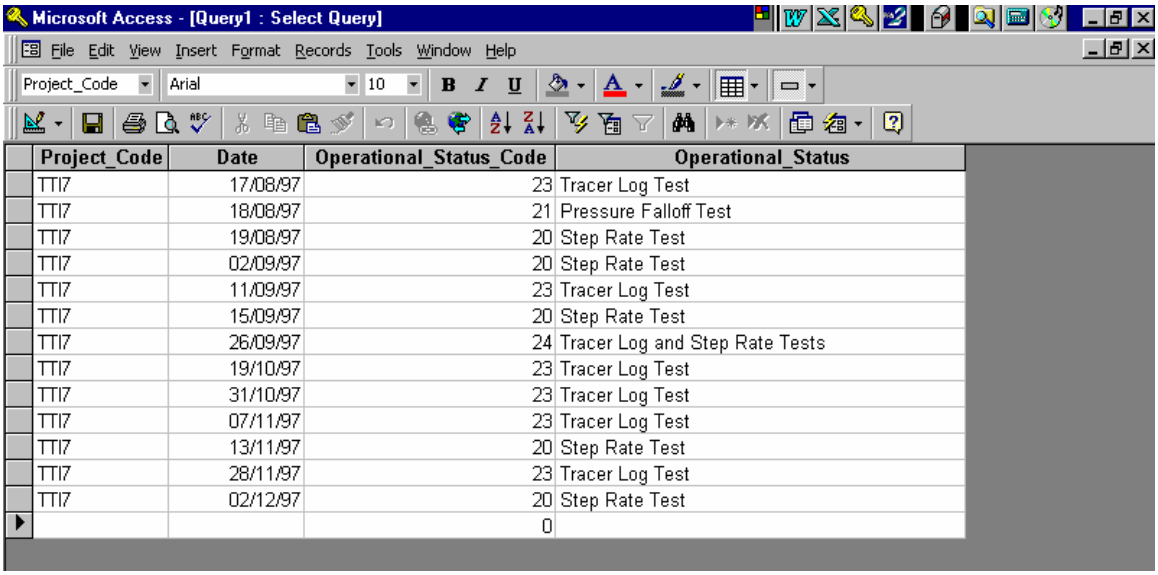

Project_Code	Date	Operational_Status_Code	Operational_Status
TTI7	17/08/97	23	Tracer Log Test
TTI7	18/08/97	21	Pressure Falloff Test
TTI7	19/08/97	20	Step Rate Test
TTI7	02/09/97	20	Step Rate Test
TTI7	11/09/97	23	Tracer Log Test
TTI7	15/09/97	20	Step Rate Test
TTI7	26/09/97	24	Tracer Log and Step Rate Tests
TTI7	19/10/97	23	Tracer Log Test
TTI7	31/10/97	23	Tracer Log Test
TTI7	07/11/97	23	Tracer Log Test
TTI7	13/11/97	20	Step Rate Test
TTI7	28/11/97	23	Tracer Log Test
TTI7	02/12/97	20	Step Rate Test
		0	

Figure 11: Table resulting from query in Figure 10

EMPIRICAL CORRELATIONS

Data Correlations

The SFI database was constructed to determine if certain pumping operations and formation parameters are related to each other. The "SFI Database Plotter" was used to plot individual variables against each other. This section discusses the more significant plots, from which conclusions about relative correlations between parameters can be determined.

When applicable, cross-project correlations, as well as project-specific correlations, use 'normalized' variables (for example pressure gradients instead of absolute pressures or percent materials instead of absolute volume of materials). This will help identify relationships that are independent of the differing formation properties and unique operating conditions of individual projects. An example of a useful cross project correlation is permeability versus injectivity. Project-specific correlations are also important, as they can gauge the effectiveness of various operating strategies, for example, the change of permeability with time as operating strategies change.

Effect of Cumulative Wastes on Closure Gradient

As waste materials are continuously packed into a disposal formation, it would be expected that pressure required to open the fracture (closure pressure) should increase. Figure 12 shows this trend of slightly rising closure pressures. "Cumulative material" means the total of all wastes including sand, slop, drilling muds, and soil & pit materials.

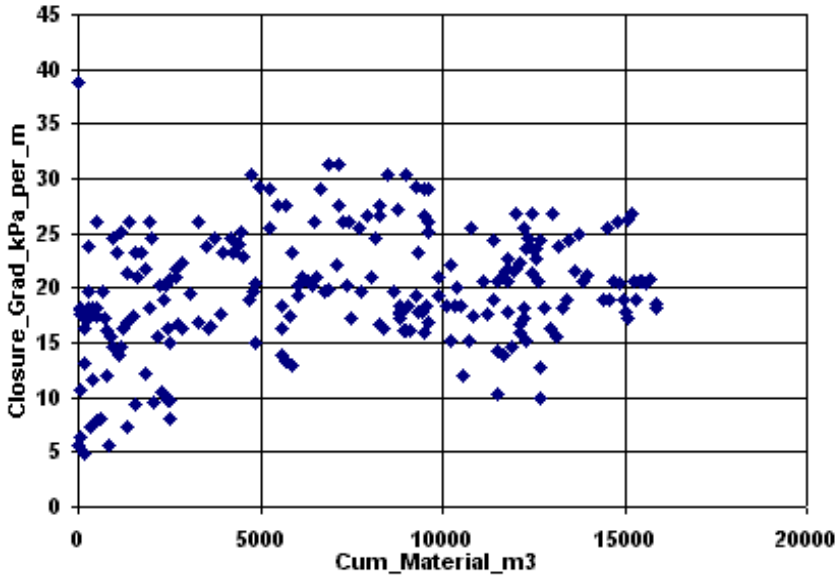

Figure 12: Closure Gradient vs. Cumulative Materials

Figures 13 and 14 show the impacts of individual waste components on closure gradient. The impact of cumulative sand injection in Figure 13 is similar to Figure 12 (combined waste volumes), with a weak rising trend. The effect of cumulative mud injection in Figure 14 does appear to be a slightly increasing closure gradient with time. There is less scatter in this plot than the others since mud was only injected in projects TTI6 and TTI9. The abnormally low closure gradients (below 10 kPa/m) present in Figures 12 and 14 came from project TTI9 which was injecting into a depleted zone at 1250 m depth as opposed to an average depth of 400 to 1000 m for the other projects.

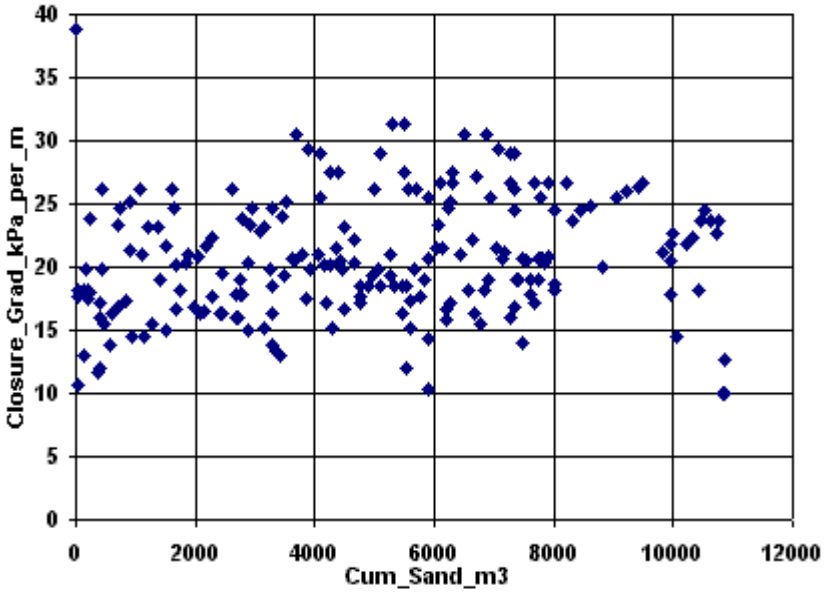

Figure 13: Closure Gradient vs. Cumulative Sand

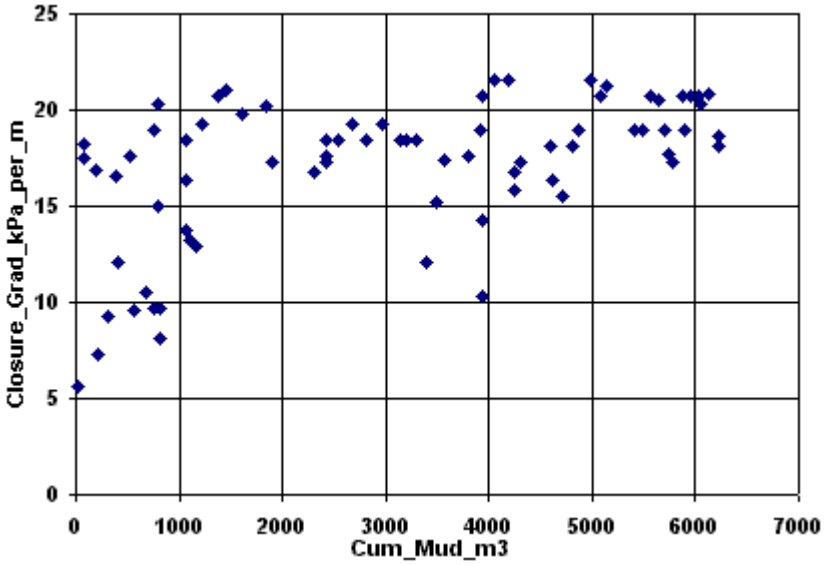

Figure 14: Closure Gradient vs. Cumulative Mud

Impact of Slurry Component Percentages on Closure Gradient

The waste material percentages refer to the average volume ratio between the waste component and the total slurry volume during an entire day. It appears in Figure 15 that increasing the percentage of waste materials in the slurry causes an increase in the closure pressure gradient. If this were true, it would be advisable to reduce the waste percentage in the injected slurries to minimize stress increase in the target formations.

However, this is not true when you look at the same plot on a project-by-project basis. It can be seen in Figures 16 and 17 that within each project the closure pressure gradient appears to be independent of percentage of waste material. In both cases the trend is horizontal and the scatter is significant, indicating that closure pressures are governed by conditions other than slurry content.

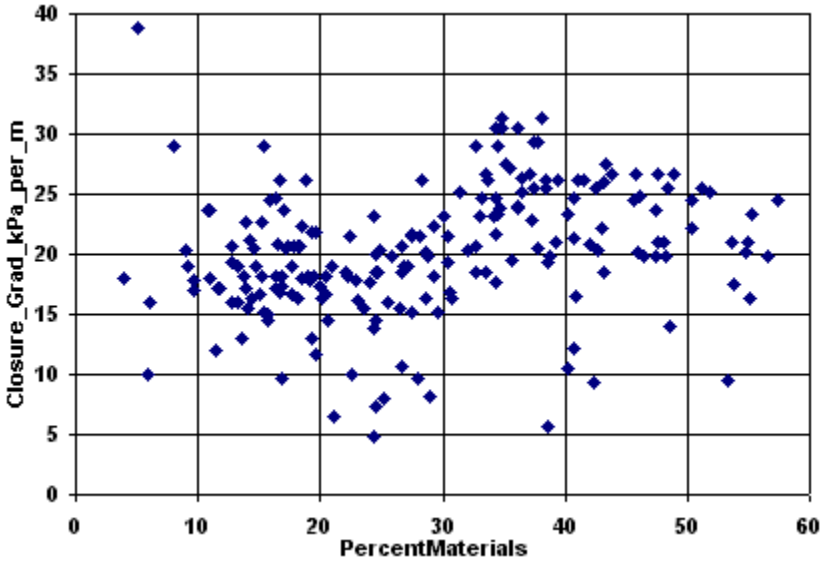

Figure 15: Closure Gradient vs. Percent Materials

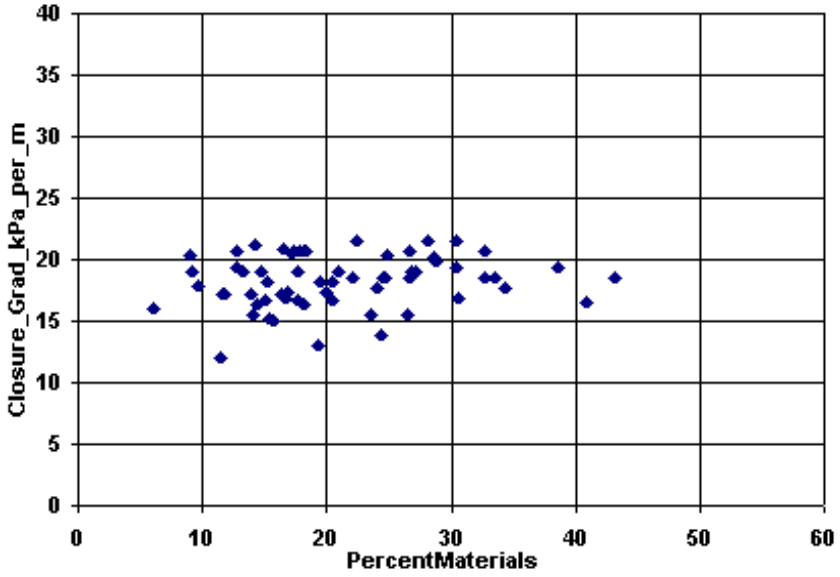

Figure 16: Closure Gradient vs. Percent Materials for Project TTI6

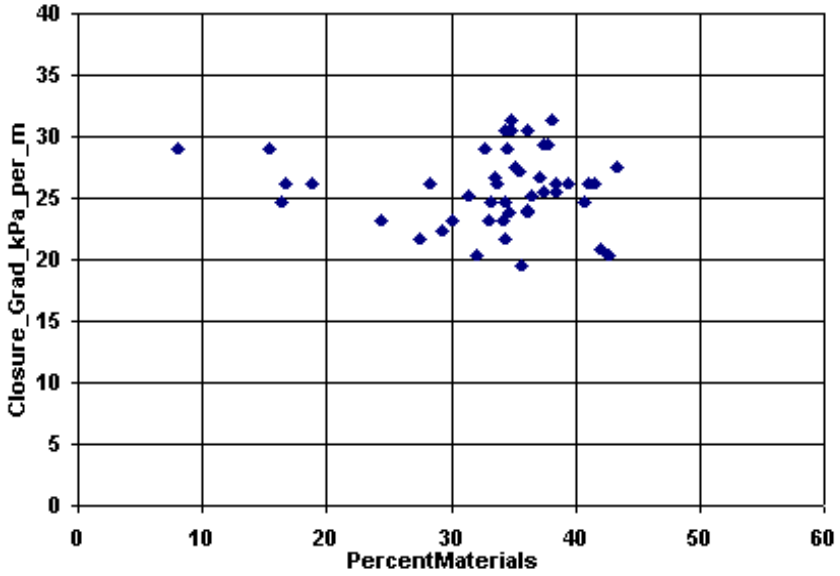

Figure 17: Closure Gradient vs. Percent Material for Project TTI7

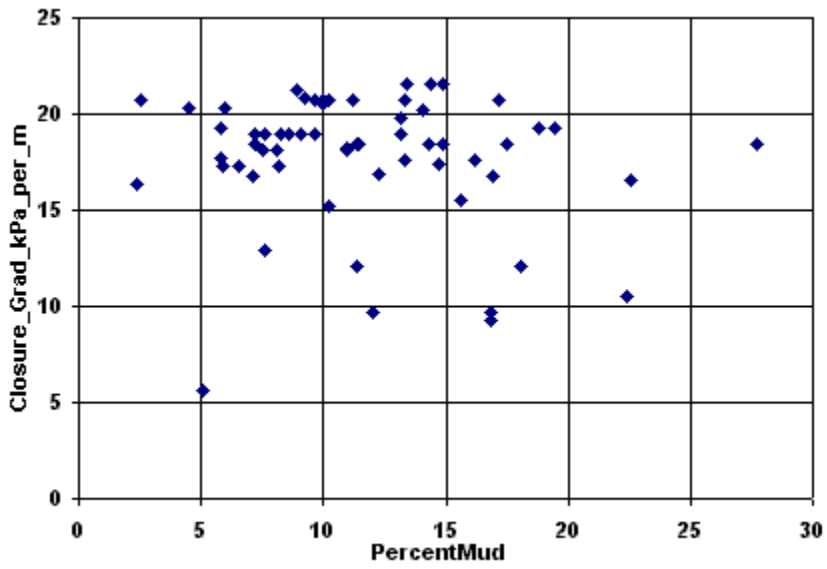

Figure 18: Closure Gradient vs. Percent Mud

Figure 18 presents the effect of an individual slurry component on closure gradient. It can be seen from this plot that the percent mud has no correlatable impact on closure pressures.

Effect of Cumulative Slurry Volume on Injectivity

Injectivity is equal to the average pumping rate divided by net pressure (average injection pressure – virgin reservoir pressure), and gives an indication of how well the formation is accepting fluid during a given injection episode.

Over the course of an SFI project, it might be expected that as more waste materials are placed within the target formation, the injectivity would tend to reduce over time. Figure 19 shows that this theory is not true, and in fact remained in a consistent band between 0.1 and 0.3 m^3/min/MPa. The points above this band typically occurred during water pumping days and points less than 0.1 m^3/min/MPa usually occcurred when the injection well was plugged.

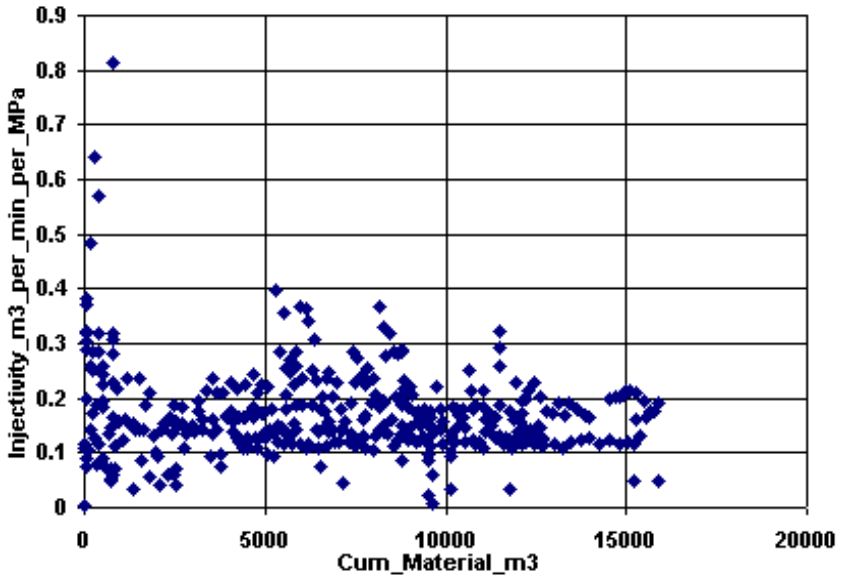

Figure 19: Injectivity vs. Cumulative Material Volume

Effect of Slurry Components Percentages on Injectivity

It would be expected that slurry containing a relatively high volumetric content of materials should be more difficult to inject into the formation, i.e., result in a low injectivity. Figure 20 shows the relationship between percent materials and injectivity. There appears to be an envelope which causes slurries with higher percent materials to cause lower injectivities. Below this envelope, the correlation is not strong.

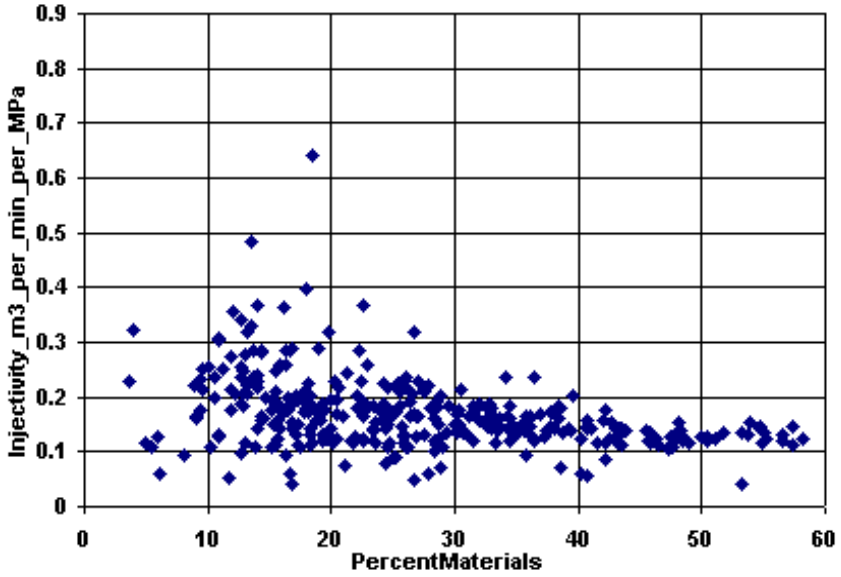

Figure 20: Injectivity vs. Percent Materials

The injection of a viscous material such as mud should result in a lower injectivity, as the slurry would be more difficult to pump. Figure 21 shows the relationship between injectivity and percent mud. There is only a small indication that higher mud content negatively impacts injectivity, independent of other factors.

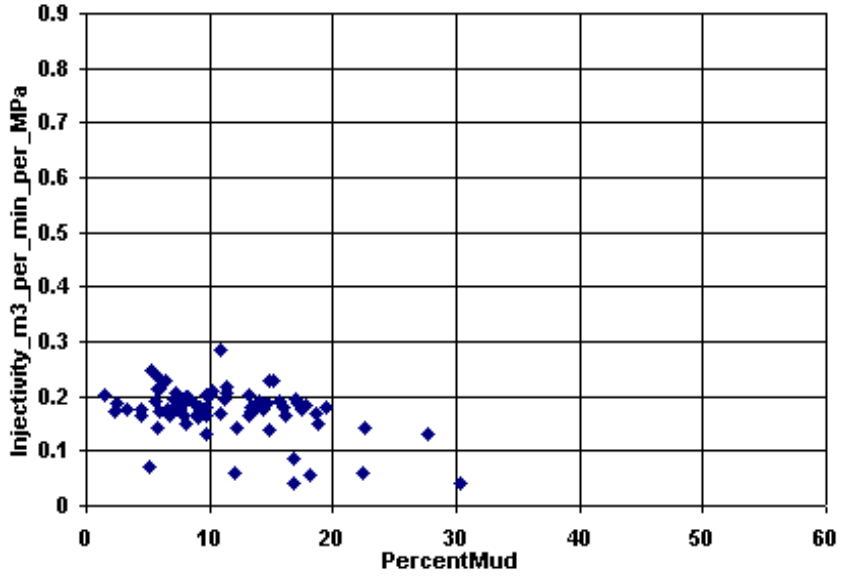

Figure 21: Injectivity vs. Percent Mud in Slurry

Figure 22 appears to show a very strong relationship between the injectivity and the sand percentage in a slurry. It appears that the injectivity is highest when the percent sand is less than 10%, with injectivity as high as 0.40 m^3/min/MPa. Above a sand percentage of 20%, the injectivity falls in a band between 0.10 and 0.20 m^3/min/MPa. This indicates that injectivity can be improved by using a slurry with a small amount of sand.

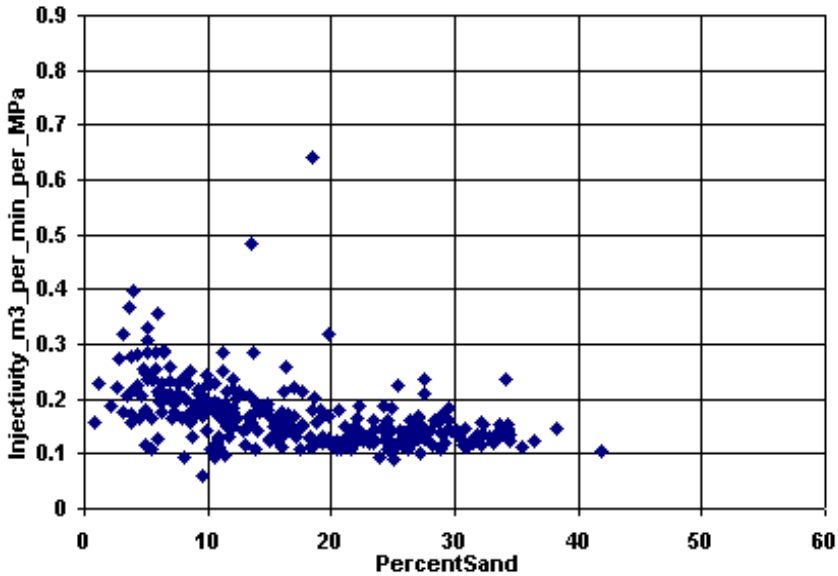

Figure 22: Injectivity vs. Percent Sand in Slurry

It appears in Figure 23 that there is no correlatable behavior between injectivity and the percent slop contained in the slurry. The broad band of data between 0.10 and 0.40 m^3/min/MPa, and the lack of a trend or envelope behavior indicates that injectivity is governed by factors other than the slop contained in the slurry.

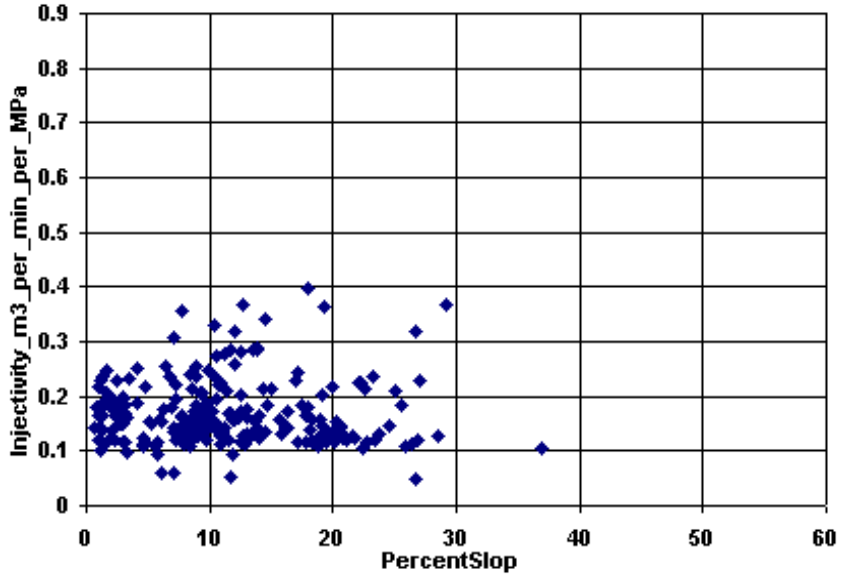

Figure 23: Injectivity vs. Percent Slop in Slurry

Effect of Viscosity on Injectivity and Permeability

Viscosity has also been correlated against slurry content. The following correlations were performed: viscosity vs. percent mud, viscosity vs. percent sand, viscosity vs. percent slop, and viscosity vs. percent materials. All show the same trend: up to about 20-30%, the viscosity is unaffected specifically by the component in question, but after this, the viscosity increases rapidly. An example correlation is shown in the following plot of viscosity vs. percent material (Figure 24):

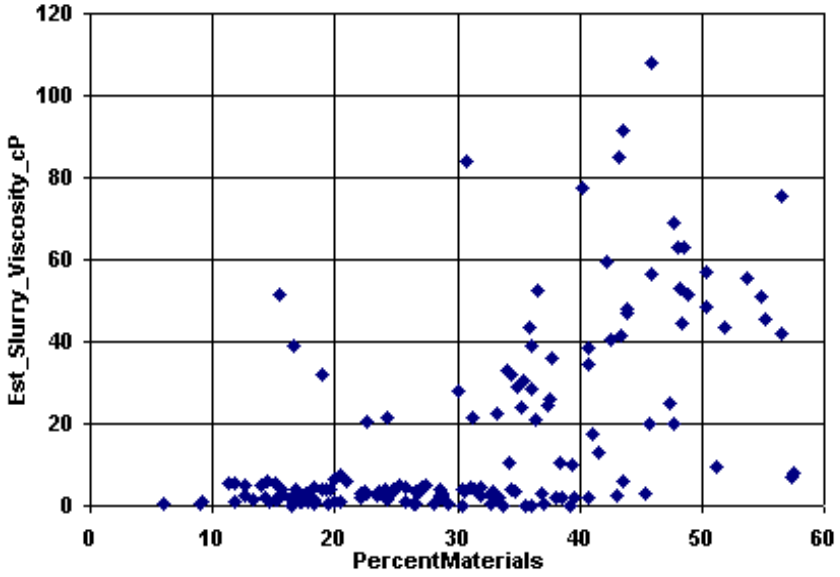

Figure 24: Slurry Viscosity vs. Percent Materials

The viscosities seem to be reasonable. The waste portion of the slurry has little effect on the viscosity until it reaches about 30% by volume; after this, average viscosity increases significantly. Now, it is of interest to see how viscosity affects permeability and injectivity. It is reasonable to expect high viscosity slurry to reduce injectivity. It would also be interesting to see the effect of viscosity on near-well permeability. Figures 25 and 26 show these correlations.

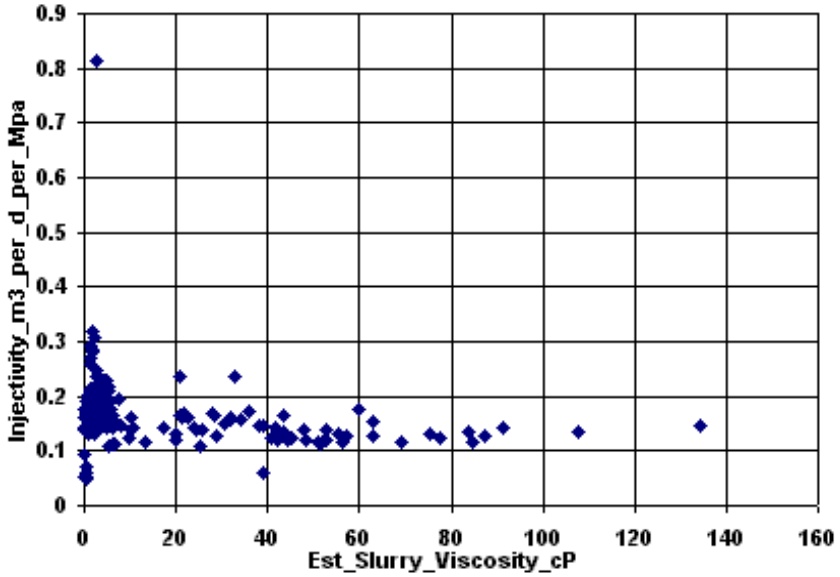

Figure 25: Injectivity vs. Slurry Viscosity

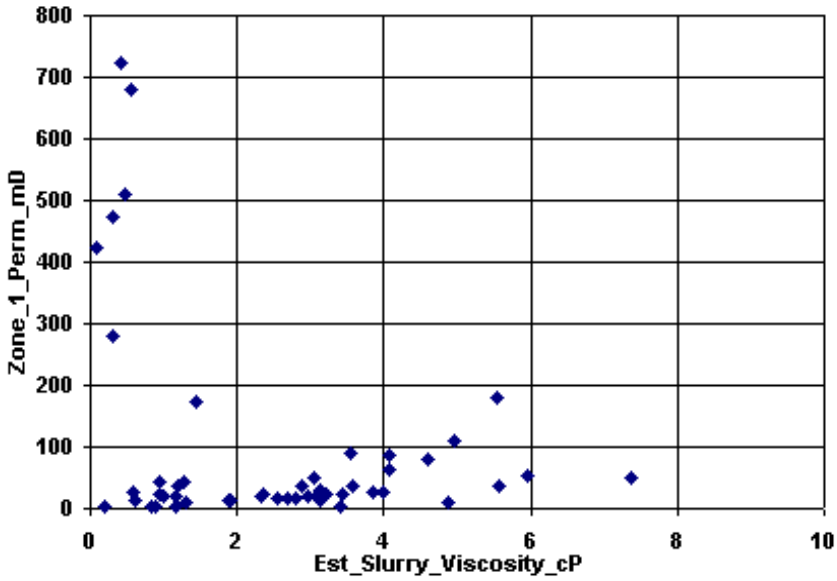

Figure 26: Near-Well Permeability vs. Slurry Viscosity

The expected behavior is seen in Figure 25; a high viscosity slurry will result in a low injectivity as it is more difficult to inject into the formation, whereas a low viscosity slurry is more easily accepted by the formation. Note that slurries with viscosity greater than 40 cP no longer have the capacity to further reduce the injectivity; it remains relatively constant after this point.

The expected trend is not seen in Figure 26. In fact, the trend seems to be opposite of what is expected. What is likely the case, however, is that on a day to day basis, the two parameters are unrelated, and the above trend is coincidental. Certainly, the continuous addition of slurry into the formation should reduce permeability over time, but on a given day, the slurry viscosity should not radically change formation permeability.

Effect of SFI Operations on Formation Permeability

At Terralog project TTI6, one of the components of the slurry was a thick, viscous mud-like material, actually a derivative of drilling mud with a small sand and water component. This was an unusual component; normal SFI slurry components are sand, slop (tank bottoms), and water. Mud injection mixed with sand and some slop was the primary make up of the slurry until September 12. Up to this period, there were difficulties in controlling bottom hole pressure, and it was suspected that the mud was starting to plug off the near-well formation. One of the strategies applied to solve the problem was the alternating injection of mud and sand (1-2 hour frequency) in hopes that the sand phase would break up the plugged off zone. The strategy, adopted on September 12 worked, and the bottom hole pressures dropped to acceptable levels. Clearly, the mud was causing a decrease in near-well permeability, and it is of interest to see if the permeabilities obtained from well-test analysis reflect this. Figure 27 shows the change in permeability with time at Terralog project TTI6.

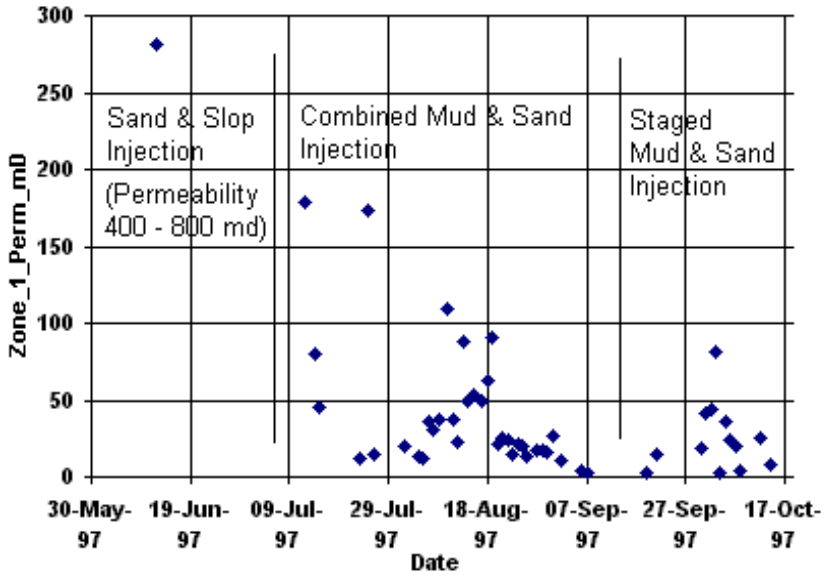

Figure 27: Near-Well Permeability vs. Time for TTI6

Starting on August 20, the permeability dropped significantly, indicating the beginning of plugging problems. The plot shows that the permeability recovered somewhat, shortly after the alternating mud-sand strategy was adopted on September 12. However, the mud apparently did enough damage to limit the permeability to 50 mD or less, whereas nearer to the beginning of the project, it was often 400 mD or more (these points not shown on plot).

Relationship between Permeability and Waste Material Percentage

Figure 28 is a plot of near wellbore permeability versus waste material percentage in the slurry. It can be seen that permeability occurs in a fairly even band between 1 and 100 md regardless of the waste percentage. Since most of the permeability analyses are from project TTI6, Figures 27 and 28 together tell us that the history of injections has a greater impact on permeability than the composition of slurry on any single day.

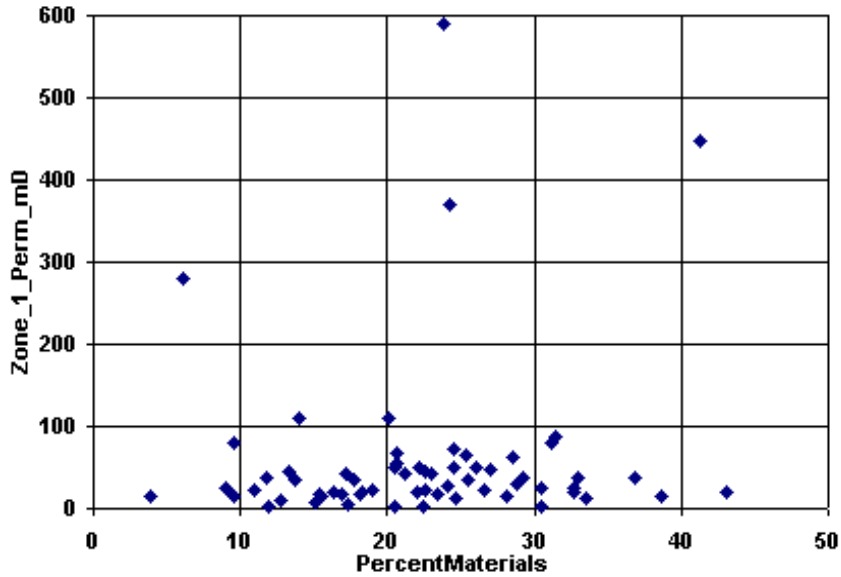

Figure 28: Near Wellbore Permeability vs. Percent Waste Materials

Relationship between Injectivity and Near Wellbore Permeability

Since injectivity and permeability both measure the ease of fluid flow into a formation, it would be expected that they should correlate well to each other. Unfortunately, when they are plotted against each other the answer is not so clear (Figure 29). Final judgement on this relationship should wait until more permeability data has been entered into the database.

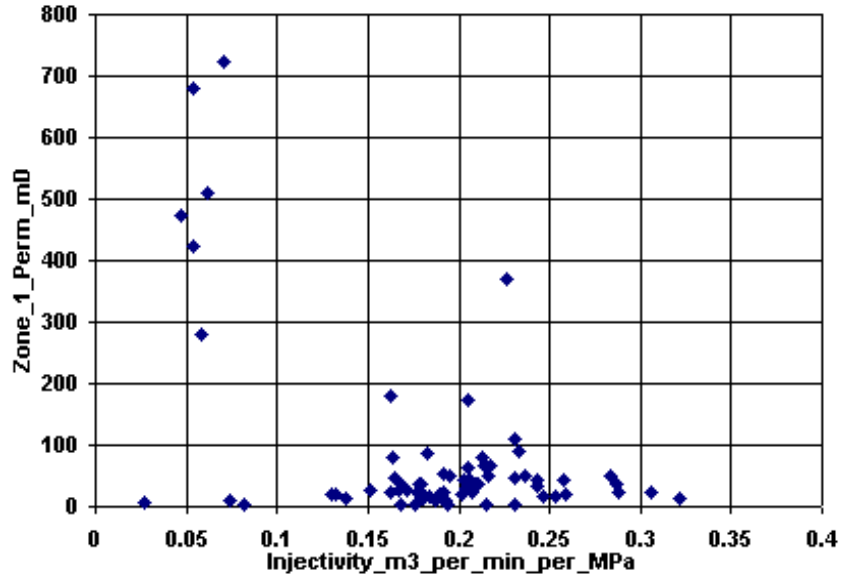

Figure 29: Near Wellbore Permeability vs. Injectivity

Effect of Injectivity, Viscosity, and Cum. Material on Growth Rate

This section deals with PKNLL growth rate and how it is affected by various parameters. It is expected that a high injectivity, which indicates that the formation is accepting fluids well, could result in longer fractures. Also, it is reasonable to suggest that high viscosity fluids will result in longer fractures, because there would be less leak-off of fluid through the fracture walls, and more fluid energy available to extend the fracture. Finally, the growth rate might change over time as material is continuously injected into the formation. These behavior mechanisms are investigated in Figures 30 through 32.

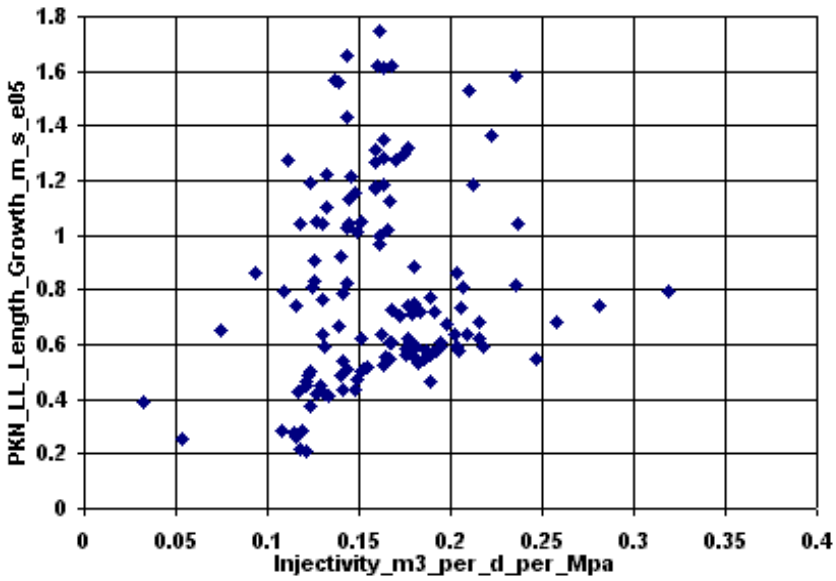

Figure 30: PKN Growth Rate vs. Injectivity

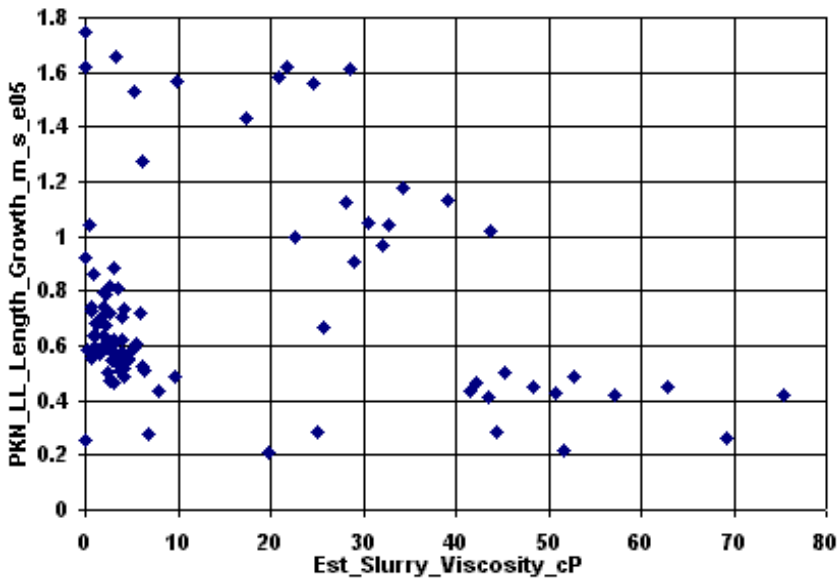

Figure 31: PKN Growth Rate vs. Slurry Viscosity

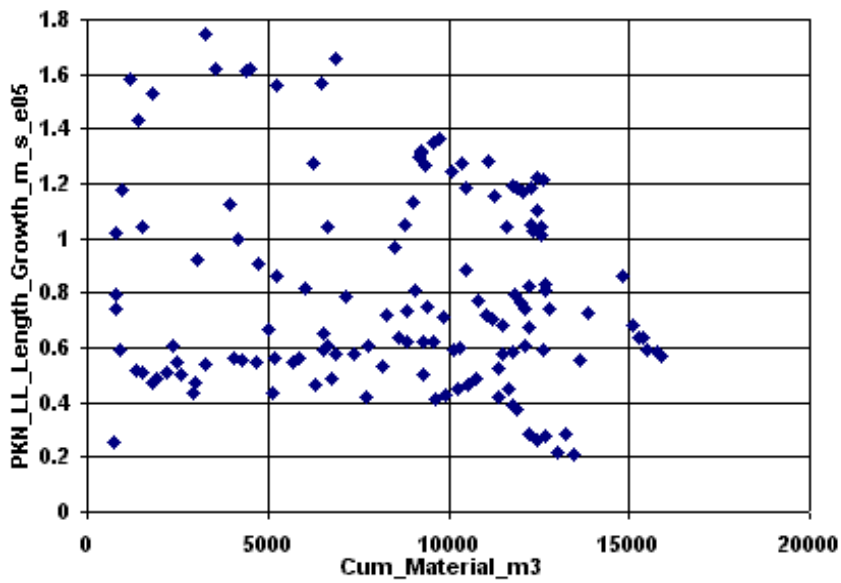

Figure 32: PKN Growth Rate vs. Cumulative Materials Injected

Figure 30 shows that a higher injectivity leads to faster fracture growth. In the case of a high injectivity, the formation is accepting the slurry well, because of the presence of a deeply penetrating fracture. In this sense, it is more prudent to say that a quickly growing fracture results in a high injectivity, rather than the opposite. Figure 31 does not show the anticipated trend. It is evident from the plot that higher viscosity fluids do not generate faster-growing fractures despite the inhibited leak-off. The reason may lie in the effect that viscosity has on injectivity. High viscosity tends to decrease injectivity (as seen previously in

Figure 25), and this indirect effect apparently has more influence on fracture development than does restricting fluid leak-off. Figure 32 indicates that fracture growth rate, in general, tends to decrease with the accumulation of slurry material in the formation. The trend is not strong, however, and might not be applicable to every project, as each has associated with them different operating conditions and formation properties.

Effect of Cum. Material, Growth Rate, and Closure on Shear Modulus

The following plots show how PKNLL shear modulus correlates with parameters such as cumulative material, PKNLL growth rate, and closure determined from well test analysis. It is reasonable to suggest that continuously packing waste into the formation would cause the local formation to become stiffer. This would be reflected by a large shear modulus developing over time. Also, it would be interesting to see whether or not a stiff formation results in fractures that are more difficult to extend. Finally, the stiffer the local formation is, the more difficult it should be to open a fracture, i.e., the higher the closure value. These relationships are investigated in Figures 33 through 35.

Figure 33 shows that the size (volume) of the waste pod does not influence how stiff the near-well formation becomes. The spike shown in the plot is actually from project TTI3. Wellbore failure was followed shortly after the spike in shear modulus occurred. Whether or not failure was a direct consequence of this is not yet fully understood.

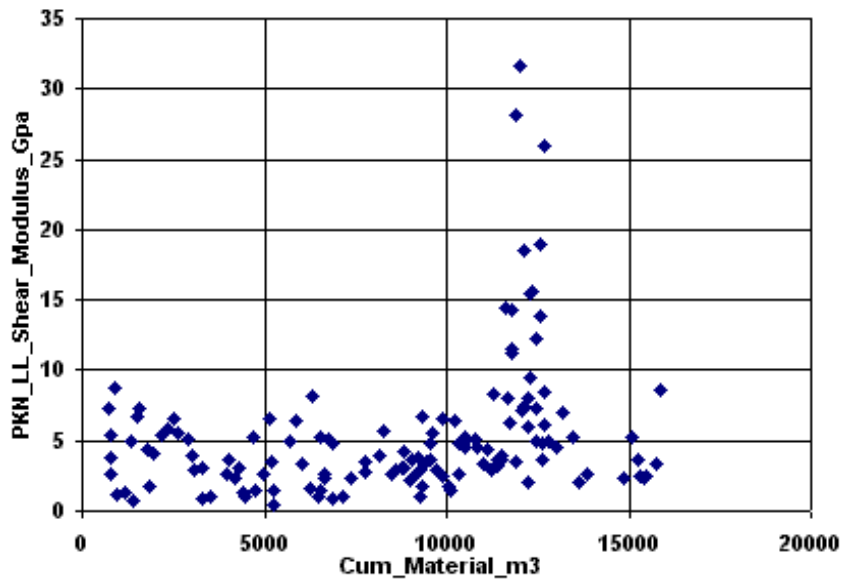

Figure 33: PKN Shear Modulus vs. Cumulative Materials Injected

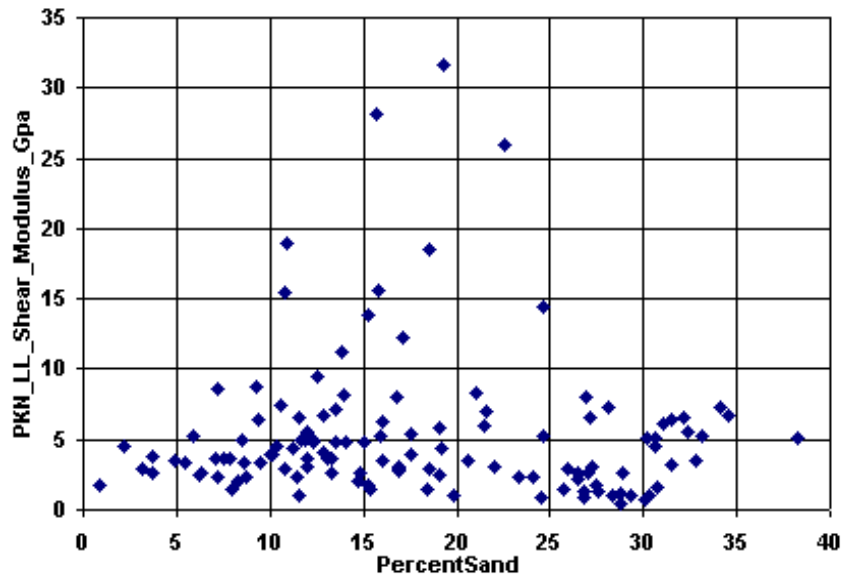

Figure 34: PKN Shear Modulus vs. Percent Sand in Slurry

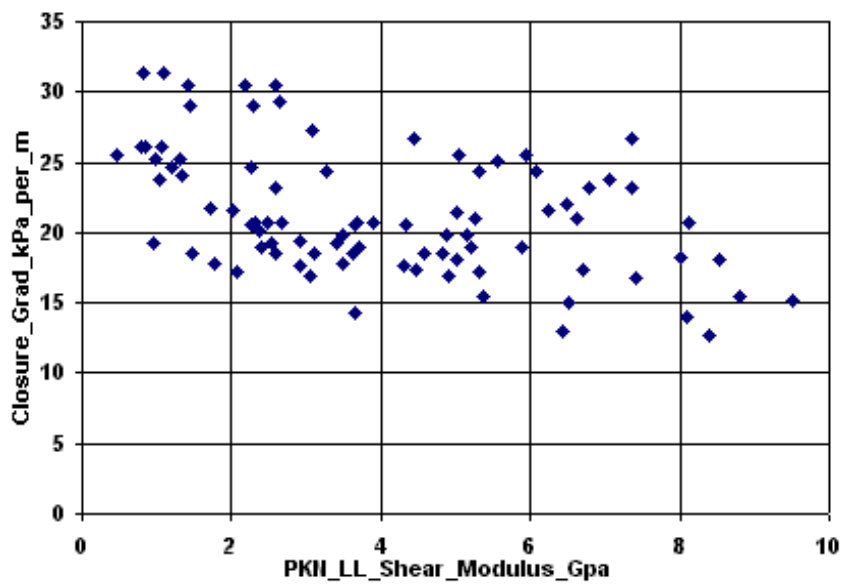

Figure 35: Closure Gradient vs. PKN Shear Modulus

Figure 34 indicates that formation stiffness is not changed in any particular direction by the sand content of the slurry. Figure 35 does not display the expected trend of increasing shear moduli causing increasing stiffness. Instead, it indicates that an increase in shear modulus results in lower closure values, i.e., fractures that open more easily.

The poor correlations demonstrated in Figures 31 through 35, and the fact that they are somewhat inconsistent with physical expectations, suggests that linear elastic fracture models have only limited usefulness in analyzing high volume injection in soft media. This provides further motivation to investigate alternative modeling and diagnostic techniques, as described later in this report.

Summary of Correlations

A summary of the correlations presented in this report is given in Table 7. A "positive" trend indicates a correlation between variables that is increasing, a "negative" trend indicates a correlation between variables that is decreasing, "no trend" indicates that the two variables are independent of each other, and "uncertain" indicates that a judgement cannot be made given the available data at this time.

The following general observations can be made based on the correlations discussed in this report:

- Closure pressure gradient tends to increase slightly as wastes accumulate in the target formation.
- On a daily basis for individual projects, however, there is little correlation between closure gradient and percent waste material.
- Injectivity has a distinctive maximum envelope that is highest for low percentages of waste material and sand. Mud and slop percentages appear to have no impact trend on injectivity.
- Near well permeability reflects the impact of accumulating materials and material injection strategy into a formation, but is not dependent on the daily changes in slurry composition.
- Injectivity appears to be more closely related to fracture growth than it is to formation permeability.

Table 7. Summary of Correlations Investigated

Figure	Relationship	Observed Trends
8	Closure gradient vs cumulative materials	Slight positive
9	Closure gradient vs cumulative sand	Slight positive
10	Closure gradient vs cumulative mud	No trend
11	Closure gradient vs percent materials	Slight positive
12	Closure gradient vs percent materials for TTI6	No trend
13	Closure gradient vs percent materials for TTI7	No trend
14	Closure gradient vs percent mud	Uncertain
15	Injectivity vs cumulative material volume	No trend
16	Injectivity vs percent materials	Negative envelope
17	Injectivity vs percent mud	No trend
18	Injectivity vs percent sand	Negative envelope
19	Injectivity vs percent slop	No trend
20	Slurry viscosity vs percent materials	Uncertain
21	Injectivity vs slurry viscosity	Negative envelope
22	Near well permeability vs slurry viscosity	Uncertain
23	Near well permeability vs time for project TTI6	Related to sand-mud strategy
24	Near well permeability vs percent materials	No trend
25	Near well permeability vs injectivity	Uncertain
26	Wellbore storage vs injectivity	Positive (?)

27	PKN growth rate vs injectivity	Positive
28	PKN growth rate vs slurry viscosity	Slight negative
29	PKN growth rate vs cumulative materials	Uncertain
30	PKN shear modulus vs cumulative materials	No trend
31	PKN shear modulus vs percent sand	No trend
32	Closure gradient vs PKN shear modulus	Negative

A comprehensive database of waste injection operations has been assembled and evaluated. This database can now be used by operators to evaluate potential influences of operational changes on injection and formation response in order to optimize operations. It also provides some insight into large scale slurry injection in high porosity media. Some of the observed trends are consistent with expectations. Some are not, however. For example, closure gradient does increase with cumulative materials over time, but is not particularly sensitive to daily changes in slurry composition. Injectivity appears to be more sensitive to sand concentration then to slop concentration. These types of observations are useful to guide future operations.

In addition to providing insight on basic operating strategies, the database is also useful to evaluate existing and new fracture modeling and diagnostic techniques. In the current work, for example, we have modeled fracture propagation with a traditional Perkins-Kern-Nordgren analytic approach. With this model neither fracture growth nor shear modulus appear to correlate well with cumulative waste injection or slurry concentration. Closure gradient seems to actually decrease with shear modulus. These observations are not consistent with physical expectations, suggesting that linear elastic fracture models cannot adequately explain the behavior of large-scale waste injection in very soft, porous media. Improved model and diagnostic techniques are required, as discussed in the following sections of this report.

FIELD OBSERVATIONS

Our review and analysis of waste injection projects in Canada and the United States has led to a number of critical observations which distinguish large-volume fracture injection from typical short-term fracture stimulation. Some of these observations include:

1. In-situ stress, near wellbore permeability, and formation and fracture behavior vary with time.
2. A single fracture does not take all the waste. Instead, multiple fractures at varying orientation are created during repeated injection episodes.
3. Formation response, including injectivity and stress relaxation, can be controlled by varying waste injection properties.

There are some general, long-term changes in formation response with cumulative injection, such as the gradual increase in average closure stress illustrated in Figure 12. However, there are also daily fluctuations in formation response. For example, Figure 36 presents a summary of net pressure (defined as bottom-hole injection pressure minus closure pressure) and shut-in pressure behavior for four sequential days of waste injection. The data illustrate that net pressure increased and subsequent shut-in pressure declined less rapidly for injection episodes 1, 2, and 3. On the 4th day of injection, however, the net pressure and shut-in behavior declined and returned to conditions observed for injection cycle 1. We interpret this as a gradual buildup of stress and decrease in near wellbore permeability as more material is sequentially packed into the same process zone, followed by a breakthrough to a new process zone and return to initial conditions.

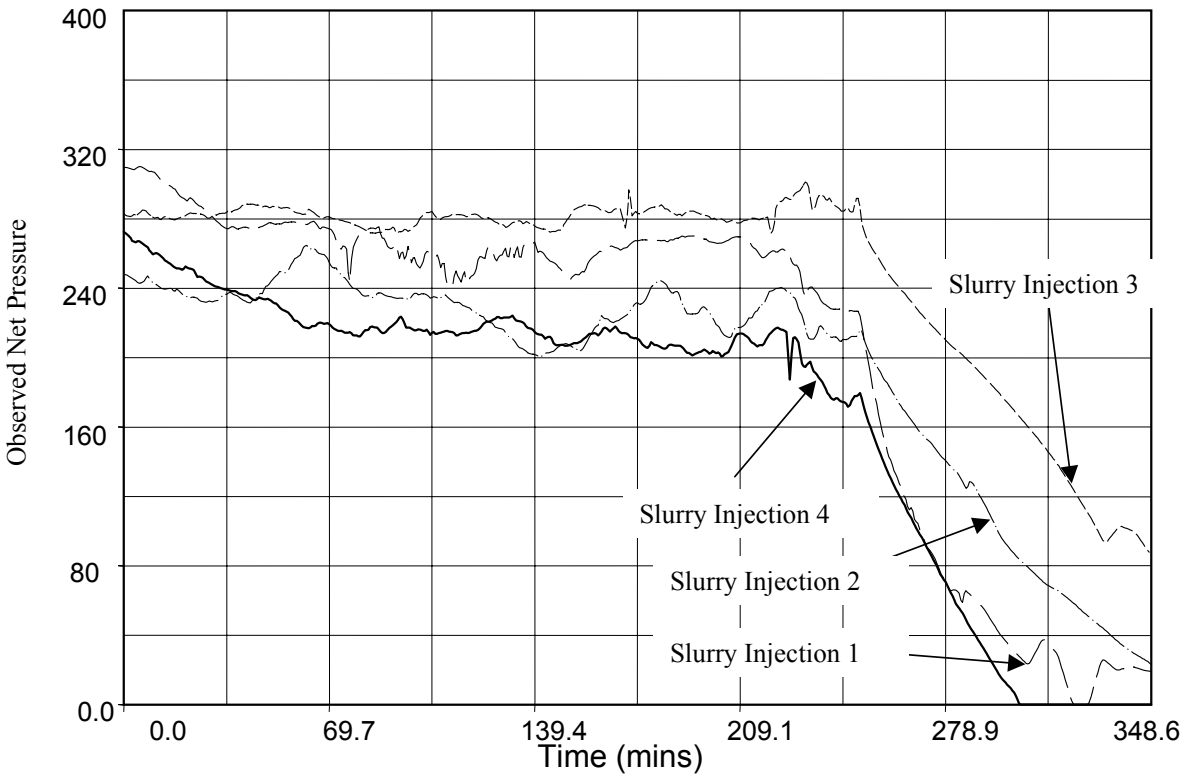

Figure 36: Varying net injection and shut-in pressures for sequential injection episodes.

In many instances breakthrough to a new process zone is accomplished not by simple fracture extension, but by generation of a new fracture at a different orientation. For example, Figure 37 presents data on changing fracture orientation, as measured with surface tiltmeters, during one week of repeated injection episodes at project TTI 4. Such fracture re-orientation can often (although not always) be correlated with changing net pressure and closure stress, as illustrated in Figure 38.

Recognizing this apparent tie between stress buildup, permeability and leakoff reduction, and eventual fracture re-orientation, one can then monitor formation response and sometimes modify injection operations to access new process zones, thereby increasing or maintaining injectivity without sustained increase in shut-in pressure. For example, Figure 39 presents an example in which relative ratios of mud and sand were varied in order reduce shut-in pressures while maintaining moderate injectivity.

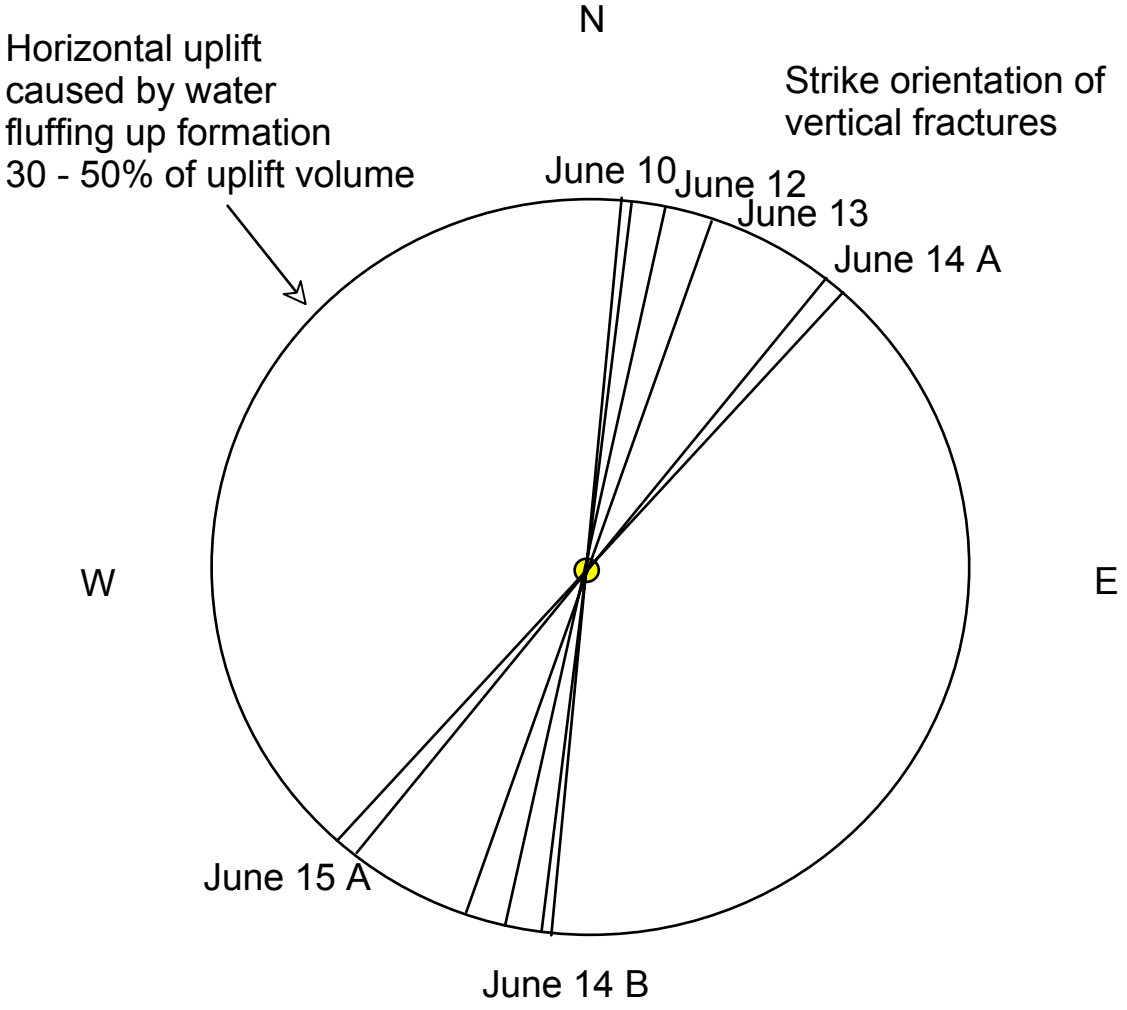

Figure 37: Fracture re-orientation during sequential injection episodes at project TTI 4

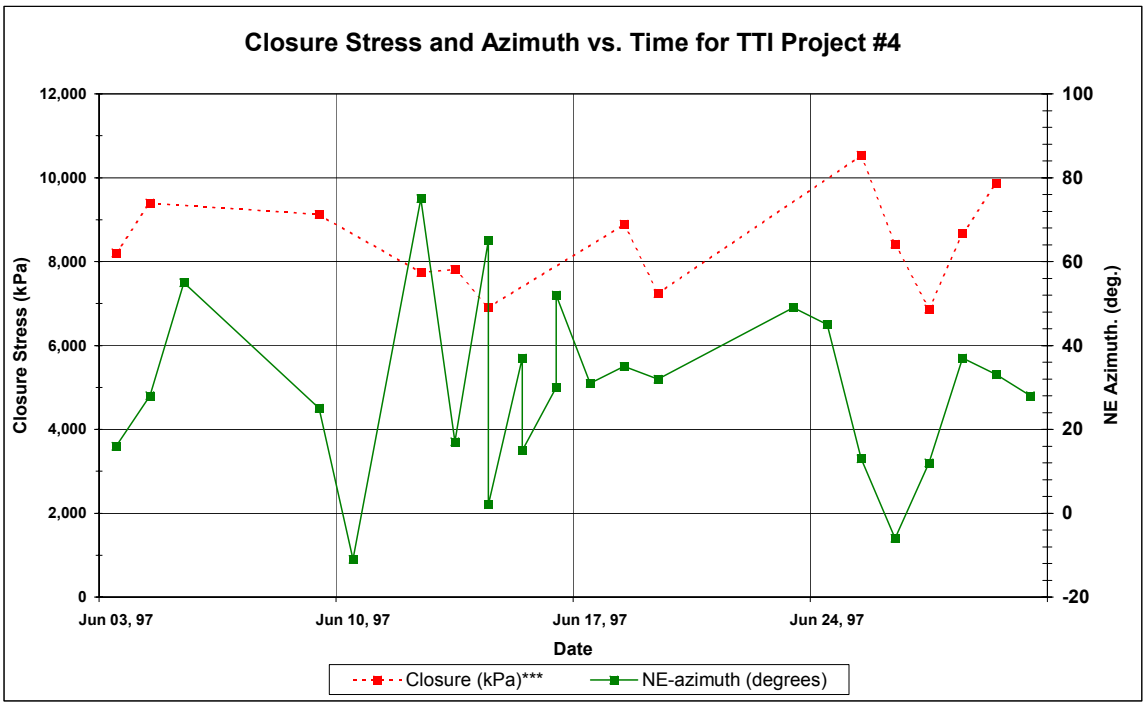

Figure 38: Closure Stress and Azimuth vs. Time for Project TTI 4

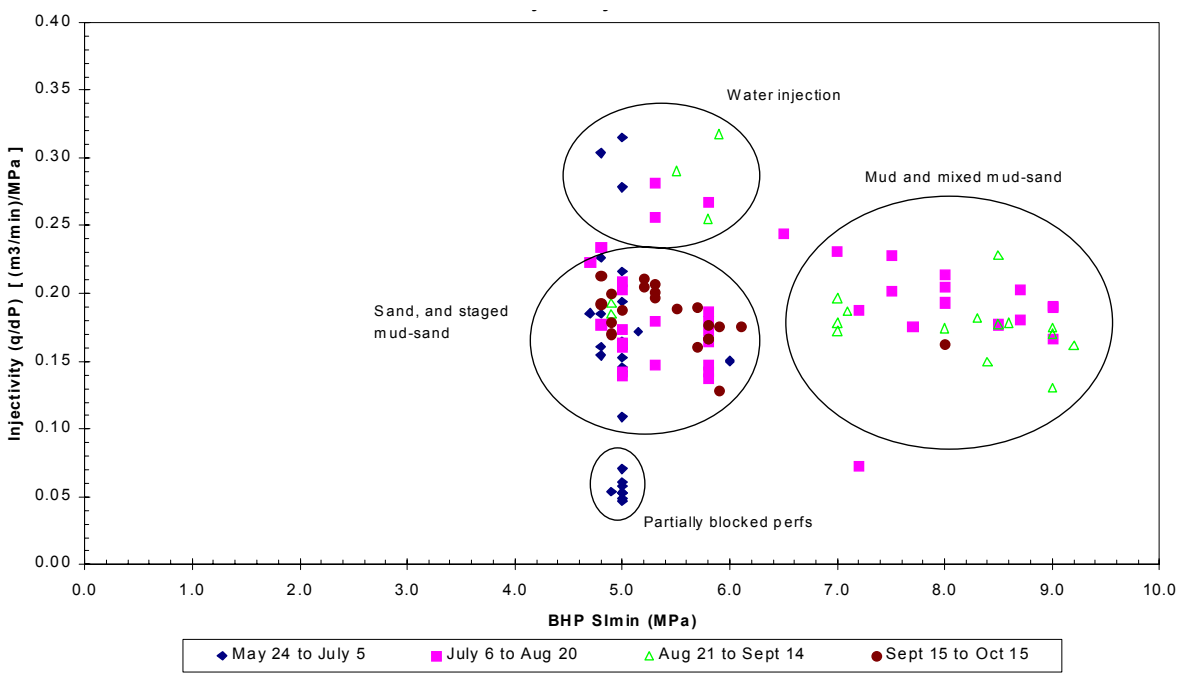

Figure 39: Injection scheme can be modified to maintain injectivity and improve pressure decline after shut-in

FRACTURE MODELING CONSIDERATIONS

It is clear from observed fracture and formation response during SFI operations that large-volume waste injection into very porous media results in volume dependent changes in stress, permeability, and fracture orientation. Such phenomena are not captured in current fracture models, which are based on physical assumptions for single, discrete, brittle fracture propagation. The key differences between large-volume waste injection in high porosity media, and typical hydraulic fracturing for stimulation purposes can be summarized as follows:

1. Large-scale dilation and inelastic deformation takes place in the soft media, so that a generalized parting and thick dilation zone is created rather than a thin, discrete, brittle fracture;
2. Because the sands can sustain little shear stress, fracture toughness and linear elastic fracture mechanics are not relevant. Rather, the process is controlled by large, inelastic deformation mechanics;
3. The particle size and permeability of the injected material is typically less than that of the formation material, in contrast to hydraulic fracture "proppants" which are inherently designed to create fractures of enhanced permeability;
4. The result is that subsequent injection is not pre-disposed to simply extend existing fractures, but rather to either create a new fracture within the existing low permeability "waste pod", or at a new orientation into zones of lower stress.

In order to properly capture these phenomena which are unique to waste solids injection in high porosity media, new modeling approaches are required. In the following sections of this report we first briefly review the current state-of-the art of fracture modeling and describe their limitations, and then we discuss our investigation of alternative techniques.

State of the art of fracture models and their limitations

A robust engineering simulation of a process requires that at least the first-order physical processes are included in the simulation. (First-order processes are those that can affect the results by 10% or more.) In hydraulic fracturing, the two major sets of physical processes are fluid hydraulics, all fluid processes with viscous energy dissipation including porous media flow and proppant transport; and geomechanics, the stress-strain-strength behavior of the rock mass. This introduction briefly describes specific aspects that must be accounted for in fracturing, with focus on geomechanics.

Intrinsic Fracture Resistance

It is often assumed that the resistance to fracture propagation afforded by fracture toughness at the advancing tip is an important aspect of fracturing. This may be true for early fracturing stages in a rock with substantial tensile strength. However, at a large scale, most reservoir rocks have joints and fissures, so that the macroscopic fracture toughness is minimal. Similarly, unconsolidated sandstones offer no resistance to tensile parting. Furthermore, when a fracture is long, even a small increase in pressure within the fracture can bring a large tensile stress concentration to the fracture tip, so large that any tensile fracture propagation resistance becomes minimal. Apparently, the role played by intrinsic fracture propagation resistance is minimal once the fracture has propagated away from the borehole region ($L > 10\text{-}20D$, where D is the diameter of the borehole). Current semi-analytical fracture mechanics models either assume an unreasonably high tip resistance and a sharp fracture termination, or else the model is

based on elliptical equilibrium fracture shapes (the Sneddon crack) where a tip resistance is not part of the model, only a geometry based on volume balance.

Tip resistance serves a useful function in several versions of fracture simulators; it allows the mathematical problem to be treated as a static solution, with stability afforded by the tip resistance. All simulators of hydraulic fracturing are in fact serial solutions to static equilibrium problems, there is no such thing as a truly dynamic simulation. If tip resistance is disallowed on physical grounds, then this version of simulator cannot achieve a solution. Many have argued that there is a "process zone" in advance of a fracture tip, and this "process zone" is a region that affords resistance to propagation through some strange "clamping stress" or "back stress", purportedly arising through shear dilation or other processes. These arguments are all physically suspect, and it is hard to imagine a granular material such as an unconsolidated sandstone behaving as a metal or a dense (low porosity) limestone where substantial bond strengths must be overcome.

The issue of tip resistance in models that use it remains physically ill-defined, and some recent research simulators have been developed to overcome this restriction.

Shearing Resistance, Dilation

Currently, no fracture models in commercial use account for the shear behavior of the rocks (Mode II fracture; the opening mode is called Mode I fracture). In fact, other than a function that allows a tip resistance to be calculated in some models, there is no provision whatsoever for Mode II under conditions of high shear stress and elevated pore pressure. The basic assumption, therefore, is that the flanks of the fracture are very strong, and cannot shear or exhibit dilation. Figure 40 presents a picture describing Mode II fracturing, and shear energy dominance over Mode I fracturing, in soft, weak rocks.

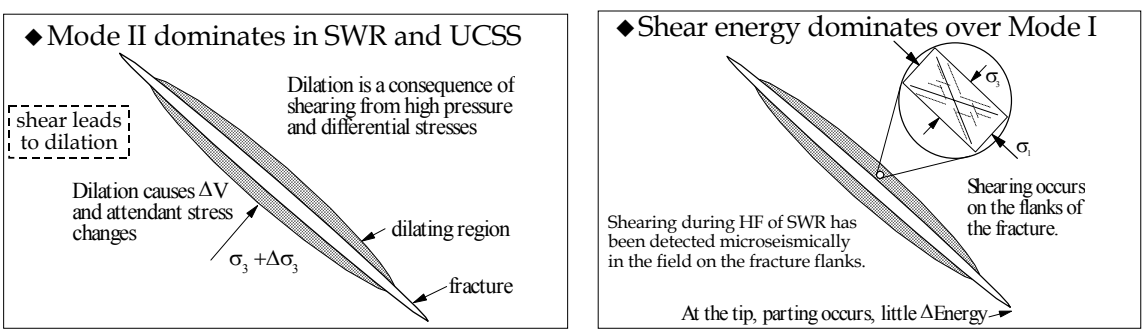

Figure 40: Mode II fracturing in SWR (soft weak rocks) and UCSS (unconsol. sandstones)

Hydraulic fracturing processes in unconsolidated or poorly consolidated sandstones and in highly jointed (fissures) rock masses show clearly that there is a great deal of shearing taking place on the flanks of the fracture. This has been demonstrated by microseismic monitoring *in situ*, showing that shearing events cluster along the flanks of the fracture, not at the tip. Discrete element simulations (2-D) show that dilation occurs on the flanks of the fractures. It is relatively easy to argue from a purely physical basis that the elevated pore pressures generated near the wellbore during hydraulic fracturing reduce the effective stresses to the point of dilation and shear. The argument for the case of poorly consolidated sandstones and highly fractured reservoirs, can be stated as:

- Hydraulic fracturing requires high pressures, therefore, near the well, $p_f > \sigma_3$ (pore pressure is greater than minimum principal stress)
- Except in cases where polymers, solids or oil block pores, this leads to a condition within the fracture wall where the effective confining stresses approach zero
- There is invariably an anisotropic stress field in the ground ($\sigma_{Hmax} > \sigma_{Hmin}$)
- So, as pressure rises and effective stress (σ') drops, deviatoric stress leads to dilation and shearing
- Energy consumption from shear and dilation is far greater than tip processes
- Depending on permeability and the nature of the fracture fluid, the elevated pore pressures propagate outward from the fracture plane, therefore the dilation and shearing process also propagates outward from the fracture plane.
- Dilation tends to close the fracture (increase in closure stress, σ_{Hmin}), thus p_f must rise slowly to counteract this closure.

In addition to shearing, energy dissipation, and dilation, another important effect that occurs during fracturing is this: the increase in pore pressure ($p_f\uparrow$) that causes a drop in the effective confining stress normal to the fracture ($\sigma'_3\downarrow$) causes a <u>volume increase</u> in the rock near the injection point because of the compressibility effect ($\Delta V = -C_c \cdot \Delta\sigma'$, where C_c is elastic compressibility). However, the increase in p_f leads to a <u>volume decrease</u> in the far-field, because of an increase in the distant effective stress where the elevated pore pressures do not reach. In general, these effects are not accounted for in hydraulic fracture simulators. Figure 41 pictorally describes the concept of the drop in confining stress (poroelastic effect).

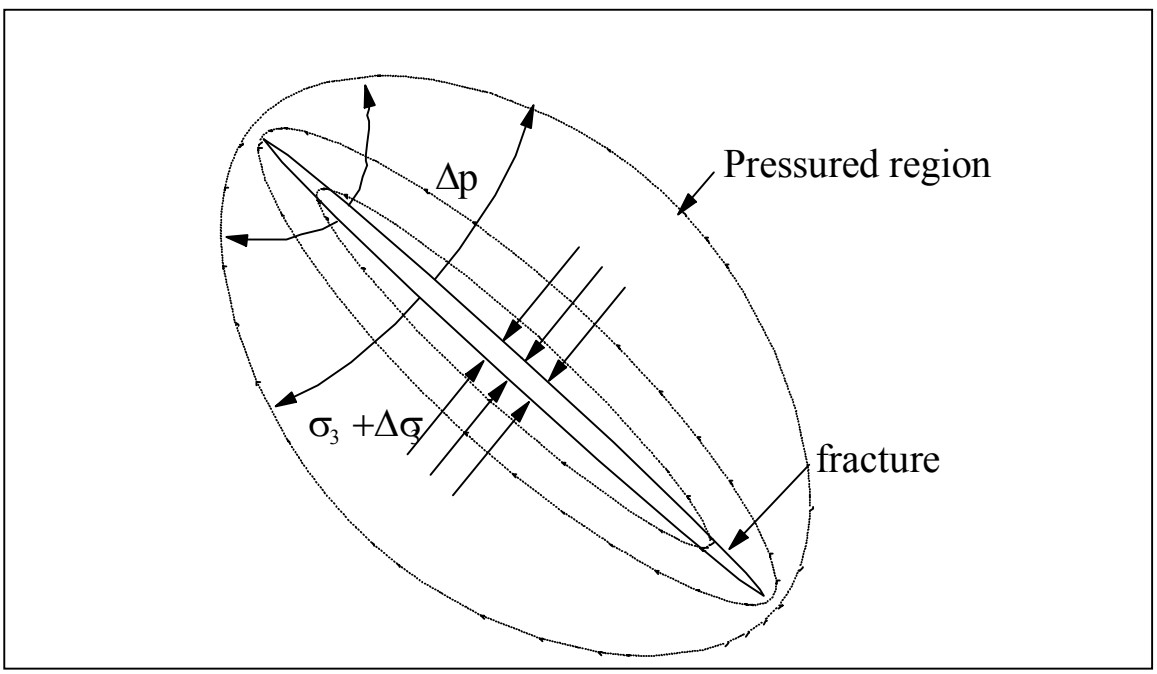

Figure 41: The poroelastic effect

Pore Pressure and Bleed-Off

In all semi-analytical hydraulic fracture simulators, there is a leakoff coefficient, usually a function of the square root of time, that stipulates how much of the liquid enters the porous medium and how much remains in the fracture, giving the volume potential to propagate the fracture an additional distance. The leakoff behavior will change if more viscous fluids that can build a filter cake are used. (For example, it is widely believed that if fracturing is carried out with a high content of heavy oil or waste emulsion, this material forms an almost impermeable skin on the fracture, reducing the bleed off coefficient to almost zero.) Any liquid entering the formation is assumed to "disappear", in terms of any potential to change the effective stresses or volume (see above).

This shortcoming is extremely difficult to overcome in a rigorous manner in a simulator. Ultimately, it appears that the only way is to move toward a fully coupled 3-D finite element approach. All other methods have deficiencies that lead to an incomplete coupling between hydraulic and geomechanics processes, or are excessively linearized so that processes such as shearing or skin development cannot be incorporated except in a purely empirical manner.

Natural Stress and Properties Differences

There is now conclusive evidence that, in addition to the differences in material properties among beds being intersected by a hydraulic fracture, there are differences in the lateral stress (σ_{Hmin}) that are large enough to affect fracture propagation. For example, if an overlying bed has a particularly low value of σ_{Hmin}, fracture containment will be problematic, because as soon as the fracture contacts the low-stress bed, growth only in that zone is favored. On the other hand, containment will be excellent in cases where the horizontal stress in the overlying bed is larger than in the target bed.

Any fracturing model based on a Sneddon crack, a Barenblatt crack, or similar semi-analytical or integral solutions, cannot handle these issues of stiffness and stress differences. They can only be handled by a finite element (or perhaps a modified boundary element) formulation that permits different stresses and properties to be introduced as initial and boundary conditions.

Numerical "pseudo-3D" simulators, such as Fracpro or M-Frac which do attempt to include heterogeneous material properties and stress fields, must deal with generally poor knowledge of initial stress and stiffness conditions. Geophysical log data provide some constraints to the choice of stresses and material properties, but in general, there remains considerable uncertainty. There is no easy or economic way of overcoming these difficulties in defining the system conditions, and the effects can easily be first order (>10% effect on the "predictions"). This places a real limit on simulation "precision".

Pressure, Stress Gradients and Fracture Rise

Consider a static but open vertical fracture induced with water in a material with a low permeability. The pressure gradient in the water is ~10 kPa/m (γ_w); however, the gradient of the lateral stress ($\sigma_{hz} = d\sigma_3/dz$) is usually about 17-24 kPa/m (depending on tectonic and geological burial history). This means that if the vertical fracture is maintained open at the injection point by a pressure $p_f \sim \sigma_3$, there is an excess driving pressure at the upper tip of $Z_u \cdot (\sigma_{hz} - \gamma_w)$, where Z_u is the vertical open fracture height above the injection point, and a deficient driving pressure of $-Z_d \cdot (\sigma_{hz} - \gamma_w)$ where Z_d is the vertical open fracture height below the injection point. Therefore, fractures tend to rise, and any tendency to drop tends to be

over-ridden by this gradient effect. The effect is greater in gas filled fractures (γ_g is very small), less so if dense slurries are used for fracturing. Clearly, this effect will also tend to cause "horizontal" fractures (where $\sigma_v = \sigma_3$) to rise at some angle; because this rise angle is at an angle to the principal stresses, high shear stresses will be generated in advance of the rising tip. These effects are known to be large enough to lead to shear of cased wellbores that are unfavorably located with respect to the fracture plane (e.g. Amoco Gregoire Lake).

Simulators based on semi-analytical or integral solutions do not incorporate these effects. In particular, for the case of "quasi-horizontal" fractures that rise at shallow angles (10º - 30º) away from the injection points, there are shear stresses that develop that are so large that shearing must occur along bedding planes or interfaces between zones of different cohesions (generally below shale beds). As mentioned before, perhaps the only method of incorporating this behavior is with a fully coupled finite element analysis approach.

Changes in Fracture Direction

"Quasi-horizontal" fractures can change their dip as they rise and interact with bedded strata of different properties. Fractures propagating through a medium with weak joints but a strong matrix (e.g. a dense but jointed limestone or sandstone) will follow local propagation paths dictated by the presence of the joints, although the large-scale (macroscopic) fracture direction will still be approximately normal to σ_3. It is generally acknowledged in this case that predictions are not substantially affected by local changes in fracture direction, as long as the overall macroscopic fracture plane is normal to σ_3.

However, there is another very important aspect of direction changes. Consider a vertical fracture in a material that has no significant fracture toughness, such as poorly consolidated sandstone. As a fracture grows in length during active injection, it must also grow in aperture. This increases the "reaction" stress ($\sigma_3\uparrow$) and eventually leads to a condition where it is clearly easier to propagate from the borehole in another direction. Such changes in fracture direction are well known from measurements of deformation at the surface and flow at depth. No simulator can handle this behavior properly, as it is extremely sensitive to other factors such as dilation, shearing, and so on.

Status and Future of Fracture Simulations

There is a basic difficulty in all petroleum geomechanics problems, but particularly for complex ones where there is full hydraulic coupling to stress changes (as well as coupled diffusion processes and temperature changes if hot or cold fluids are used). It is impossible to determine all the boundary conditions and material properties with sufficient accuracy to account rigorously for all the phenomena outlined above. This gives rise to a number of options:

- Treat the hydraulic fracturing problem purely empirically, using models that we know are seriously incomplete, but that appear to be robust enough to handle the great majority of cases, with careful calibration.
- Continue the development of full 3-D finite element simulations, accounting for the various factors of non-linear behavior and material properties, while simultaneously trying to improve our knowledge of those boundary conditions and material parameters.
- Try to develop models in new directions, such as boundary element methods that can handle only some degrees of non-linear behavior, but can handle issues such as pressure gradients easily, or discrete element models that can clearly simulate physical processes better, but may be limited in the size of problems that can be analyzed.

Fracturing in weak materials, particularly where there are processes such as fracture skin development, shearing, fracture direction changes, dilation, permeability changes, and so on, is sufficiently complex that the following approach to simulation is the most rational one available:

- Carefully assess the impact of various processes, and use a hydraulic fracture simulator that is as simple as possible, given the perceived dominant processes.
- Use the simulator in a parametric mode to explore a range of reasonable conditions that could happen in situ.
- Take monitoring information (BHP, surface deformation, pressure decay after fracturing, etc.) to try and understand what is happening and whether the effects are rational, compared to the physical predictions of the hydraulic fracture simulation.
- Improve the simulator predictions as much as possible through "calibration" all the while recognizing the limitations of calibration and fitting if the basic simulator does not have all of the relevant physical processes incorporated in it.
- Apply a "common-sense" filter to the data and the simulations, and then, use the simulator as a predictive tool for future jobs in the same reservoir or conditions.
- Do not try to push this process too far, in terms of rock properties, stresses, etc.
- Continue some development of other simulation approaches in a research mode.

With these thoughts in mind, and taking into account recent field observations compiled through this project, we describe several alternatives to modeling in the following sections of this report.

MODELING AND DIAGNOSTIC INVESTIGATIONS

Our observations of fracturing and formation behavior during large-volume waste injection operations suggest a new physical model for episodic injection. When a vertical fracture is first induced in a virgin reservoir, its tendency will be to open against the least regional principal stress, σ_3, and extend in length parallel to this direction. During slurry fracture injection, the stream of waste slurry being pumped into the formation causes a fracture to open and material to dilate around the fracture, or within a "process zone". The waste becomes trapped in the formation when pumping stops and the fracture and dilation zone closes. The fluid component of the slurry will bleed off. The solid component of the slurry is left behind.

This large amount of solids packing the fracture and dilation zone alters formation properties and behavior. The stresses within the process zone increase and the permeability within the process zone decreases. Subsequent injection episodes will then cause fractures to break through the waste pod, in a direction still parallel to σ_3, but with increasing difficulty. This is indicated by increased net pressure and less rapid pressure decline after shut-in, as illustrated in Figure 4. The minimum stress within the waste pod increases and, eventually, fracture re-orientation away from the σ_3 direction occurs. The general process is illustrated schematically in Figure 42.

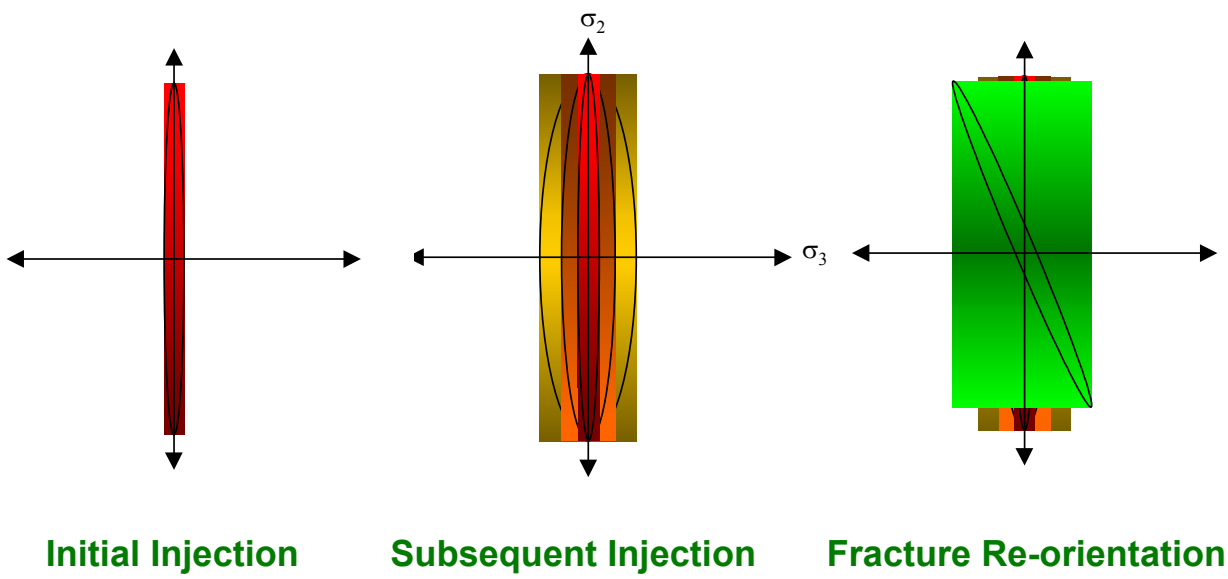

Figure 42: Fracture re-orientation due to stressing of waste pod

We consider here a relatively simple model to account for such a "packing effect" as a waste pod grows with continuous solids injection. We assume that a waste pod initially grows in the the preferred direction of fracture orientation (i.e., perpendicular to σ_3). The growth of the waste pod induce increases stress (ΔP) on the system acting in the direction of σ_3. We can define a compressibility relationship as follows:

$$C = \frac{1}{V}\frac{\Delta V}{\Delta P} \qquad [8]$$

where V is the effected volume around the fracture, or within the process zone. For example, we might consider a cylindrical volume around the fracture where $V = H \cdot \pi L_1^2$. H is the constant height of the fracture and L_1 is the half-length of the largest fracture to have developed in the primary direction before deviation occurs). C is the compressibility of the sand formation and waste. The term ΔV is the cumulative volume of the waste pod before deviation occurs (effectively, the perturbation inflicted upon the system). The term ΔP represents the increase in stress of the system due to the perturbation (ΔV), and represents the amount by which σ_3 increases. We assume that until the point of deviation, episodic fracturing always occurs with the same orientation as the waste pod. It is also assumed that the compressibility of the waste material is equal to the compressibility of the surrounding formation.

Initially, the half-length L_1 of the fracture could be determined by PKN large leak-off theory:

$$L_1 = \frac{\frac{1}{2} q\sqrt{t}}{\pi C h} \qquad [9]$$

where q is the average volumetric slurry injection rate for the injection episode; t is the duration of the injection episode, C is Carter's leak-off coefficient (units $L/T^{1/2}$), and h is the fracture height. For our purposes here, we assume that the fluid component of the slurry completely leaks off into the formation without increasing pore pressure, and the remaining solids component of the slurry forms the linear waste pod as described above. The formation is stressed by the factor ΔP in equation [8] in the direction of σ_3. As the cumulative volume ΔV increases, ΔP increases.

We can propose that the maximum deviation of the fracture from the primary orientation is the angle θ. We can determine a potential deviation angle θ by comparing the increased stress in the waste pod perpendicular to the initial fracture orientation, $\sigma_3 + \Delta P$, to the normal stress on a deviated fracture angle caused by the unperturbed far-field stresses.

$$\sigma_3 + \Delta P = \sigma_3 \cos^2\theta + \sigma_2 \sin^2\theta \qquad [10]$$

Equation [10] can be solved for θ, with the following result:

$$\theta = \arccos\left[\sqrt{\frac{(\sigma_2 - \sigma_3) - \Delta P}{(\sigma_2 - \sigma_3)}}\right] \qquad [11]$$

This represents the maximum angle of deviation of a fracture from the preferred orientation, for any given ΔP.

Figure 43 presents a plot of the change in fracture orientation with the cumulative addition of solids in the formation based on Equation [11]. "Stress Ratio" is the ratio between the maximum and minimum horizontal stresses. For example, typical horizontal stress ratios for Western Canada are on the order of 1.5. As shown in Figure 8, when the initial stress ratio is small, the addition of small volumes of solids to the waste pod will cause fracture reorientation to occur with greater magnitude than when the initial stress ratio is large. Such a model would predict changes in fracture orientation on the order of 30 to 60

degrees for cumulative injection of about 2000 m^3 to 5000 m^3. This estimate is consistent with field observations at Project TTI 4 for varying fracture orientation, as illustrated in Figures 37 and 38.

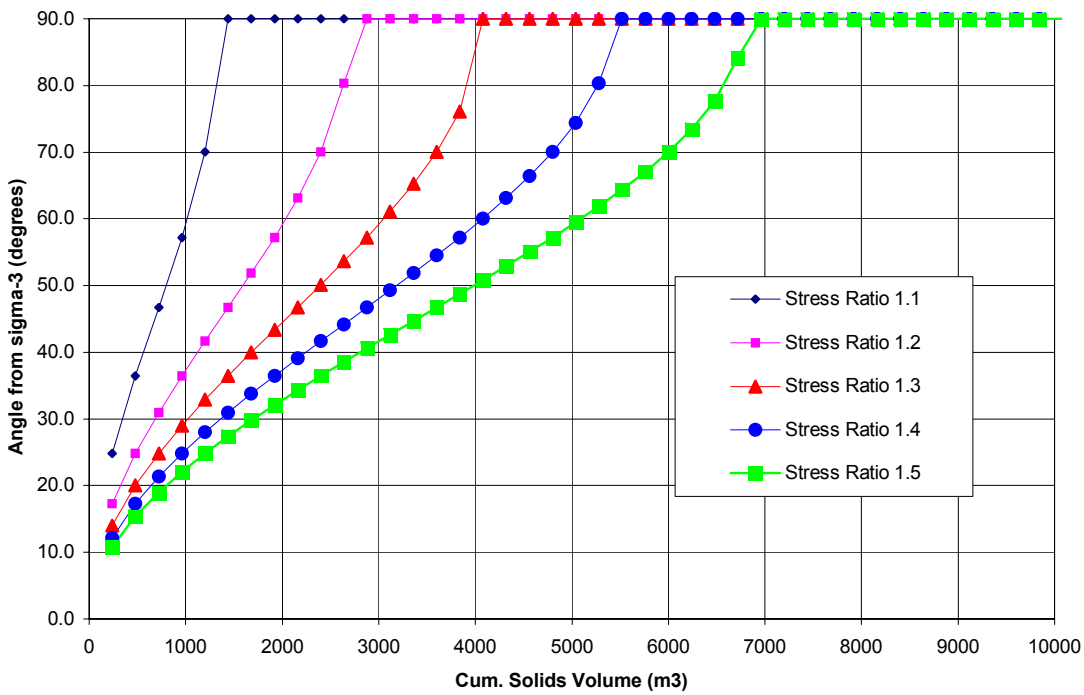

Figure 43: Fracture re-orientation vs. cumulative injected volume

Two Dimensional Analytical Models with History Matching

The simple model and process described above seems to explain observed fracture re-orientation. To address observed changes in net pressure and leak-off behavior, we next consider application of simple two dimensional analytical models. These analytical models assume fracture growth is occuring in a linear elastic medium. Fracture growth is limited to the length & width dimensions, keeping the fracture height consistent.

The Perkins-Kern-Nordgren (PKN) Model

The PKN fracturing model represents fluid-induced fractures with constant vertical height and laterally-extending growth propagating in linear elastic media (Perkins & Kern, 1961, Nordgren, 1972). The theory, based on the geometry of the PKN fracture (Figure 44) and the leakoff conditions of the reservoir, predicts that BHP_{net} will increase during pumping. PKN theory neglects the tip effects and any concept of

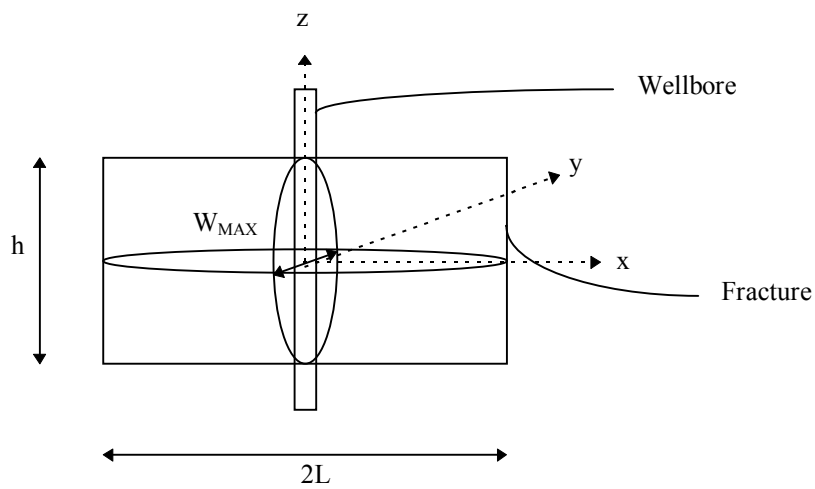

Figure 44: PKN Fracture Geometry

stress intensity, making it physically consistent for formations that have no tensile strength. Reservoirs used for SFI, typically permeable, unconsolidated sandstones, fall into this category.

For the large leak-off case, pressure behaves as follows:

$$\mathrm{BHP_{net}} = \Delta p(x=0,t) = 4\left[\frac{2G^3\mu(\mathrm{q_{inj}}/2)^2}{\pi^3(1-\nu)^3 Ch^5}\right]^{1/4} t^{1/8} \qquad [12]$$

where $\mathrm{BHP_{net}}$ is net pressure at the wellbore ($\mathrm{BHP_{net}} = \mathrm{BHP} - \sigma_3$), G is the shear modulus of the local reservoir, q_{inj} is the pumping rate, μ is the fluid (slurry) viscosity, ν is Poisson's ratio, C is Carter's leakoff coefficient (Howard and Fast, 1957), h is the constant fracture height, x is the distance from the wellbore (x=0 indicates the wellbore wall), and t is time (measured from start of pumping). It is evident from [12] that $\mathrm{BHP_{net}}$ increases with time to the power of 1/8.

The following equation represents pressure behavior for the zero-leakoff case, using physics that do not consider reservoir leakoff:

$$\mathrm{BHP_{net}} = \Delta p(x=0,t) = 2.5\left[\frac{G^4\mu(\mathrm{q_{inj}}/2)^2}{(1-\nu)^4 h^6}\right]^{1/5} t^{1/5} \qquad [13]$$

Clearly, the leakoff coefficient, C, does not occur in [6]. This equation indicates that for the zero-leakoff assumption, $\mathrm{BHP_{net}}$ increases with time to the power 1/5. While it is reasonable that SFI reservoirs will cause large leak-off due to their high permeability, it is possible that local reservoir plugging and other features may evolve during the course of a project that lead to zero (or at least small) leakoff situations. This model therefore provides a useful check on reservoir behavior.

Regression Analysis

Regression analysis can be used to rapidly match predicted PKN behavior to measured data. Equations [12] and [13] are of the form $\Delta p = A \cdot t^B$. This is identical to the following expression: $\log(\Delta p) = \log A + B \cdot \log(t)$, which can be analyzed using regular linear regression techniques. Therefore, reducing the net-pressure data to a log-log plot of net-pressure vs. time yields a series of possibly linear field data points. If the trend is linear or nearly so, and has a small positive slope, then it can be modeled using PKN large- or zero-leakoff assumptions.

The modeling is performed by fitting the best-fit straight line y=mx+b (or $\log(\Delta p) = \log A + B \cdot \log(t)$) through the field data. An example is presented in Figure 45. The best fit is obtained by iterating over the closure pressure, affecting the ordinate $\log\Delta p = \log(\text{BHP-closure pressure})$. This process can be done by initially ignoring the intercept term, A, and solving for the closure stress to match the theoretical slope. The optimum fit involves the closure that yields the highest r-squared value in the linear regression process. PKN large-leakoff closure is the optimum closure for which B = +1/8; similarly, PKN zero-leakoff closure is the optimum closure for which B is +1/5.

A similar iterative procedure matching model and field data is used to determine the intercept, once the closure is known. The intercept A on a log-log plot contains all the leading terms multiplying $t^{1/8}$ or $t^{1/5}$ in equations [12] or [13]. Reservoir, fluid, and operational data are included in this intercept term. The flowrate and viscosity of the injectate is generally known and the fracture height may be assumed. We can therefore solve for either the combination of shear modulus and leakoff coefficient based on equation [12] if the slope is close to 1/8 or the simply the shear modulus based on equation [13] if the slope is close to 1/5.

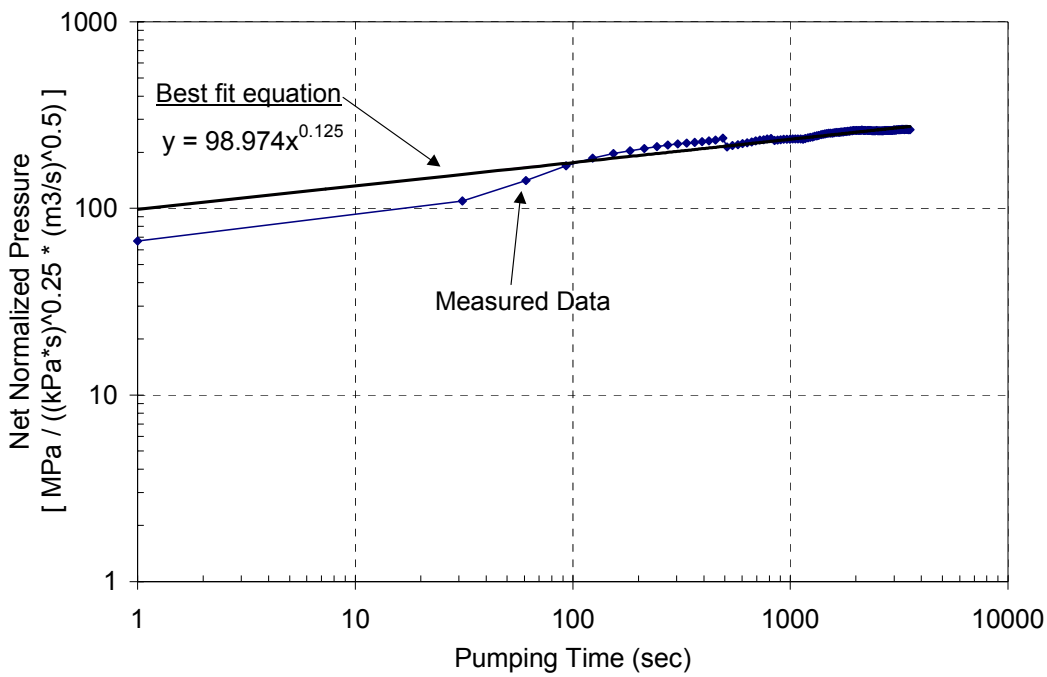

Figure 45: Log-log plot of measured net normalized pressures and best-fit PKN model line

In summary, the regression process first attempts to fit the PKN models to the data by altering closure pressure to match a 1/8th or 1/5th slope vs. time on a log-log plot. Next the corresponding shear modulus and leakoff coefficient are varied to match the intercept between the model and observed field data. Fracture dimensions such as length and width may then calculated using the standard PKN equations once these parameters have been determined.

PKN-Large Leakoff Analysis: Case Study

Ten consecutive injection days were chosen from an SFI project for analysis using the PKN Large Leakoff model as described above. Naturally occurring radioactive material (NORM) contaminated soils were injected during Project TTI 11 into a deltaic sandstone of Miocene age at a depth of 1380 m. The soil volumes injected in this project were very large, and as of October 18, 1999 the cumulative soil volume injected into this formation was 76,850 m^3.

The ten days chosen for analysis were from October 18 to 29, 1999 (Figures 46 and 47). This suite of days was chosen since a step rate test was performed on October 25, 1999, which was used to estimate fracture initiation pressure and rate. The duration of each daily injection period varied from 4 to 11 hours, during which time slurry volumes of 525 to 1440 m^3 (3310 to 9060 bbl) were injected.

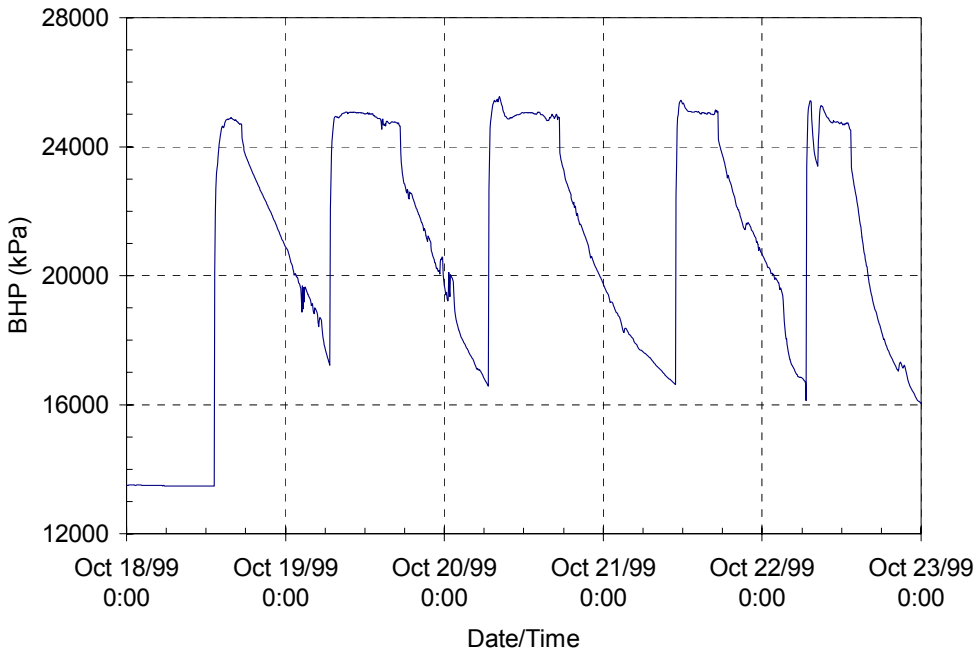

Figure 46: Injection and shut-in pressure data for October 18 to 22, 1999 (TTI 11)

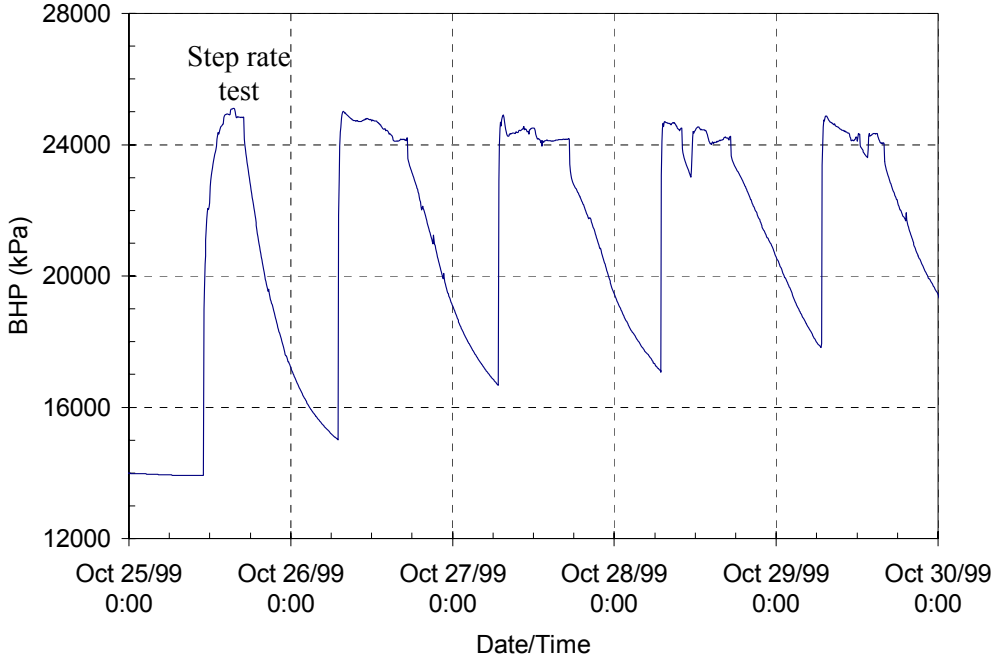

Figure 47: Injection and shut-in pressure data for October 25 to 29, 1999 (TTI 11)

Each of the days used for modeling showed increasing pressure behavior for the first hour or two, and then constant or decreasing injection pressures for the remainder of the day. The physics of the PKN model indicate that bottomhole pressures should increase throughout injection. To make the analyses common for each day, only the first hour of injection was analyzed. This substantially improved the fit of the PKN model to the data.

The step rate test of October 25 could not be modeled regardless of the model settings chosen. Stable fracture growth and PKN pressure behavior do not occur when multiple injection rates are used. Only twenty minutes of data were analyzed on October 22 since some BHP data points were not recorded in the first hour.

The PKN model was run in two modes: (a) allowing the computer to find the best-fit closure pressure and then solving for the stiffness/leakoff term, and (b) entering a fixed closure pressure from which the program would solve for the stiffness/leakoff term.

The results from using the best-fit closure approach are presented in Table 8. In using this approach, the closure pressures typically fell in the range of 17000 to 20500 kPa (Figure 13). The closures steadily rose from 17060 to 18330 kPa during the first week and were mostly steady around 20100 kPa during the second week. This range of closure values appears reasonable, although perhaps a bit low, equivalent to horizontal stress gradients (σ^3/z) of 12.9 to 15.5 kPa/m (0.57 to 0.68 psi/ft). Typical horizontal stress gradients are in the range of 16 to 18 kPa/m (0.7 to 0.8 psi/ft) for the area.

The stiffness/leakoff ratio ($G/C^{1/3}$) is the grouping of two important variables affecting fracture growth: formation stiffness (shear modulus – G) and fluid leakoff (C). Shear modulus (G) can be calculated when leakoff (C) is known, but C is typically based on estimated permeability and porosity which are poorly

known. Therefore $G/C^{1/3}$ can provide a relative estimate of stiffness and leakoff behavior of fracture in the "near" region of the target formation. With the exception of the October 22 and 26, the stiffness/leakoff ratio ($G/C^{1/3}$) was about 155 GPa/$(m/s^{1/2})^{1/3}$ on the first week and about 90 GPa/$(m/s^{1/2})^{1/3}$ during the second week (Figure 49).

Table 8: PKN-Large Leakoff analysis summary table (TTI 11)

	October 18	October 19	October 20	October 21	October 22
Closure (kPa)	17059	17490	18270	18520	22780
$G / C^{1/3}$ **	148.0	164.6	152.2	149.0	46.7
Shear Modulus (GPa)	6.827	7.765	7.170	7.101	2.270
Slurry Viscosity (cP)	2052	2024	2289	2104	1860
Leak-Off Coefficient ($m/s^{1/2}$)	9.74E-05	1.06E-04	1.05E-04	1.09E-04	1.15E-04
Injected Volume (m^3)	124.6	127.2	122.0	128.0	42.3
Fracture Volume (m^3)	26.7	26.9	27.6	26.5	16.4
Fracture Aperture (mm)	13.6	13.3	14.0	13.7	15.4
Fracture Half Length (m)	87.2	89.4	87.5	85.7	47.2
Constant Height (m)	18.3	18.3	18.3	18.3	18.3
Fit quality (r^2)	0.510	0.912	0.896	0.866	0.900
Analysis Time (hr)	1.0	1.0	1.0	1.0	0.33
Total Injection Time (hr)	4.0	10.6	10.7	6.2	4.9

	October 25	October 26	October 27	October 28	October 29
Closure (kPa)	n/a	17400	20406	19915	20119
$G / C^{1/3}$ **	n/a	171.4	84.8	96.9	94.7
Shear Modulus (GPa)	n/a	8.100	4.026	4.587	4.489
Slurry Viscosity (cP)	n/a	2083	2108	2070	2107
Leak-Off Coefficient ($m/s^{1/2}$)	n/a	1.07E-04	1.06E-04	1.07E-04	1.07E-04
Injected Volume (m^3)	n/a	127.0	125.4	124.8	122.4
Fracture Volume (m^3)	n/a	25.6	31.5	30.5	29.0
Fracture Aperture (mm)	n/a	13.1	15.7	15.3	15.0
Fracture Half Length (m)	n/a	86.9	88.6	88.5	85.7
Constant Height (m)	n/a	18.3	18.3	18.3	18.3
Fit quality (r^2)	<0.15	0.898	0.798	0.733	0.816
Analysis Time (hr)	n/a	1.0	1.0	1.0	1.0
Total Injection Time (hr)	6.0	10.3	10.6	10.4	9.2

** - Units: GPa / $(m/s^{1/2})^{1/3}$

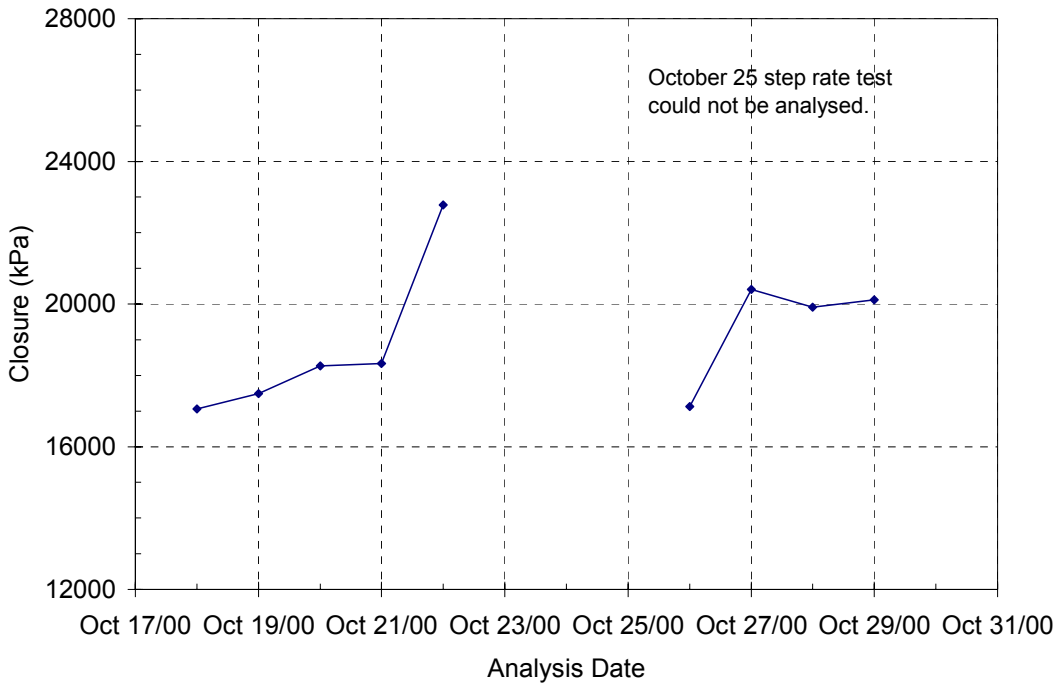

Figure 48: Closure pressures determined by best-fit methods to analyzed injection periods

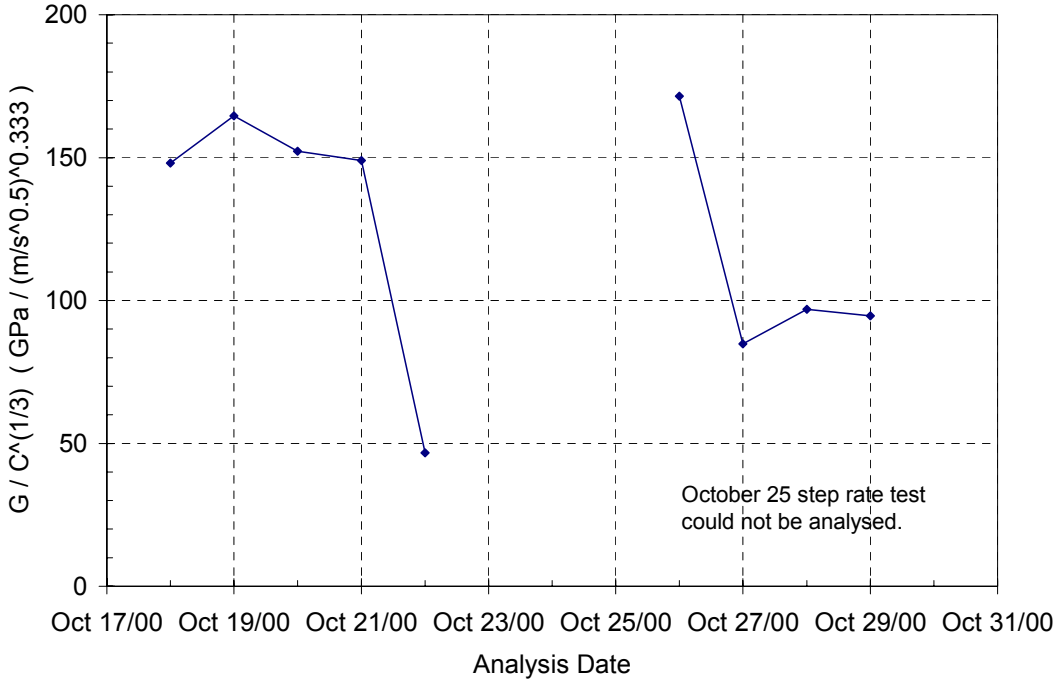

Figure 49: Stiffness/leakoff ratios ($G/C^{1/3}$) determined for best-fit daily closures

The problem with allowing the closure to float to a best fit is that closure pressure and stiffness are inversely related as can be seen in Equation 12. In comparing Figures 48 and 49 it can be seen that closure and stiffness/leakoff ratio ($G/C^{1/3}$) for the analyzed days are closely related to each other. Using this technique closure pressure and $G/C^{1/3}$ cannot be solved independently of each other and need an external method of determining either closure or stiffness. The stiffness and closure values determined purely by best-fit approach should be taken with caution.

The second approach used in modeling was to choose a fixed closure pressure to use on all injection days. The best choice of closure pressure should be determined from the pressure fall-off of the step rate test of October 25. Unfortunately, no characteristic closure pressure was visible in the pressure fall-off. The breakdown injection pressure was 24680 kPa at an injection rate of 1.27 m^3/min. This pressure is higher than true formation closure pressure (σ^3) due to friction effects at the perforations (which could not be predicted with confidence).

Since a unique closure pressure could not be determined, each injection day was modeled with three fixed closure pressures: 18000, 20000 and 22000 kPa. Figure 50 shows the stiffness/leakoff ratios ($G/C^{1/3}$) determined for each day at these closure pressures. The average stiffness/leakoff ratio at 18000 kPa was 160 GPa/$(m/s^{1/2})^{1/3}$, at 20000 kPa the ratio was 99 GPa/$(m/s^{1/2})^{1/3}$, and at 22000 kPa the ratio was 48 GPa/$(m/s^{1/2})^{1/3}$. $G/C^{1/3}$ is clearly inversely related to closure pressure.

Regardless of the closure pressure chosen, the stiffness/leakoff ratio ($G/C^{1/3}$) increased steadily during the first week (October 18-22) and stayed constant during the second week of injections (October 26-30). The increase during the first week could be caused by either increasing formation stiffness or decreasing leakoff and permeability. Stable stiffness and leakoff conditions were maintained during the second week assuming that the closure pressure remained constant.

Fracture dimensions were quite consistent for each of the 1 hour analyses (October 18-21 and October 26-30). The fracture height of 18.3 m was set based on the thickness of the sand formation. It is known from periodic temperature and gamma ray logs that primary fracture growth was confined within this zone. The widths from the fractures shown in Table 1 ranged from 13 to 16 mm, and the half-lengths from 85 to 90 m. The fracture dimension results for the runs shown in Figure 50 were similar in magnitude.

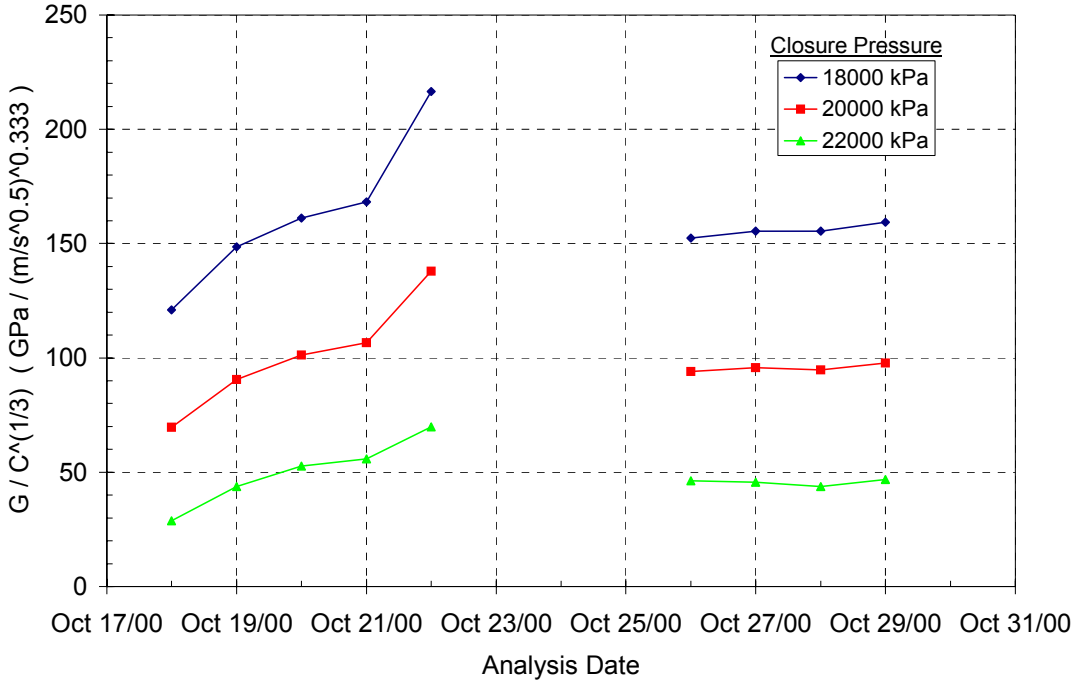

Figure 50: Stiffness/leakoff ratio ($G/C^{1/3}$) determined for three fixed closure values

Another potential source of error is appropriate estimation of the slurry viscosity. Slurry viscosity is estimated using a laminar pipe flow equation based on the wellhead and bottomhole pressures and slurry flow rate. The typical calculated viscosities have been about 2000 centipoise, significantly higher than the likely true value. The viscosity overestimates would affect the absolute magnitude of the stiffness, leakoff and fracture dimensions, but the distortion will be constant in most cases.

PKN-Zero Leakoff Analysis: Case Study

Analysis of the case study data using the PKN-Zero Leakoff assumptions did not fit any of the injection periods well. In most cases the PKN-Zero Leakoff model extrapolated pressures that were higher and increased more rapidly than the actual injection pressures. An example of this type of poor fit is shown in Figure 51.

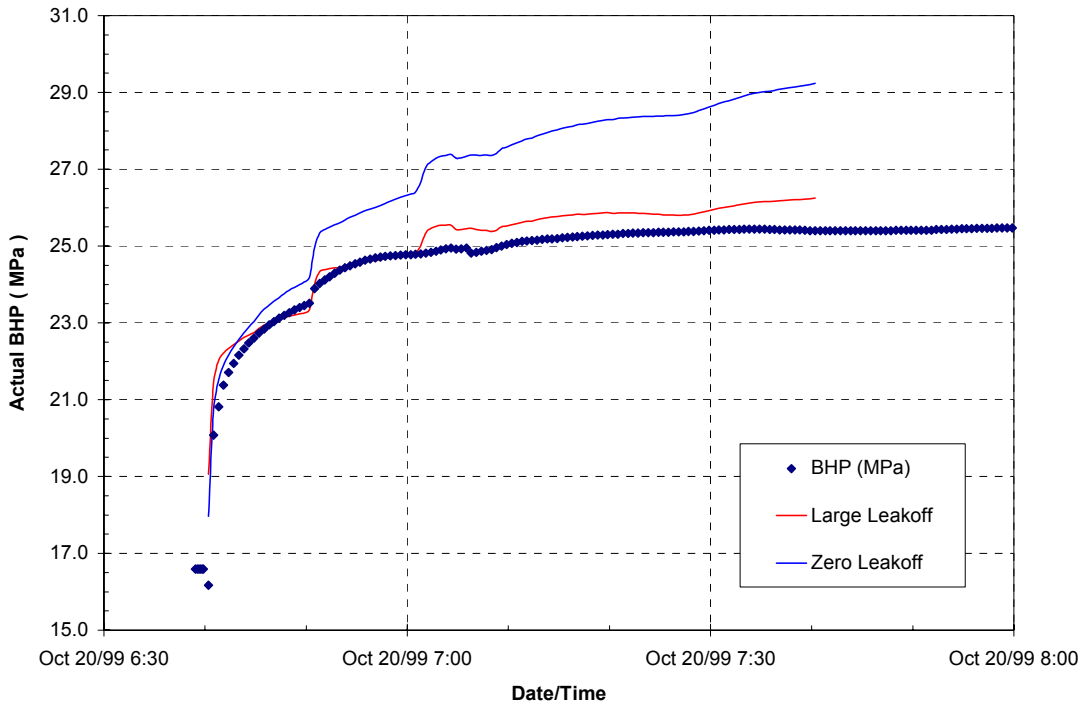

Figure 51: Fit of PKN-Large Leakoff and PKN-Zero Leakoff models to October 20, 1999

It makes sense that the PKN-Zero Leakoff model does not fit the data. The fundamental assumption of this model is that no fluid leaks off from the fracture into the surrounding formation. Like most high volume injection projects, the injection formation of project TTI 11 had a permeability of at least 500 md, and the waste pod had a permeability of around 10 md. Considerable fracture leakoff would occur at either of these values, thus reducing the pressure build-up during injection.

Analytic Modeling Discussion

Our proposed physical model for large volume slurry injection into suggests that repeated "packing" of a fracture and dilation zone by the injected solids increases the local stress and modulus (and may decrease the leakoff) until a new fracture breaks through in a different orientation. We present here a technique to use simple analytical equations, with variable closure, shear modulus, and leakoff, to model such a situation. Such models can match observed pressure data and do indicate slight changes in closure and stiffness/leakoff ratios. However, it is difficult to isolate the relative influences of individual factors if both are allowed to vary. The preferred approach is to estimate closure independently, generally with a step-rate test, and then evaluate changing stiffness/leakoff ratio.

Pseudo-3D Numerical Models with History Matching

Introduction

In addition to investigating modifications to simple analytic expressions for fracture in order to capture observed SFI phenomena, we have also investigated the use of state-of-the art three dimensional models. In two dimensional hydraulic fracture models, one of the fracture dimensions is held constant in order to solve for the other two dimensions. With the PKN fracture model used in this project, the fracture height was held constant so that length and width could be determined. In three dimensional fracture modelling the fracture height, length and width are solved together. This is more difficult mathematically, but additional degrees of information can be entered to create a more realistic fracture growth. Such models are not truly three dimensional, because they do not allow fractures to grow out of a single plane (the third dimension is merely a changing thickness), hence they are referred to as "pseudo-3D".

The primary variables which govern hydraulic fracture growth are injection pressures and rates, slurry concentration and flow behavior. At the fracture level, pseudo-three dimensional (pseudo-3D) models require information about each of the formation units. Formation data includes permeability, horizontal stress, elastic modulus, Poisson's ratio, and fracture toughness. Characteristics of the injection slurry that are required are liquid density, viscosity, rheology at different temperatures, and proppant density, diameter, settling and flow behavior.

There are several commercial programs available which perform pseudo-3D hydraulic fracture modelling, such as MFrac by Meyer & Associates, and FracProPT which is based on development work by the Gas Research Institute. Modeling in this project was performed using FracProPT by Pinnacle Technologies Inc. A brief description of the model components follows (Pinnacle, 2000, Crockett et al, 1986):

Wellbore Flow: The primary goal of this component is to determine pressure drop that occurs in the tubular goods due to viscosity and proppant properties. Since bottomhole pressures were monitored continuously, this information is of less importance than when only a wellhead pressure sensor is present.

Fracture Geometry: Fracture geometry is determined based on spatial variations in formation stress, modulus, pressure and flow distribution. However, instead of calculating fracture width at each point using a finite element mesh, the effects of each of the formation variables are integrated into functional coefficients of the governing differential equations. This greatly simplifies the calculations of fracture dimensions. The details of the equations used are too lengthy for the purposes of this discussion, but are described in Crockett et al, 1986.

Leakoff Model: Leakoff of fluid from the fracture is an important mechanism determining fracture length and width. If high leakoff is occurring, less fluid is available to increase the fracture length or height. Fluid leakoff from the fracture is governed primarily by formation permeability and apparent fluid viscosity. Plastering of a filter cake onto the walls of a fracture can cause reduction of fluid leakoff. In the case of SFI fractures, the filter cake is probably composed of clays and heavier oil components in the slurry.

Proppant Transport and Placement: Proppant transport inside a fracture generally appears to be a convective process. Settling of the solid particles can be progressively hindered by increasing

concentration. The growth of a settled bank of solid particles at the bottom of a fracture limits downward fracture growth.

Other Model Components: Heat transfer from the formation to the fluid can be important when fracturing fluids have rheological properties that are very sensitive to temperature. This is not the case with SFI where the rheologically simple liquids of water and oil are the only fluids present. Modelling the effects of acids in fracturing is also possible, but again is not applicable in this case.

Case Study

Injection data from Project TTI 11 was used for testing the capabilities of FracProPT pseudo-3D fracture modelling software. Data from the ten injection days from October 18 to November 2nd, 1999 were used, the same dataset evaluated in the PKN case study described above. The complete Pinnacle analysis report is provided in Appendix A. We present here a summary of their results and comparison with analytical modeling results.

Pinnacle Technologies evaluated 5 different fracture growth scenarios that address potential mechanisms that could result in rock mechanical property changes in waste injection wells. Table 9 provides an overview of the different scenarios that were evaluated.

Table 9: Fracture growth scenarios

	Sand Closure Gradient (psi/ft)	Shale Closure Gradient (psi/ft)	Matching Variables		
Scenario	(psi/ft)	(psi/ft)	Permeability	Opening Fact.	Modulus
1	0.736	0.886	x	x	
2	0.736	0.886	x		x
3	x	0.886	x		x
4	0.736	0.786	x	x	
5	0.662	0.812	x	x	

Two matching variables are used in each of the 5 scenarios. During net pressure matching, it is important to match both the level of the net pressure and the pressure decline slope following the injection. Matching the level of the net pressure is mainly controlled by changing the Young's modulus of the rock or the fracture opening factor. The opening factor represents the level of fracture growth complexity, and assumes that multiple fractures open against each other to "compete" for fracture width. Matching the slope of the pressure decline is achieved by changing the leakoff multiplier, which is roughly proportional to the permeability squared.

In general the net pressure and falloff behavior for each injection could be matched reasonably well regardless of which variables were adjusted. For example, Figure 52 presents typical pressure matches for scenario 1, in which permeability and fracture complexity are varied, and Figure 53 presents typical pressure matches for scenario 2, in which permeability and Young's modulus are varied. The variables required to achieve these matches are presented in Figure 54, as well as the resulting fracture dimensions. Comparing Figures 53 and 54, it is clear that multiple fracture opening factor has nearly the same influence as modulus.

FRACPRO Modeling Discussion

There are some interesting similarities in behavior modeled with both the analytical technique and the FRACPRO simulation. For example, the changes in shear modulus to leakoff ratio shown in Figure 49 from the analytical modeling are consistent with the changing modulus multiplier shown in Figure 54. They ar relatively constant during the first four days of injection during week 1, and are relatively constant and lower by about half for the last four days of injection during week 2. As with the analytical models, it is clearly possible to match observed pressure behavior during waste injection by varying closure, leakoff, and stiffness modulus. However, it remains difficult to use treating data alone to determine how individual properties might vary independent of the other variables in the models.

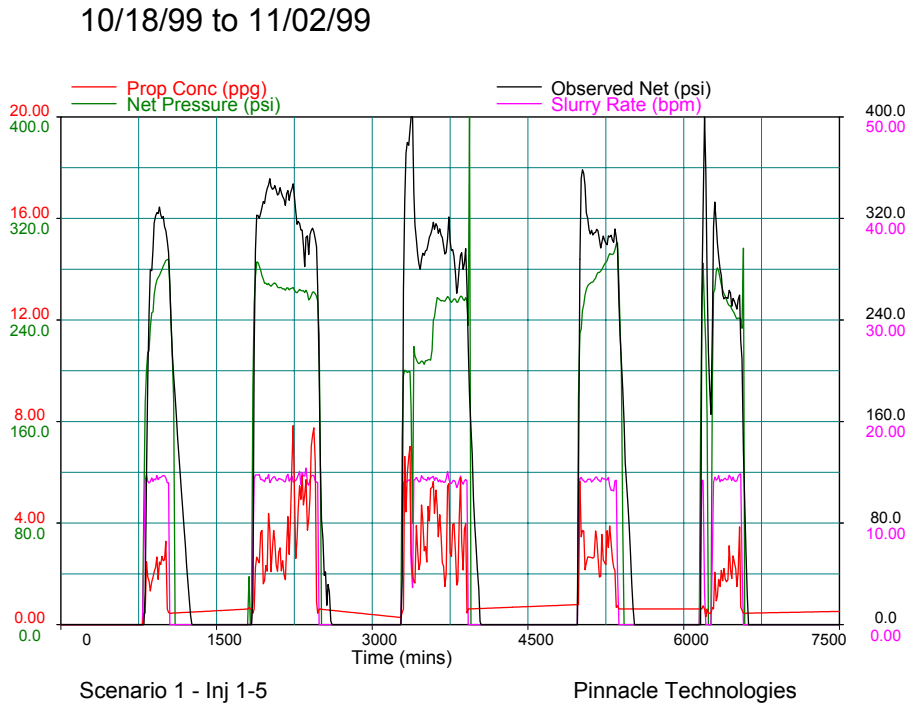

Figure 52: Net pressure match for injection 4-6 using scenario 2.

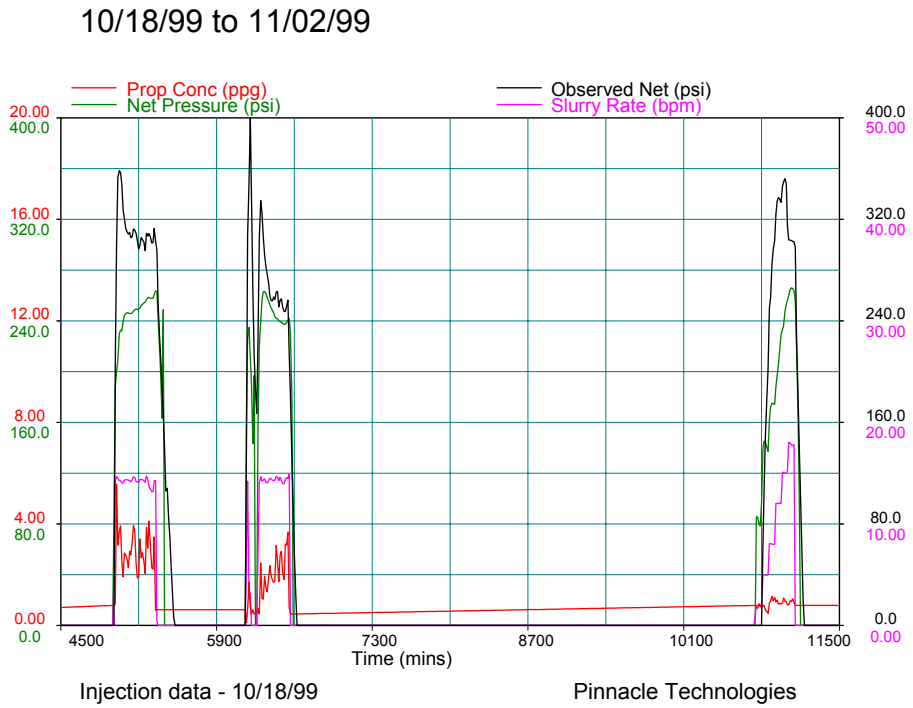

Figure 53: Net pressure match for injection 4-6 using scenario 2.

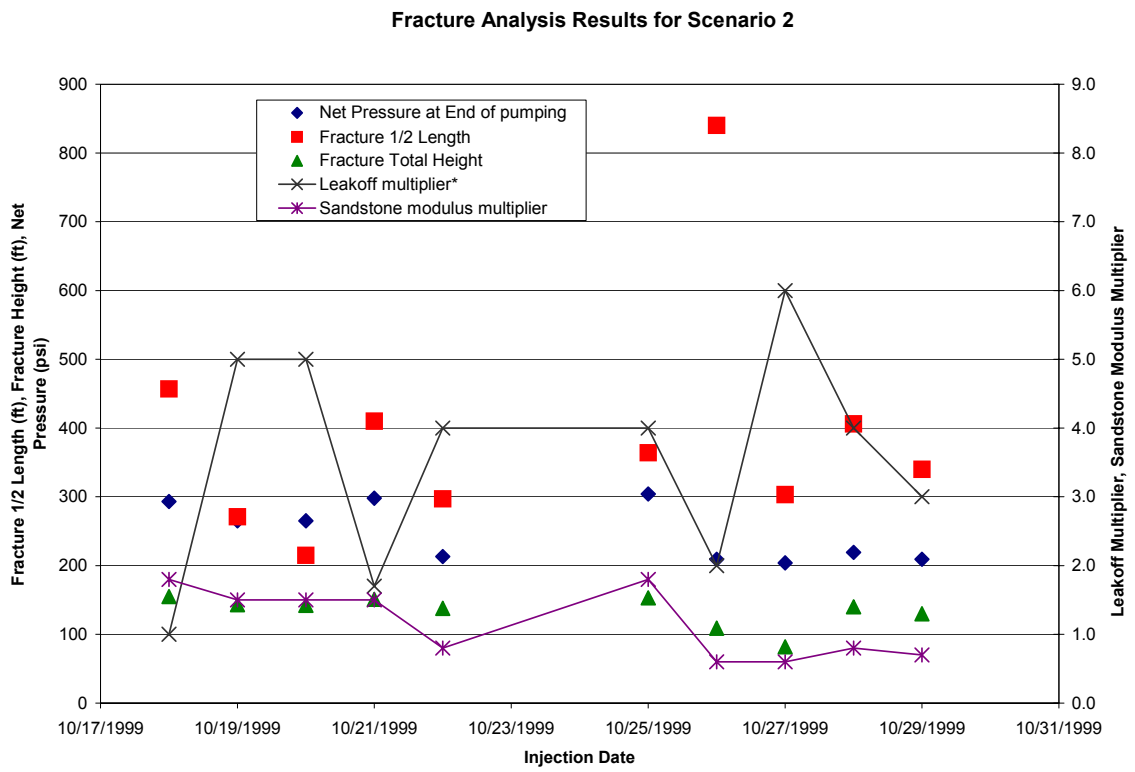

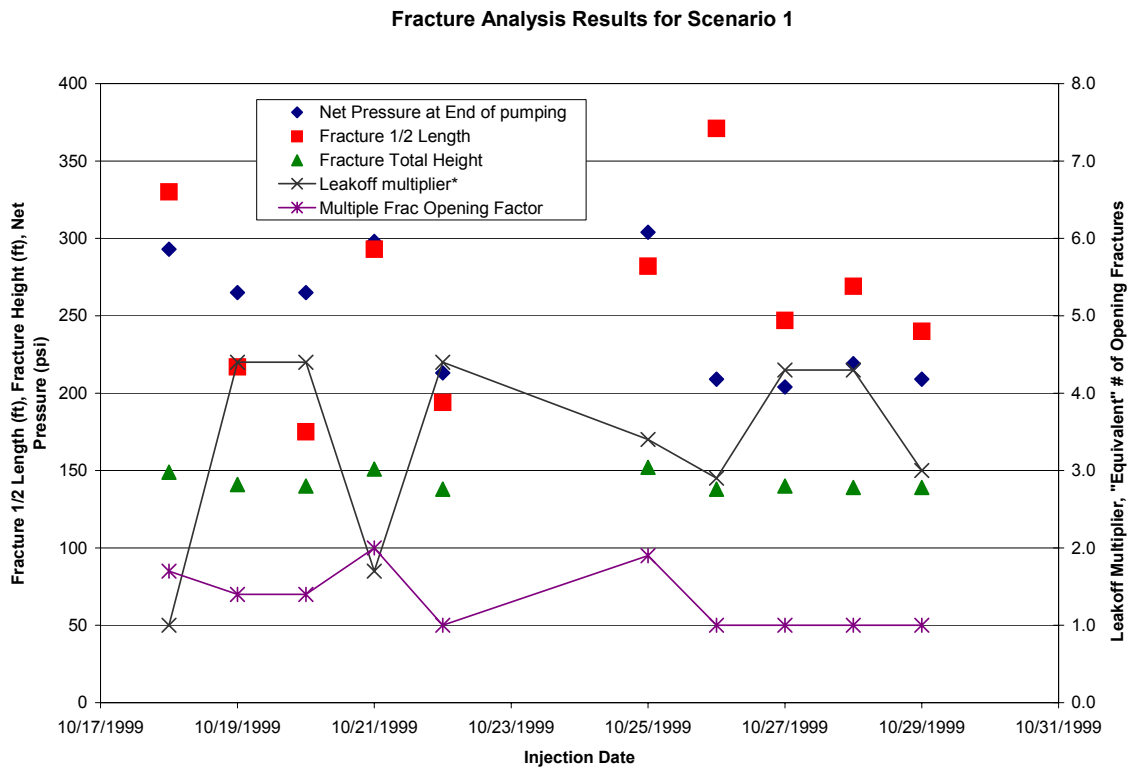

Figure 54. FRACPRO variables required to match pressure behavior for scenarios 1 and 2.

Discrete Element Modeling

Fracture and large scale dilation of granular media are inherently "discontinuous" processes. Continuum models have difficulty capturing the basic physical processes of microcracking, disaggregation, and grain movement which occurs during waste injection in weakly consolidated media. Therefore, Terralog has investigated the application of particle models to better simulate the SFI process. Discrete element or particle models, which model interparticle mechanics explicitly, can often provide a more realistic simulation of granular material deformation and flow.

Background

Numerical simulation of cohesionless granular assemblies with discrete elements was introduced by Cundall and Strack (1979), and has since been modified and expanded by a number of researchers. In these models, the movements and mechanical interaction of particles are tracked over time with an explicit finite difference procedure. Particle interaction is modeled by damped force-displacement relations at each contact. The resulting forces and moments are related through Newton's second law to the particle mass and acceleration. Contact forces on the microstructural level may be related to macroscopic boundary stresses through the principal of virtual work, as described by Bathurst and Rothenburg (1990).

Discrete element models for grain assemblies have been applied to investigate stress induced microcracking and induced permeability anisotropy in sandstones (Bruno and Nelson, 1994) and to investigate sand production around perforations and wellbores (Bruno et al, 1996). Cementation is modeled as tension and shear bonds between grains. Fluid flow can be accommodated explicitly by adding a pore space network flow model to the assembly, solving for the pore pressure field at each time step, and then resolving pressure gradients into body forces at individual grains. Alternatively, a continuum flow model can be run concurrently with the granular model, and using the particle model to update porosity and permeability fields for the flow model. Terralog has applied this latter approach for this project.

Cementation Influence on Brittle Fracture and Dilation

We first investigate how particle models can capture observed physical processes in weakly cemented media and provide insights on material parameters which influence changes in fracture behavior from discrete brittle fractures (as occurs in stiff formations) to general dilation (as occurs in very soft formations). Figures 55 through 60 present a series of fracture simulations with varying cementation properties. Particles are shown with orange circles, and contact bonds between particles are shown with dark lines. In each simulation, an initial fracture is extended simply by applying normal, outward forces to the starting fracture face, consistent with the forces that would be applied by fluid pressure within the starting fracture. The particle movement and change in contact bond pattern illustrate fracture and deformation patterns resulting from assemblies with varying cementation properties.

As illustrated in Figure 55, for strongly cemented granular assemblies, fractures propagate in a discrete, brittle manner simply by extending forward. However, for weakly cemented materials (lowermost assembly in Figure 55), deformation is accommodated by general dilation and deformation around the original fracture face, with very limited fracture extension. This transition from brittle fracture extension to general dilation is primarily controlled by shear bonding between particles, as demonstrated in Figures 56 and 57. That is, a decrease in the shear strength alone between particles produces dilation whereas a decrease in the tensile strength alone does not.

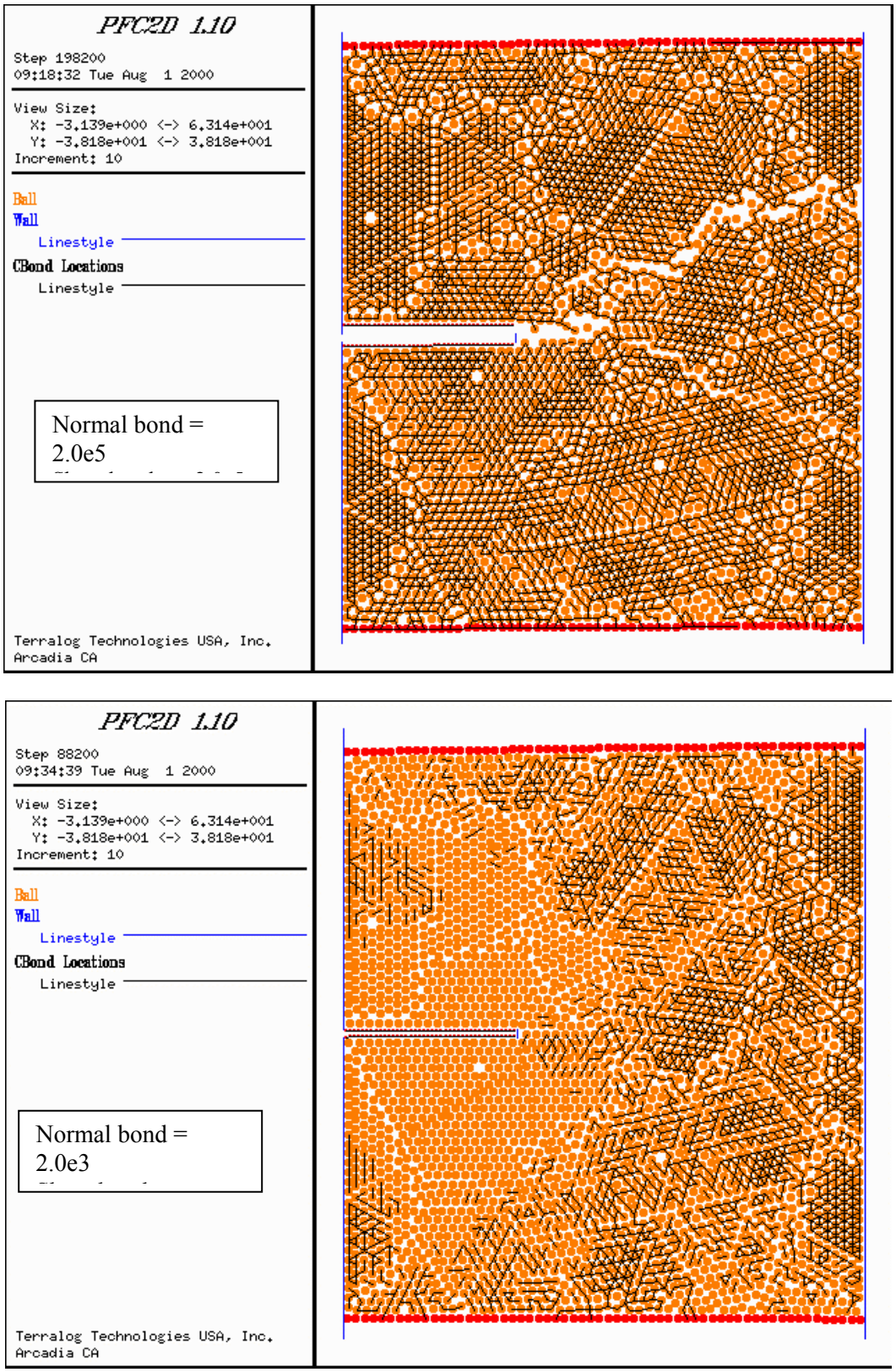

Figure 55: Transition from discrete brittle fracture to process zone dilation by decreasing bond strength.

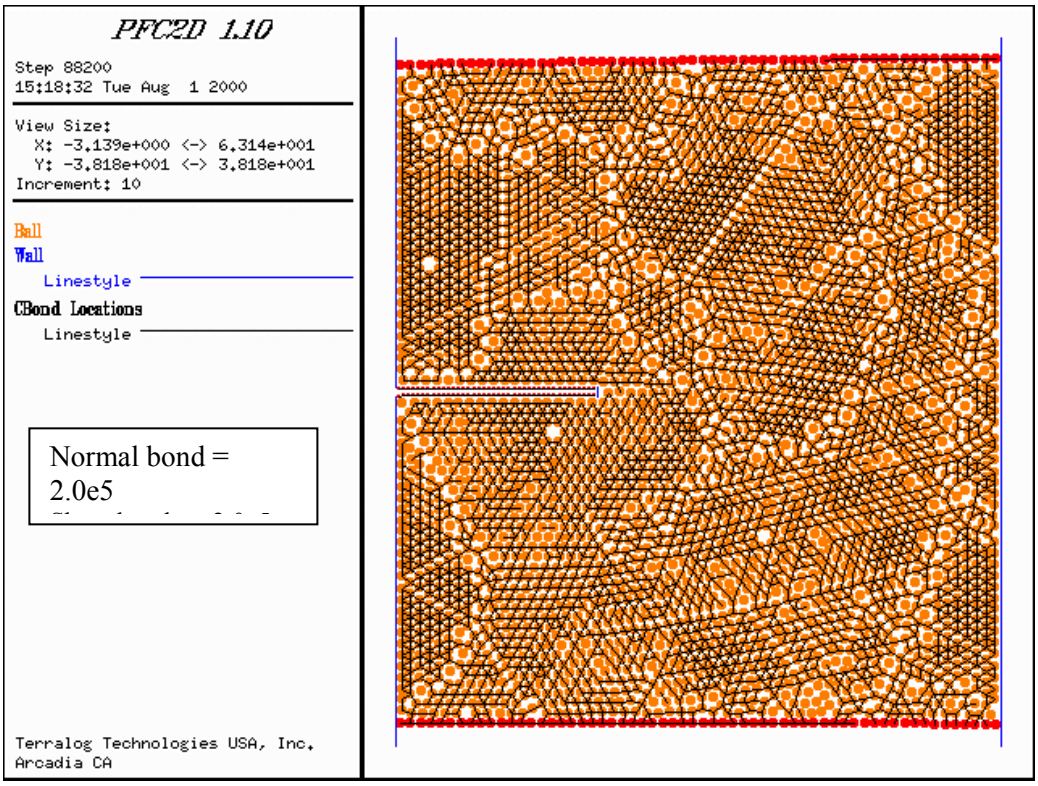

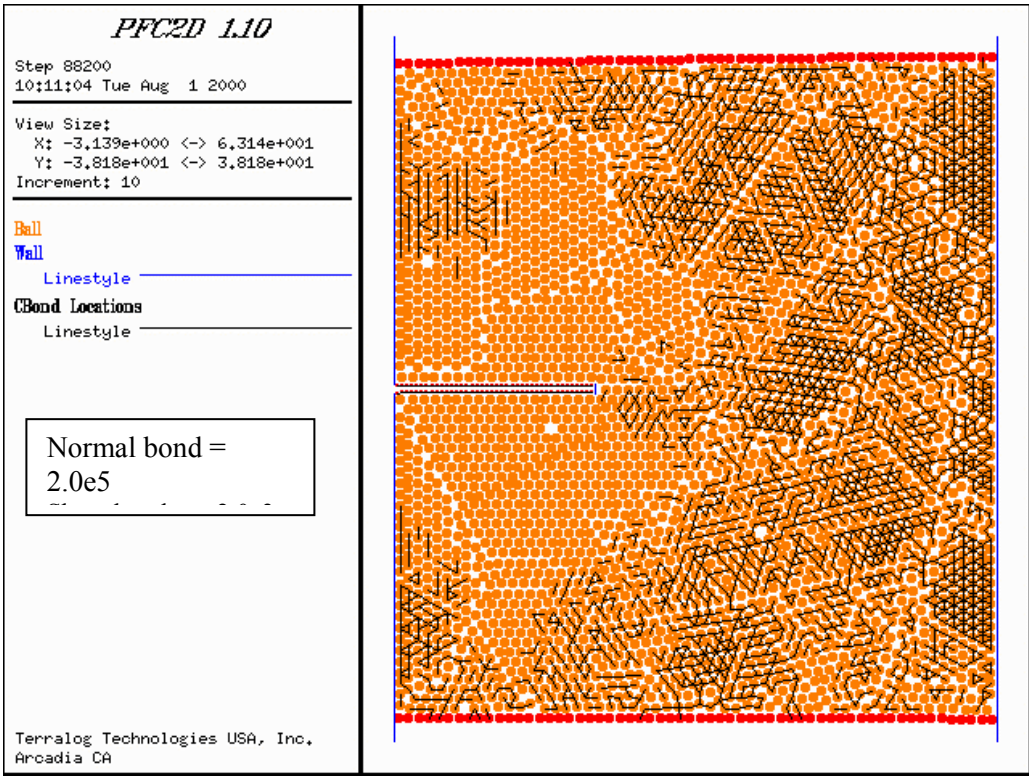

Figure 56: Dilation behavior is caused by decrease in shear bond strength alone.

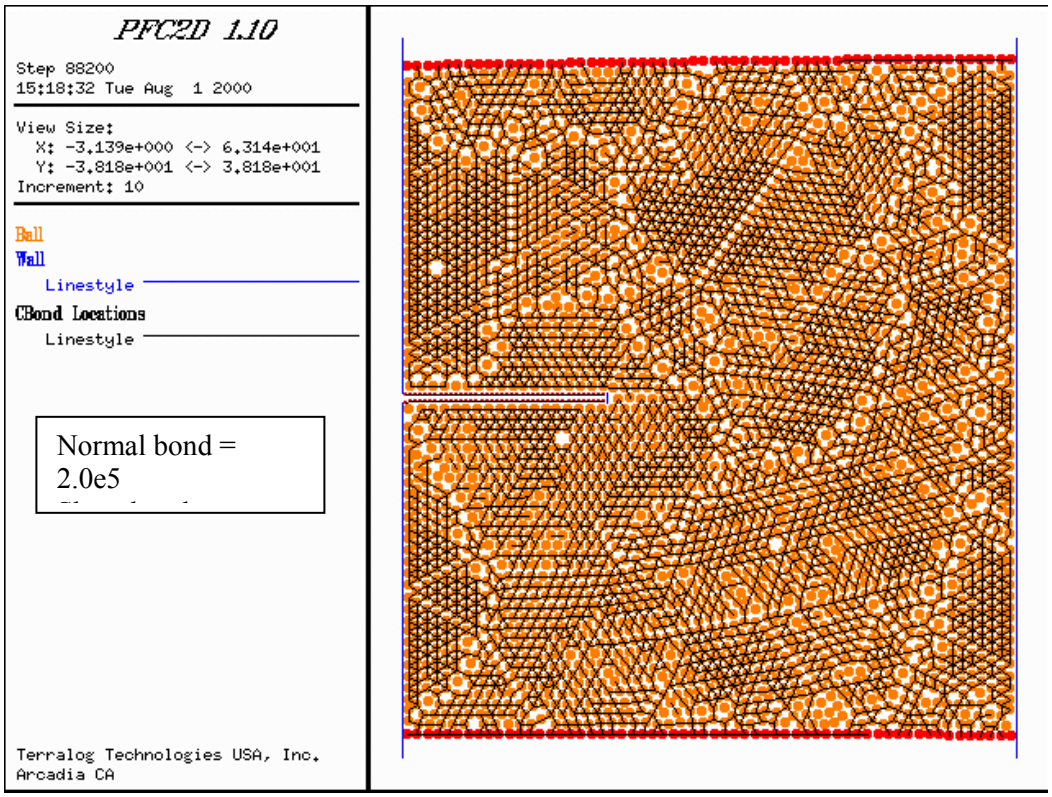

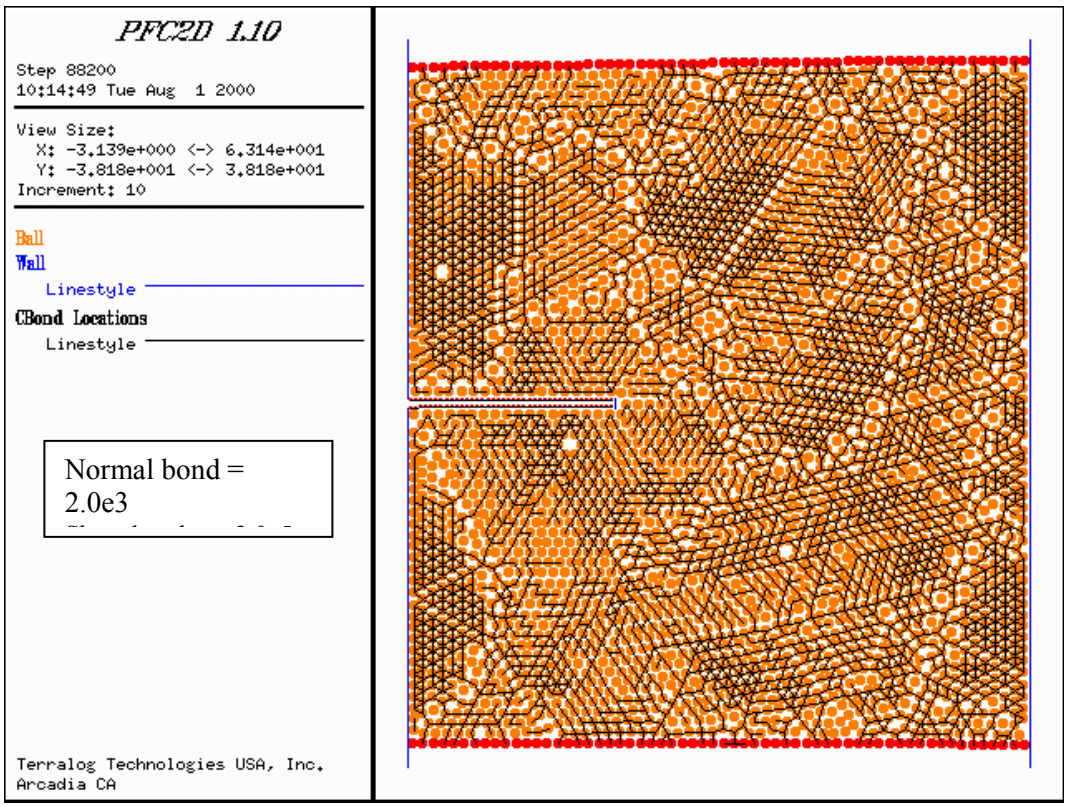

Figure 57: Decrease in normal bond strength does not lead to dilation.

Coupled Fluid Flow and Particle Flow Simulation

Next we investigate the process of slurry injection by analyzing the coupled fluid flow and particle mechanics process. We use ITASCA's FLAC program to model fluid flow in a fully saturated media and the PFC program to model the particle movement. The general coupling process is illustrated in Figure 58. A Windows interface used to assign properties, call individual subroutines, and track solution progress is illustrated in Figure 59.

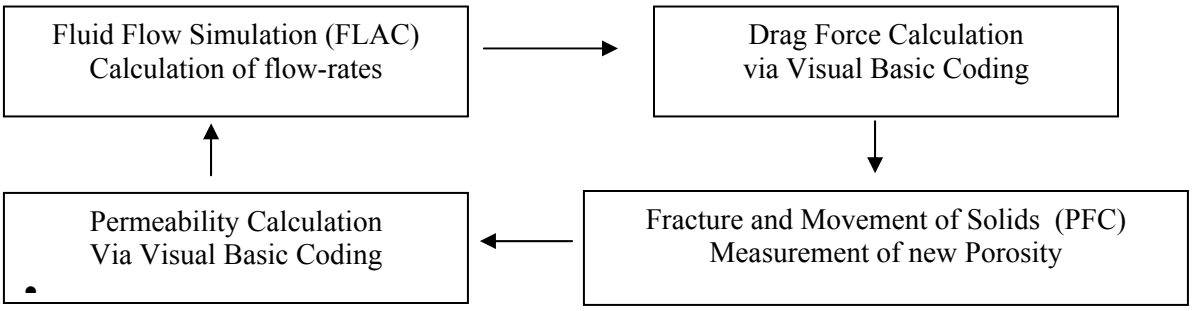

Figure 58: Schematic representation of the iterative coupling process

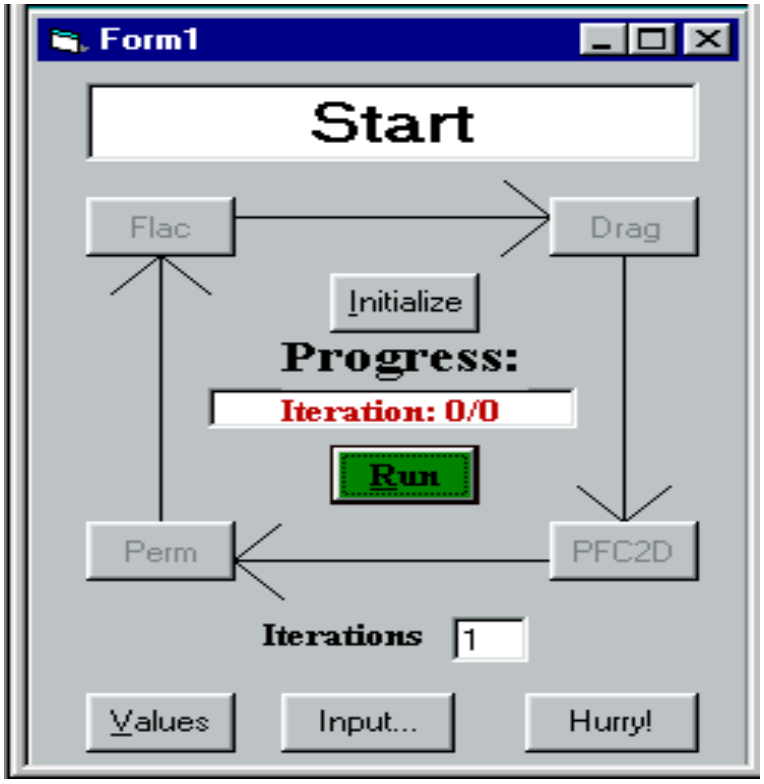

Figure 59: Windows interface developed to couple fluid flow and particle models

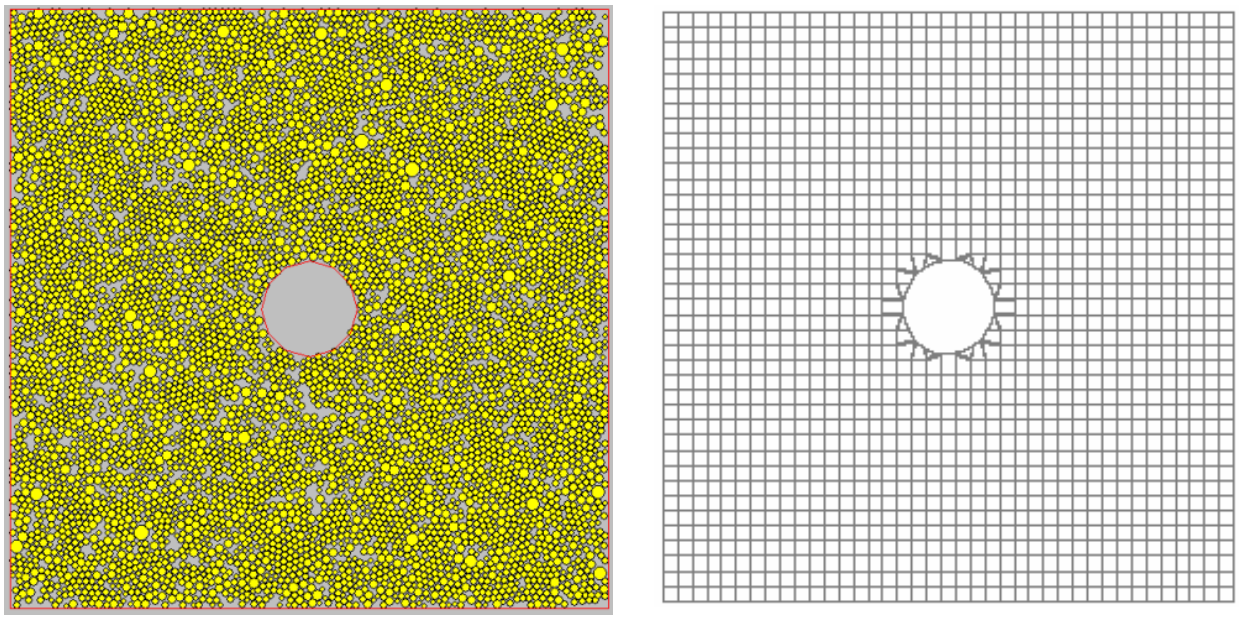

Figure 60: Initial particle assembly and fluid flow mesh to simulate slurry injection

To initiate the coupled fluid and particle fow simulation, a matrix of solid particles is first generated with PFC to simulate the weakly cemented sand formation. Neighboring elements in the matrix are connecting by weak bonds, which are allowed to fail upon creation of a limited stress state in the link itself. A corresponding and overlapping FLAC mesh is also generated to model fluid flow, as illustrated in Figure 60.

Porosity values from the particle model shown on the left of Figure 60 are used to define an initial permeability field for the fluid flow mesh. In our initial studies, we assume there is a relatively simple relationship between permeability, K, and porosity, ϕ, of the form taken by a Kozeny-Carman equation:

$$K = C\,\phi^{n} \quad , \qquad [14]$$

where the proportionality constant, C, and the exponent, n, are generally related to the specific surface area, grain size, and tortuosity in a granular assembly. In our simulations we use an exponent n=3.0, providing a relatively strong dependency on porosity.

The injection process is simulated by prescribing a flow rate at the borehole and maintaining a constant pressure boundary condition at the outer walls in the model. The assembly is assumed to be completely saturated. For the given initial permeability field and borehole flow rate, FLAC is then run to determine the resulting pore pressure field. For example, Figure 61 below presents a sample pressure field determined by the FLAC model.

Figure 61: Pore pressure distribution in model after a few iterations

The gradient of this pore pressure field, acting in the direction of fluid flow, induces drag forces on the particles. Drag is the resistance to fluid flow posed by the porous matrix (Bear, 1972). The drag force is introduced as an equivalent body force induced by the pressure gradient across the diameter of a particle in the flow direction multiplied by the area of the particle.

$$dF_i = A\frac{\partial P}{\partial x_i} \qquad [15]$$

using the expression for $\partial P/\partial x_i$ from Darcy's equation

$$F = \left(\pi r_g^2\right)\frac{Q}{K}2r_g \qquad [16]$$

where,

F	*Drag Force*
$\partial P/\partial x_i$	*Geometric Pressure Gradient in x_i-direction*
r_g	*Radius of the Grain Particle*

At each time step the x- and y-components of this force are added to the total body-force of each particle in the PFC model for the next iteration, and the solution of the equation of motion will then provide new acceleration terms. Time integration results in new values for the vector components of particle velocity, displacement and rotation. Dilation and cracking during this iteration then increases the porosity in a local area around the borehole, and provides new fluid paths that decrease the flow resistance in the porous material. The pressurized fluid in the fracture imposes additional load on the crack faces, thereby wedging the fracture further open. The direction of crack propagation when the porous material is loaded in compression is predominantly parallel to the maximum compressive stress direction.

We introduce slurry particles of a given size into the borehole at a given rate, consistent with the desired density and fluid flow rate. These particles are then swept by the flow field into the matrix and fracture system, contributing to the calculations for determining porosity, drag force, fracturing and fluid flow.

In summary, the iterative fluid flow and geomechanics process proceeds with the following steps:

1. Start with an initial particle assembly and fluid flow mesh, assigning initial material properties;
2. Assign a permeability field to the flow mesh consistent with the initial porosity;
3. Define the desired borehole injection rate, slurry density, and far-field pressure boundary conditions;
4. Run the fluid flow simulator (FLAC) to determine a new pore pressure field;
5. Determine pressure gradients and associated drag forces to be applied to each particle;
6. Run the particle simulator (PFC) to determine deformation in the geomechanical assembly;
7. Calculate the new porosity field and associated permeability field for the assembly;
8. Return to step 4 and iterate again.

Simulation Results and Discussion

The results of such a simulation are illustrated in Figures 62 through 64. For this simulation displacements are fixed on the lateral boundaries (left and right edges of model), and a fixed compressive stress is prescribed on the vertical boundaries (top and bottom edges). This establishes an anisotropic stress field favoring fracture orientation in the horizontal direction. The close-up view in Figure 63 illustrates a number of features.

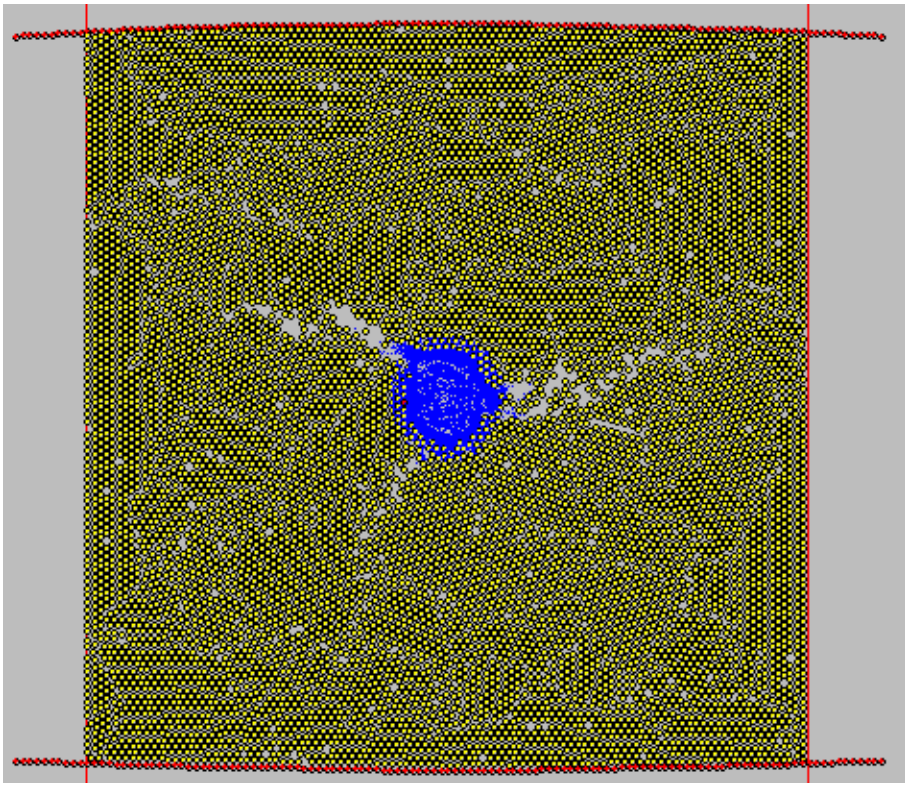

Figure 62: Discrete particle model showing fracture initiation and slurry particle injection

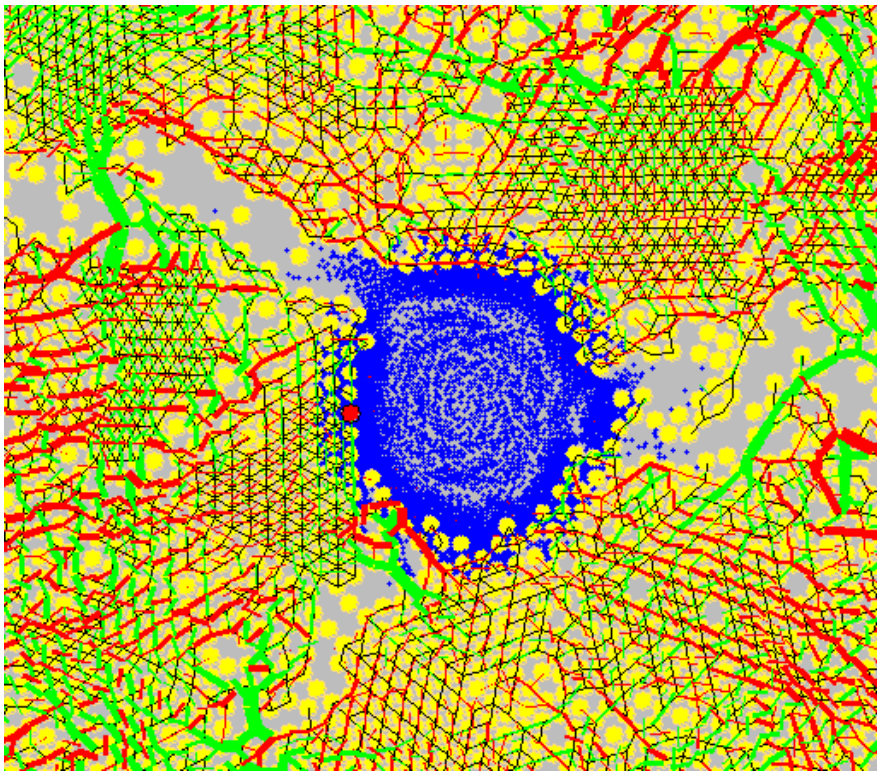

Figure 63: Closeup view of fracture initiation and slurry injection in porous media

First, injection particles (shown in blue) penetrate radially into the matrix. A wide fracture and dilation zone (zone of increased porosity) is initially established by the fluid, which then allows the injected solid particles to enter the fracture and process zone. Solids injection is therefore accommodated not only by fracture creation, but also by the matrix porosity (note penetration of slurry particles into porespace surrounding the borehole). Several fracture branches are formed, but those preferentially aligned with the stress field widen to a larger extent and ultimately accept most of the injected solid material. Pressure increases until the fracture conductivity and slurry flow matches the flow rate and then stabilizes as illustrated in Figure 64, which is consistent with field observations. Upon shut-in pressure declines. A model of small size can simulate one or two injection cycles before fracturing and deformation reaches the boundaries (indicated by little further pressure increase on last injection cycle in Figure 64).

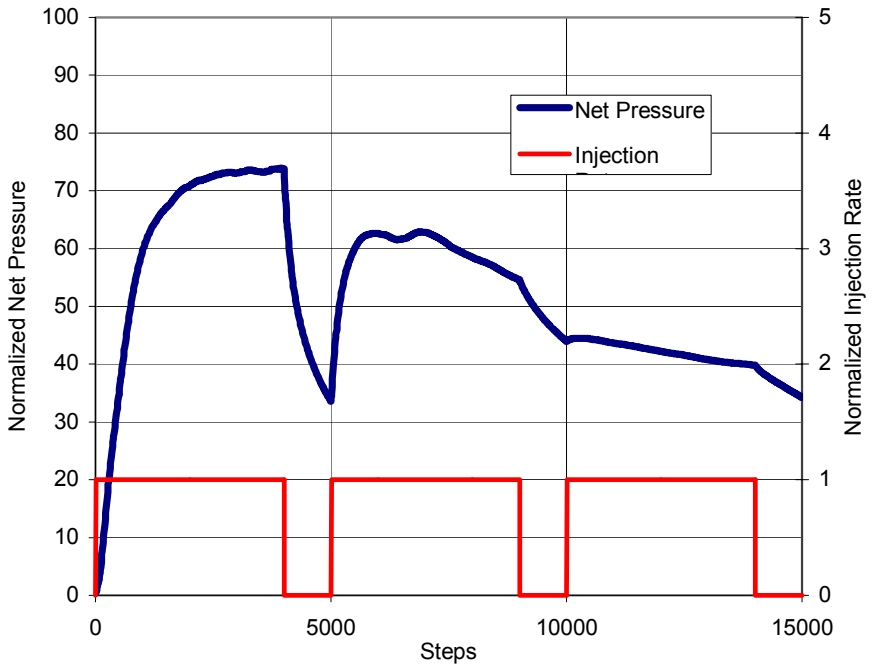

Figure 64. Typical pressure behavior for repeated injection cycles with particle flow model

These simulation results, although preliminary, appear to capture the physical processes involved in solids injection into weakly cemented media. This method shows good potential for better simulating waste injection, and warrants additional investigation and development efforts. For example, the model shown in Figure 62 is limited in size and needs to be expanded by at least a factor of ten to eliminate edge effects and allow simulation of repeated injection episodes. Terralog Technologies intends to pursue these efforts in the future.

MODEL INVESTIGATION SUMMARY

Our observations of fracturing and formation behavior during large-volume waste injection operations suggest a new physical model for episodic injection. During slurry fracture injection, the stream of waste slurry being pumped into the formation causes a fracture to open and material to dilate around the fracture, or within a "process zone". Much of the solid volume injected is accommodated by formation porosity, not simply within the fracture volume. The waste becomes trapped in the formation when pumping stops and the fracture and dilation zone closes.

This large amount of solids packing the fracture and dilation zone alters formation properties and behavior. The stresses within the process zone increase and the permeability within the process zone decreases. Subsequent injection episodes will then cause fractures to break through the waste pod, in a direction still parallel to σ_3, but with increasing difficulty. The minimum stress within the waste pod increases and, eventually, fracture re-orientation away from the σ_3 direction occurs. We propose a relatively simple analytic model to account for this "packing effect" as the waste pod grows with sequential injection, which allows prediction of fracture re-orientation as a function of injected volume. Model results are consistent with field observations, indicating that fracture re-orientation over a range of 30 to 60 degrees in azimuth can occur due to injection volumes on the order of 5000 cubic meters.

We also investigated the use of two dimensional analytical models (Perkins-Kern-Nordgren) and pseudo three dimensional models (FRACPRO) to simulate slurry fracture injection. These were modified to allow variations in shear modulus, leakoff coefficient, and closure stress with repeated injection episodes in order to capture observed formation behavior. Varying these parameters provides improvement over typical constant value assumptions, but it is difficult to recognize beforehand which parameters should be allowed to vary.

Finally we investigated the use of coupled fluid flow and particle flow models to simulate fracture and dilation processes during waste injection. These studies lead us to conclude that when formations are weakly cemented with limited shear strenght, there is a transition from brittle, discrete fracture extension, to more widescale dilation and inelastic parting. We were successful in developing a coupling process between a continuum flow model and a discrete particle model, allowing simulation of slurry particle injection and resulting fracture and dilation. These simulation results, although preliminary, appear to capture the physical processes involved in solids injection into weakly cemented media. This method shows good potential for better simulating waste injection, and warrants additional investigation and development effort.

GUIDELINES FOR SLURRY FRACTURE INJECTION

There are a number of guidelines that should be followed to operate a successful SFI project. These guidelines are based on field experience and some of the research included in this report.

A successful SFI project requires cooperation between a number of groups including regulatory agencies, the project operator and engineer, drilling and completions companies, and the site operators. Good communications need to be established between each of these groups: the success of an SFI project is sensitive to understanding and applying the guidelines by each project member.

The SFI well should be located in a formation and area that is sufficient to contain the hydraulic fracture process in a suitable permeable zone. This is discussed in more detail in the Geologic and Well Siting Guidelines. The Well Completion Guidelines discuss a number of items that increase the life expectancy of an SFI well and prevent slurry communication with overlying formations along the wellbore. Operating Guidelines cover specific recommendations regarding slurry injection practices. Finally, Monitoring and Analysis Guidelines discuss a number of techniques for determining the development and location of hydraulic fractures and the resulting waste pod.

Geologic & Well Location Guidelines

Injection of liquid wastes below fracturing pressure typically uses high permeability injection formations bounded by low permeability confining formations. However, additional geological provisions need to be considered to provide adequate confinement of hydraulic fractures and wastes created in the SFI process. Figure 65 shows an example SFI well placed in the types of formations discussed below.

Target Formation

Granular wastes disposed by SFI should be placed into a *Target Formation* which is composed of poorly consolidated sands. This formation should be of high permeability, relatively thick (> 20 m) and laterally continuous. The reasons these properties must be chosen are:

High permeability: Permits slurry carrying fluid to be carried off rapidly into the formation. This limits hydraulic fracture growth and prevents buildup of formation fluid pressures.

Thick formation: Increases the storage zone available for waste placement and increases the transmissivity (permeability×height) available for fluid leakoff.

Poorly consolidated sand: Formations with high porosity provide more void space volume into which solids can be placed than formations with low porosity. In addition, poorly consolidated formations have high compressibility, which means it can be displaced easily during hydraulic fracturing to create more volume for waste placement.

Laterally continuous: The target formation should have uniform thickness and permeability over a large area (greater than 25 km^2). A small or limited formation area would limit the maximum waste volume that can be injected and also increase the potential of raising the formation pressure due to fluid leakoff.

Containment Zone

Above the target formation should be a *Containment Zone* which is composed of shales and sands which retard upward fracture growth and fluid flow. The shales should be relatively impermable, and the sands

should of sufficient permeability to absorb any upward fluid motion. The combination of sands and shales will tend to blunt fracture growth.

A containment zone should be considered in the planning process since it is likely that hydraulic fractures may grow above the target zone, especially in long-term projects. Project TTI 11 showed an example of this process (Figure 66). The initial target sandstone lay between 1372.8 and 1386.2 m. The storage zone of the waste grew from 13.4 m height initially to about 33.5 m midway through the project. However, the fracturing height increased no further to the end of the project, during which time an additional 60,000 m^3 of soils were injected into the formation. The storage and fracture zone height was monitored using gamma ray and temperature logs. The logs showed the storage zone quite effectively since the soils contained naturally occurring radioactive material (NORM) and the slurry was cooler than the natural formation temperatures.

SFI fracture growth remained limited in height in this example because the containment zone was composed of a series of thin sands and shales. Shales tend to limit fracture growth since they have higher horizontal stresses than sands and have higher stiffness. Thin sands would limit fracture growth since fracture fluid drains rapidly into them instead of remaining in the fracture. Mechanical slippage at the sand-shale interface may also halt the upward growth of a fracture tip.

Confining Zone

The *Confining Zone* overlies the containment zone and provides the final containment barrier between migrating injected fluids and overlying formations containing fresh water, oil, gas or other valuable formation materials. This zone should be an impermeable shale which is at least 20 to 50 m thick. This zone should also be extensive in area (>25 km^2) and relatively uniform in properties throughout this area.

To date, the confining zone has not been hydraulically fractured or shown evidence of permitting fluid migration into overlying zones on any SFI projects. When a shale layer is homogenous and continuous over sufficient area, it is an effective flow barrier. However, when wells are drilled through this zone, they can become highly conductive holes through the barrier fabric.

Well Site Considerations

An SFI well should be located in an area that is most advantageous based on geological concerns and minimum intersection of the target and confining zones by nearby wells. The well should be located in an area where target, containment and confining geologic zones described above are laterally extensive.

When determining the site of an injection well, an Area of Review should be established in which all natural resources are assessed. This assessment should establish whether or not SFI will have any impact on them and corrective procedures if necessary. The radius of the area of review about the injection well should be the greater of 3 km or the radius to which elevated formation pressures will exist during SFI which could potentially cause upward fluid migration.

Ideally, SFI wells should be placed in locations where no other wells are present within the radius of influence. The analytical and pseudo-3D fracture models indicate the fracturing half-length is at least 400 m. The preferred minimum interwell distance should be at least 800 m. If there are wells within the radius of influence, they should be well cemented throughout the injection interval and confining zone. These wells should then be monitored periodically with temperature logs to verify that they are not providing a pathway for waste injection fluid migration out of the injection interval.

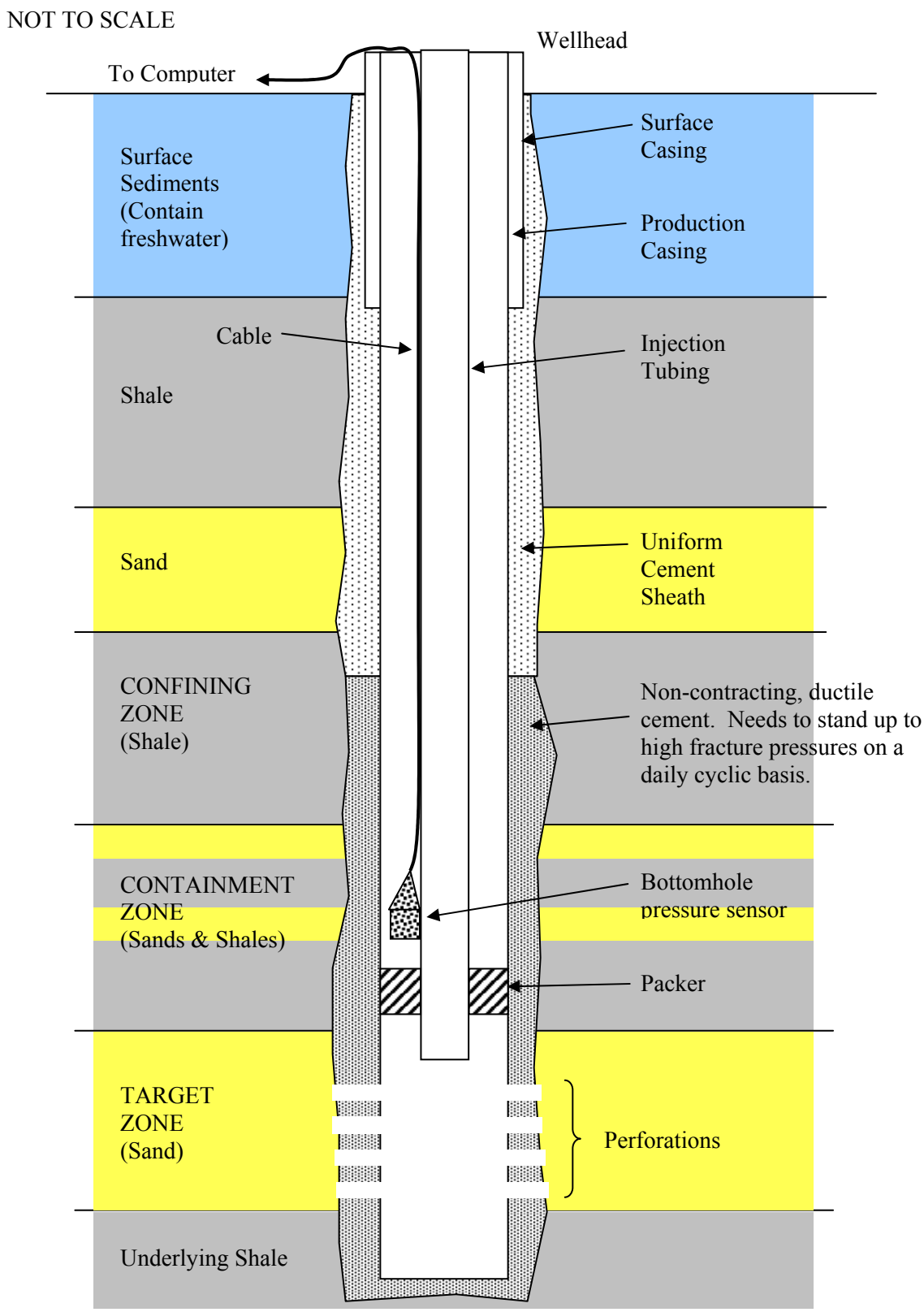

Figure 65: Suggested well construction guidelines

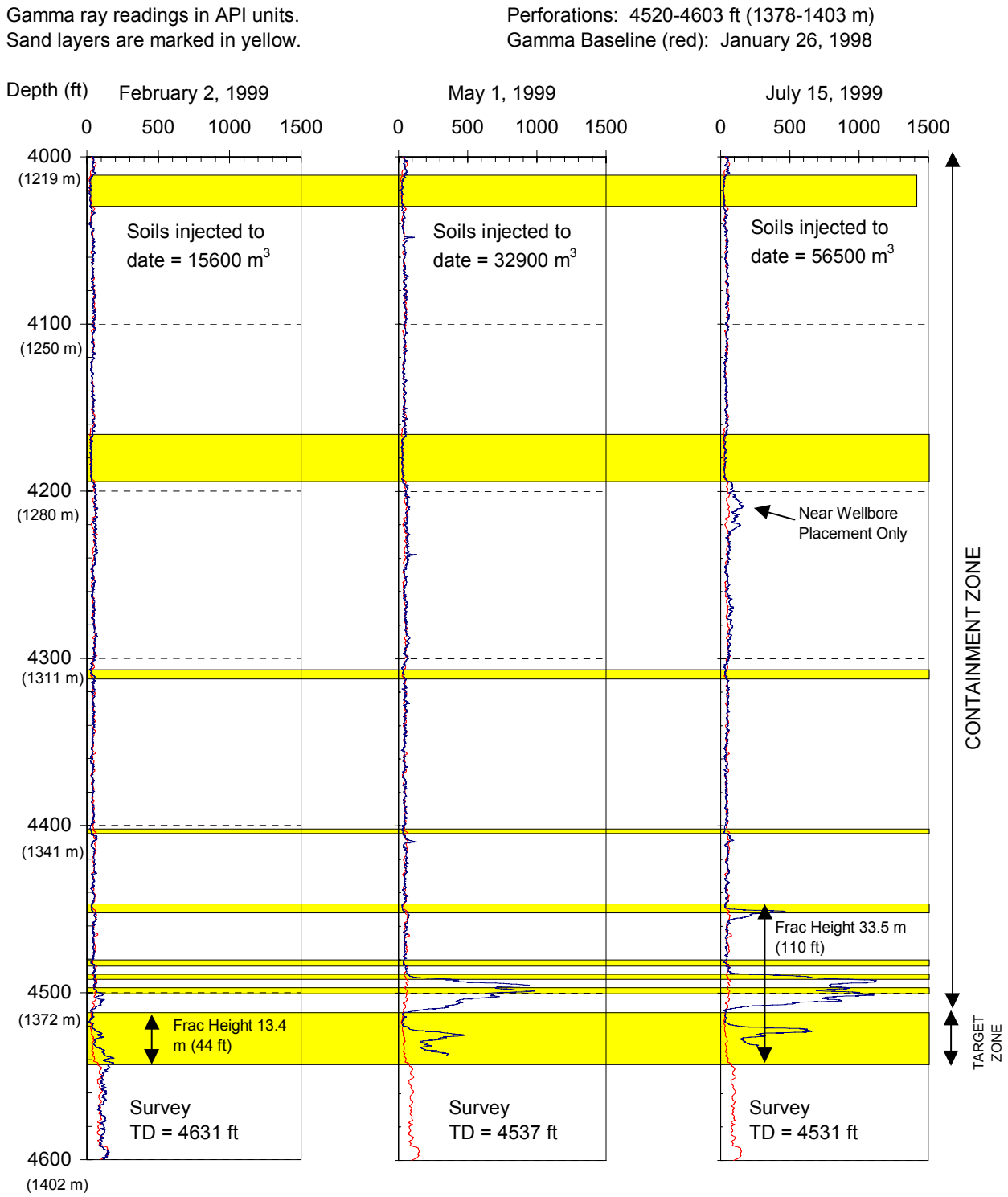

Figure 66: Fracture height growth into the Containment Zone, Project TTI 11.

Well Completion Guidelines

The injection well has to be completed in a manner that prevents fluid and waste communication between different geologic zones, and is also robust enough to handle multiple hydraulic fracturing episodes. Figure 65 shows a number of suggested guidelines for construction of an SFI well.

Well Cementing

The cement between the well casing and the surrounding rock is the weakest link in containing injected slurries in the target formation. The life expectancy of a well can be significantly increased if good or excellent cement bonds exist from 60 to 100 m above the target zone. This requires controlled drilling and cementing practices.

Drilling practices which can aid good cement placement are:

- Larger than normal hole should be drilled so a thicker cement sheath can be formed.
- A good mud circulation system should be used to keep the hole clean and minimize filter cake buildup.
- The hole should be cleaned of drill cuttings and filter cake prior to installing the casing using scrapers and conditioned mud.
- Varnish should be removed from the production casing prior to installation, to improve the cement bond to the steel.
- Centralizers must be installed frequently on the casing to keep it centred in the hole.

Cementing practices which can aid in forming a good bond are:

- A final cleanout of the hole with the casing in place should be performed with a viscous mud flush. The normal preflush immediately prior to cementing should be doubled in size, and followed by 5 m^3 of scavenger slurry.
- The cement should be made up using a continuous batch mixing method, to create a cement with consistent weight and strength.
- The casing should be rotated and reciprocated throughout the cement job to make cement placement throughout the annulus.
- Do not set weight on the casing until the cement has cured.

Since the wellbore in the target formation and the containment zone will experience the greatest changes in stress due to cyclic hydraulic fracturing, this part of the well should use cement with greater durability. The cement in this zone should be a low shrinkage, ductile/pliable cement, as opposed to a high strength, high shrinkage, brittle cement. The ductile cement need only be placed in the target zone and overlying containment zone as shown in Figure 26.

A cement bond log should be run once the cement has been cured. If extensive sections of poor cement bond exist in the containment or confining zones it may be necessary to perform remedial cement squeezes. Unfortunately, the success of squeeze jobs in improving the cement bond is not guarranteed, and may in fact weaken the integrity of the casing to cyclic hydraulic fracturing.

The necessity of a good cement bond around the injection well is demonstrated in the following example. In the gamma ray logs shown in Figure 27 it is possible to see that some NORM slurry was placed in the vicinity of 1280 m by July 15, 1999. Temperature logs showed no significant slurry placement in this location, so fracturing into the formation did not occur. The location of this NORM placement matched a

stretch of poor cement bond shown in the cement bond log. The slurry probably reached this poorly bonded section through a microannulus up the wellbore from the perforations. The microannulus was sealed thereafter since no further activity was observed at 1280 m.

Well Completion

Figure 65 shows a standard SFI well completion. A production casing with tubing and packer has proven an adequate design to date. The purpose of the tubing and packer is to prevent pumping and shut-in pressure cycles from acting on the casing. Pressure cycling could cause the casing to expand and contract which would weaken the bond with the cement. Microannuli could form which would create a flow pathway to overlying formations for slurry from the injection zone.

The production casing should be about twice the diameter of the tubing. The casing should be of uniform diameter throughout to minimize workover problems. Tubing diameter should be chosen based on the expected slurry flow rate. The diameter can be increased to reduce slurry flow friction.

Operating Guidelines

SFI operating procedures should be designed so that injection zone permeability and stress behavior is kept in control, and that injection well integrity is maintained.

Slurry injection should be performed in daily cycles of pumping followed by well shut-in. The injection period should be 8 to 12 hours in duration, followed by 12 to 16 hours of shut-in. The shut-in periods permit pressures and stresses to dissipate into the formation from the fractured zone. Pressure fall-off data collected during this time can also provide good indications of the state of fracturing and dissipation processes. Cyclic injection is preferred to continuous slurry injection over the course of weeks and months since more information is gathered about the formation state. Dangerous fracturing conditions can be predicted and averted more easily than when continuous operations are used. An example of continuous slurry injection interfering with other oilfield activities is described by Schmidt et al (1999).

Injection episodes should start with a clean water preflush to clean out the well and initiate hydraulic fracturing, followed by slurry injection containing the granular wastes. At the end of an injection episode a clean water postflush should be used to wash solids out of the well.

Formation response should be monitored to confirm that pressures are declining back to baseline reservoir conditions at the end of each injection episode, and that injection pressures are not increasing or decreasing signficantly from “normal” behavior. That is, maximum injection pressures should stay consistent to within about 10% over or above their average values, and formation pressure should recover to within about 10% of its initial value. If sustained, large pressure fluctuations occur, then corrective actions should be taken using insights gained from the SFI database and analysis efforts of this project. For example, Figure 39 illustrated how the relative mix of solid components might be varied to maintain injectivity without increasing shut-in pressure. Such operational changes are evaluated on a project-by-project basis.

Monitoring and Analysis Guidelines

Since extensive hydraulic fracturing occurs during SFI, significant monitoring and analysis should occur to confirm that waste placement is contained within the correct zone and that injection behavior and formation response is optimized. The monitoring systems typically used in SFI projects are shown in Figure 67 and summarized below.

Well Logging

Well logging can be used to determine fracturing and flow behavior as it is occurring near the wellbore. There two types of well logs: passive and active. Passive logging measures formation parameters around the injection well when no fluid injection is occurring. Active logging attempts to measure fluid flow and fracturing in the formation during pumping.

Passive logs can be used when the injected slurry has physical properties that are significantly different from the native formation. If the injected slurry contains radioactive materials, these will show up strongly in a gamma ray log. Temperature logs can be used when the injected slurry temperature is markedly warmer or colder than the natural formation temperatures.

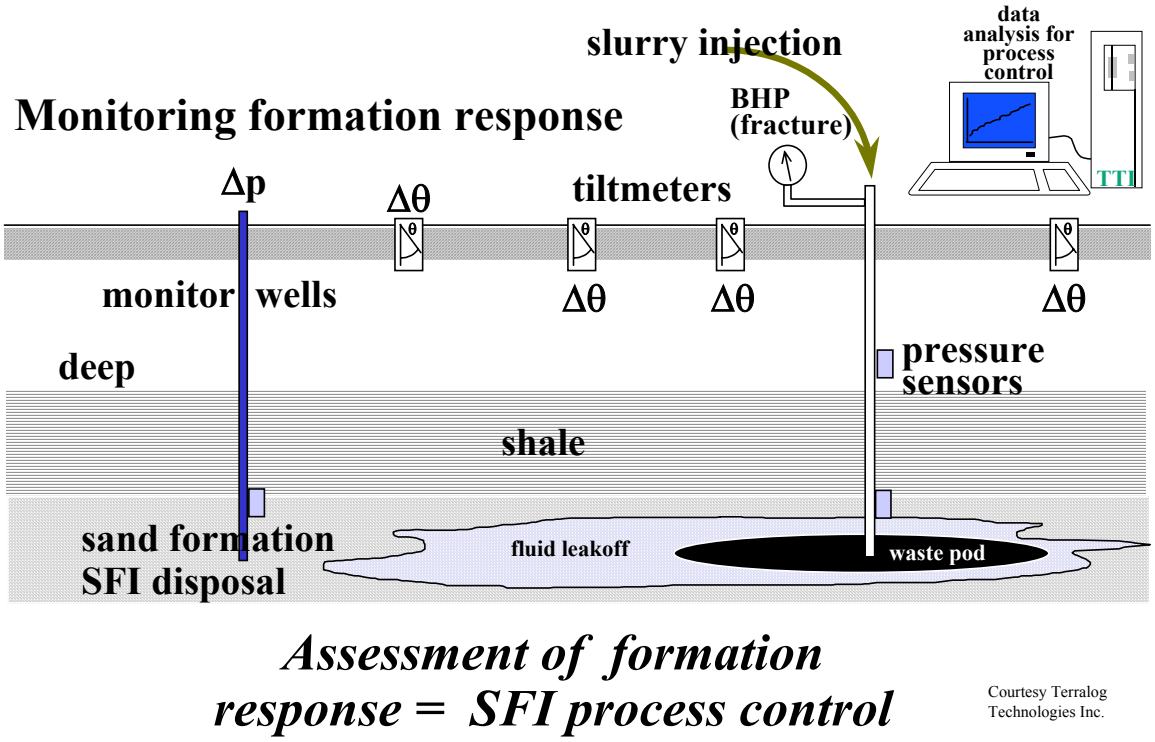

Figure 67: Techniques used to monitor the SFI process

Radioactive tracer logs are an active logging technique which can be used to determine if uphole migration of fluid is occurring. Water should be pumped through the injection well at the rate which

causes hydraulic fracturing. As this occurs, a small amount of radioactive Iodine-131 is released into the stream. A gamma ray tool is moved up and down in the well to observe the path taken by the tracer once it is into the formation. Tracer logs can also be used to determine how much fluid is passing through each group of perforations.

Whether active or passive logs are run is determined by the type of slurry material being injected. Logs should be run every two months or 50,000 m^3 of slurry injected in order to develop a good history of behavior lest odd fracturing events occur.

Injection Parameters

Continuous monitoring of the injection process must be performed so that the injected slurry can be characterized and the formation response can be determined. The critical measurements include: bottomhole pressure, wellhead pressure, well annulus pressure, injection flow rate, slurry density, and slurry volumes. Data from these sensors should be recorded with an electronic device, such as a datalogger or computer, which has battery power backup. Recordings should be made once every five minutes.

Notes by the site operators often provide information about operations that dataloggers cannot describe. These should be recorded daily and placed in an accessible library to aid in future analyses.

Bottomhole Pressure

Bottomhole pressure is the most important single parameter to measure, since it is the only sensor which is continuously observing the behavior of the formation. At minimum readings should be taken once every five minutes, and should be as frequent as once every 5 seconds during periods of rapid pressure change, as occurs at pump start-up and shut-down. A sensor with good accuracy is preferred (e.g. accurate to ±0.025% full scale), but this has to be balanced with the rapid readings and changes in pressure that can occur.

Analysis of bottomhole pressures can take the form of pressure fall-off analysis, or fracture analysis of injection pressures. From these analyses the permeability of the target formation and waste pod, fracture lengths, fracture closure stress, minimum principal stress, and formation fluid pressure can be determined. If possible, these values should be determined for each injection and fall-off period to determine how the fractures and waste pod are developing. These values and the raw pressures can be used as the basis of fracture modelling as discussed elsewhere in this report.

Formation Tests

Formation tests should be performed prior to the start of a SFI project and at regular intervals thereafter. These tests are used to determine the state of injectivity and stress in the formation and waste pod.

Step rate tests are performed to determine formation parting pressure and changes of in situ stresses. A step rate test is performed by injecting water at rates that step up every thirty minutes. Step rate tests should be run at regular intervals, at least once per month, to determine fracturing pressure and fracture extension rate. The step rate test program must use consistent injection rates and durations of each rate. A typical test program is:

Duration (min)	Water Injection Rate (m^3/min)
30	0.25
30	0.50
30	0.75
30	1.00
30	1.25
30	1.50

The step rate test is analysed by plotting the final bottomhole pressure of each rate period on a pressure vs. rate plot as shown in Figure 68. The initial steep slope of points indicates radial formation flow, and the flat or slightly positive slope indicates fracture flow. The point where these two lines intersect is the formation parting pressure, which is a good indicator of in situ stress. If a negative slope is observed, fracture height growth into overlying formations is occurring (Figure 69).

Injectivity tests are performed by injecting water into the formation at a rate below the fracture extension rate. This test is intended to determine the radial flow characteristics of the formation. A typical test would inject water at a rate of 0.25 m^3/min for 4 hours. The injection rate must be held absolutely constant to obtain good bottomhole pressure data. The bottomhole pressure data is analysed using semi-log and log-log plots, and if the data quality is good, can provide acceptable estimates of permeability and skin.

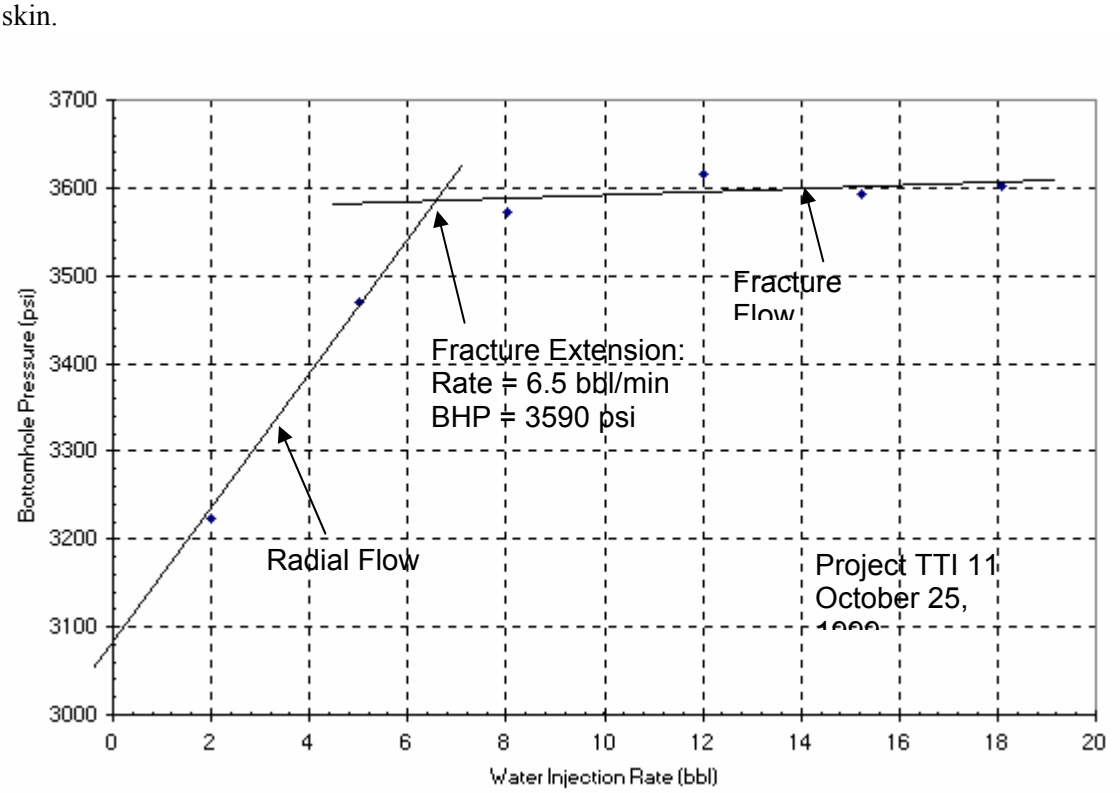

Figure 68: Example of a typical step rate test

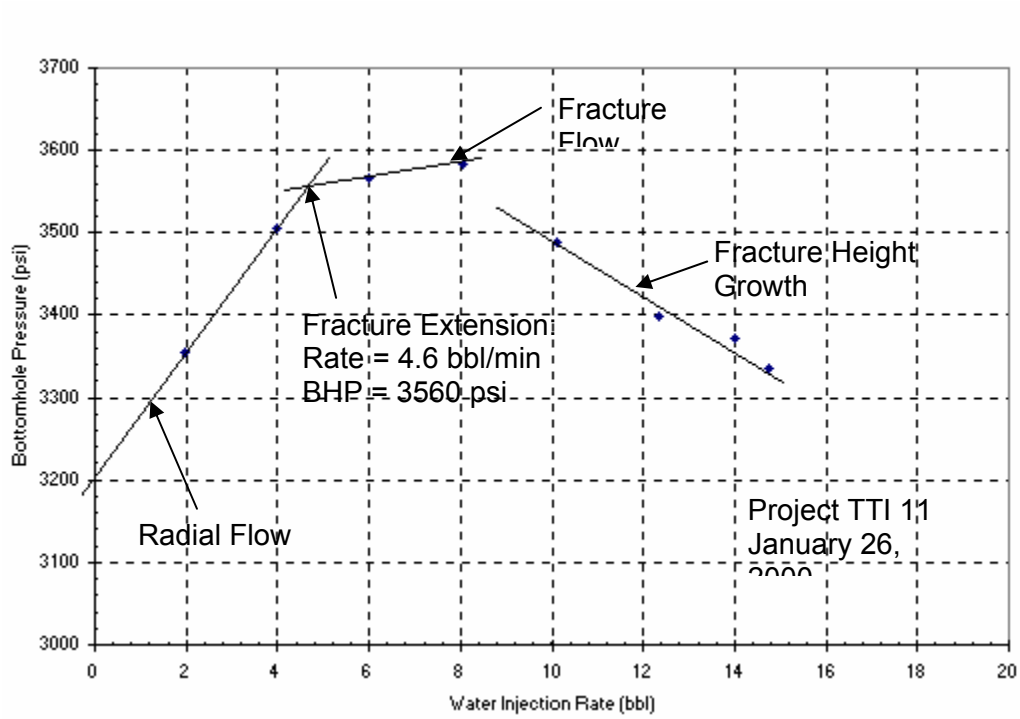

Figure 69: Example of a step rate test where fracture height growth is occurring

Pressure fall-off tests are performed by analysing the bottomhole pressure data recorded during any shut-in period immediately following slurry or water injection into the well. Pressure data should recorded at least every five minutes, and during the initial fall-off period the recording frequency should be every five seconds to capture the rapid pressure changes that occur. The data is analysed using Horner semi-log and log-log plots, which provides estimates of permeability, skin, and fracture length if linear flow is present.

Observation Wells

Observation wells can be useful to determine formation behavior at some distance from the injection well. The typical use of an injection well is to have a bottomhole pressure sensor to monitor the change in formation pressure over the course of a project. The observation well can also be used for mechanical monitoring systems such as downhole tiltmeter and microseismic arrays as discussed below. The observation well must be placed a sufficient distance away from the injection well that will not be intersected by hydraulic fractures, and must also have cement in good condition so that no upward fluid migration will occur.

Tiltmeter Systems

As a hydraulic fracture grows in a formation, it deforms the formation and slightly lifts the overlying earth. The pattern of deformation at the surface is characteristically unique enough that the fracture dip and azimuth can be easily determined. Other fracture characteristics such as location, depth, volume and length can also be determined, although with less numerical confidence. To measure the deformation at the surface of the earth an array of 12 to 16 tiltmeters should be placed around the injection well. The tiltmeter is analogous to a sensitive electronic carpenter's level which takes readings every 5 minutes.

Data from each tiltmeter is taken to determine the earth deformation during each injection episode and calculate the fracture parameters listed above.

Downhole tiltmeters are a recent development which allow much better resolution of the depths of the top and bottom of the fracture. This method requires an array of tiltmeters to be present in an adjacent observation well.

Microseismic Systems

Hydraulic fracturing causes tensile and shear failure of the sandstone fabric around the fracture to occur. These failure events are called microseismic events, and can be recorded with an array of accelerometers or geophones in nearby observation wells. The recorded microseismic events are processed to locate the source of each event and an image of the fracture geometry can be created. This technology is somewhat expensive and to date has not been used in long term SFI projects, although the costs may drop enough in the near future to make this a valuable tool.

Guidelines Summary

The guidelines recommended in this section are intended to make slurry fracture injection a process which maximizes the investment made into an injection well and facility, and also to provide good systems of providing and proving containment of the injected wastes in the target formation.

Good well drilling and cementing practices are critical in providing a good cement bond along the well. If a good cement bond exists, particularly in the 60 to 100 m above the target injection zone, the volume of slurry which infiltrates upwards is very small and the volume of waste which can be placed into the target formation can be very large relative to poorly cemented wells.

SFI is best performed as a cyclic injection process, with daily periods of injection and shut-in. This permits dissipation of pressures and stresses into the formation during shut-in periods. The pressure data collected during these cycles indicates the formation injectivity and stress conditions and can be used to predict future behavior. Continuous slurry injection does not permit dissipation processes to occur and little information is available to determine injectivity and stress states.

Well logging, bottomhole pressure recording and other monitoring and analysis techniques are crucial in determining the behavior of the SFI process. Monitoring and analysis provides information about the growth of hydraulic fractures and the waste pod, and confirms the containment of the injected wastes in the target formation. This feedback loop of information can then be used to direct future injection operations.

FIELD APPLICATIONS: PROJECT DESIGN AND PERMITTING

Guadalupe Field Slurry Fracture Injection

The Guadalupe oil field is located on the California Coast about 12 miles west of the City of Santa Maria. The field was first drilled in 1947. The field produces primarily from the Pliocene age unconsolidated Sisquoc Oil Silt and Oil Sand intervals which occur at a depth of about 3000 ft. Over 30 million bbls of oil were produced from the Guadalupe field over it's 50 year history. Most of the 215 wells (DOGGR, 1994) in the field were drilled between 1948 and 1974. The field has been shut in since 1995. All but four wells were abandoned between 1993 and 1995.

Production of the highly viscous crude oil from the field required the use of a number of secondary recovery techniques throughout the production history. Water flooding, steam flooding, and the introduction of diluent into production and well lines was typically used. Diluent, a diesel-like additive, was injected into production lines well annular spaces in volumes of two to three barrels for each barrel of oil produced. Large volumes of this diluent leaked from pipelines and storage facilities over a period of 40 years. The use of diluent to thin heavy produced oil ceased in 1990 and various remediation options, including slurry fracture, are have been proposed to regulatory agencies overseeing cleanup of the site.

Our geologic review evaluated the potential suitability of sand silt intervals within the Foxen, Sisquoc, Monterey, and Knoxville formations. We estimate solids injection capacity for these formations, taking into account net thickness, porosity, and permeability. Our well review included an analysis of historical completion practices throughout the field, with particular attention to cement coverage over potential injection intervals.

The generalized stratigraphy of the Guadalupe area consists of the Pleistocene Paso Robles formation, the Pliocene age Careaga, Foxen, and Sisquoc formations, the Miocene Monterey and Point Sal formations, and the Upper Jurassic Knoxville formation. Figure 70 presents the type section for the Guadalupe Field, as well as a field structure map and cross section.

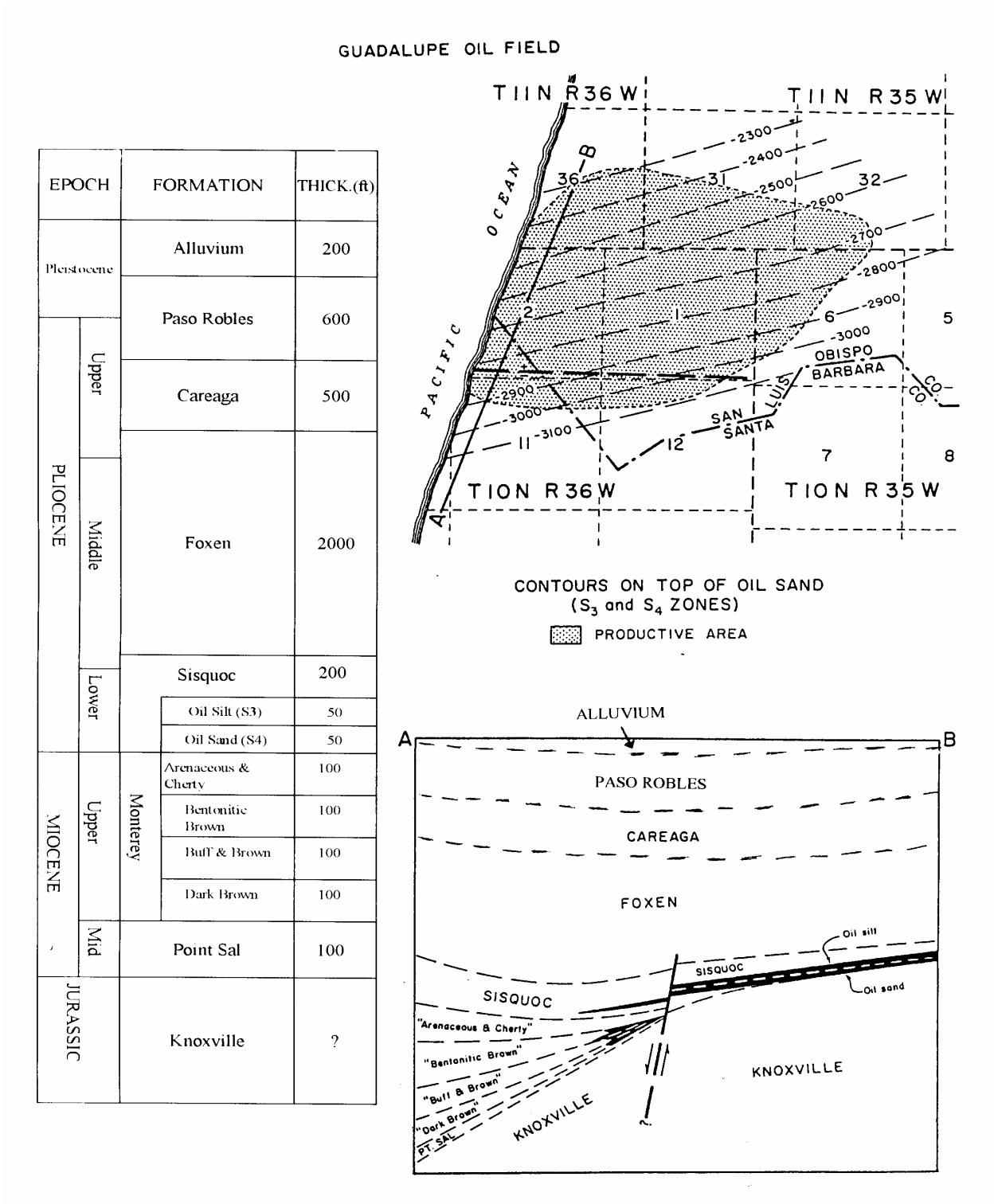

EPOCH		FORMATION		THICK.(ft)
Pleistocene		Alluvium		200
PLIOCENE	Upper	Paso Robles		600
		Careaga		500
	Middle	Foxen		2000
	Lower	Sisquoc		200
			Oil Silt (S3)	50
			Oil Sand (S4)	50
MIOCENE	Upper	Monterey	Arenaceous & Cherty	100
			Bentonitic Brown	100
			Buff & Brown	100
			Dark Brown	100
	Mid	Point Sal		100
JURASSIC		Knoxville		?

Figure 70. Type stratigraphy, cross section, and structure map for Guadalupe Field

We have evaluated four formations with respect to the appropriate geologic criteria for successful SFI. These are the Foxen, the Sisquoc, the Monterey, and the Knoxville formations. Volumetric calculations for the Guadalupe field yield approximately 2,938 acres (almost 1.3 x 10^8 ft^2) in the LeRoy lease. Table 10contains details of the volumetrics of the main producing zones of the Guadalupe field, the Oil Silt and Oil Sand units.

Table 10. Sisquoc Formation Volumetrics at the Guadalupe Field

Unit	**Volume (acre-feet)**	**Volume (yd^3)**
Gross Oil Silt	112,161	1.8 x 10^8
Gross Oil Sand	117,844	1.9 x 10^8
Net Oil Silt	13,880	2.2 x 10^7
Net Oil Sand	52,270	8.4 x 10^7

The average original reservoir temperature at a datum of 2,700 ft below surface (generally within the Upper Sisquoc) is 131ºF. The estimated original average reservoir pressure of the field in 1947 was 1,205 psi at the same datum. Average reservoir pressure in 1958 was 1,048 psi. Field pressures declined with time due to continued oil production, to a measured average of approximately 740 psi in 1976 (latest data available). The base of fresh water in the vicinity of the Guadalupe field averages 1,320 feet of depth.

There are a number of important criteria used in determining the suitability of a formation for Slurry Fracture Injection (SFI). These include:

- High permeability within the target formation with at least 50 ft of thickness,
- Porosity greater than 20%,
- Poorly consolidated formation sands which can be displaced easily by fracturing,
- The presence of a thick overlying confining unit that is impermeable and resists fracturing, and
- No nearby fault zones that may permit fluid communication to surface.

Both the Oil Silt and Oil Sand of the Sisquoc fit the above criteria, although each unit alone is on the lower end of what we would consider to be sufficient thickness to support injection of large volumes of waste. Collectively, the thickness of the productive Sisquoc zones in sufficient for sufficient volumes of waste injection. We estimate that an SFI well injecting into the Oil Silt through Oil Sand interval will accept about 200,000 yd^3 per well, assuming wells are spaced at least 2000 feet apart.

A significant advantage of these intervals is that they are underpressured due to over 40 years of oil production. Low formation pressure provides a reduced fracturing pressure and a natural pressure sink and containment zone for Slurry Fracture Injection operations. Overlying the Oil Silt and Oil Sand units is 250 feet of Sisquoc silts. Injection pressures and rates will be limited due to the limited vertical extent of these units. If large waste volumes (400,000 yd^3 or greater) were to be dedicated to an SFI project, a system of multiple wells could be considered to accommodate injection volumes into these thinner units.

The Foxen and the Knoxville formations are not viable candidates for injection due to inappropriate lithology or lack of sufficient localized lithologic data.

Overall, the stratigraphy and previous oil production operations in the Guadalupe Field indicate favorable conditions for use of SFI as a waste disposal technique. We recommend permitting the entire Sisquoc interval for injection. If substantial additional waste volumes are anticipated, further review of well data will indicate where a new well could be drilled to accommodate the added waste into the Sisquoc.

We also evaluated and compared the relative advantages and disadvantages of using one or more of the four existing water disposal wells in the field and the alternative of drilling one or more new wells for solids injection. Finally, we evaluated the costs to modify an existing well or drill a new well in the area, the capital costs for an appropriately sized slurry fracture injection system, and operating costs for a range of waste material volumes. Our review and analysis to date supports the following conclusions and recommendations:

1. The Oil Silt and Oil Sand units of the Sisquoc formation are sufficiently porous and thick to accommodate about 200,000 yd^3 of waste solids per well, assuming the wells are spaced at least 2000 feet apart. Slurry injection rates into these formations are anticipated to be about 250 cu-yds/day of soil and about 5000 bbls/day of water per well.
2. The Foxen, Monterey, and Knoxville formations do not seem to be viable injection candidates at this time due to low permeability and uncertainties with regard to their formation properties. There may be highly fractured sections of the Monterey and Knoxville which can provide useful injection targets, but current data is not sufficient for confirmation.
3. From a technical standpoint, the best option would be to drill a new well for waste injection. This well could be used to test the lower Foxen and upper Knoxville, and then completed for injection in the Oil Silt and Sand formations. The costs for drilling, testing, and completing such a well would be on the order of $350,000. In addition to solids injection capability, a new well operating at fracture conditions would provide about 5000 bbls/day additional fluid disposal capacity for the field.
4. Any of the four existing water injection wells at Guadalupe would also be suitable for SFI. From an injectivity and material logistics standpoint, the best candidate would be either well C4-A or YC-4. Re-completion costs for solids injection would be in the order of $100,000. In addition to solids injection, operating one of these existing wells at fracture conditions would also provide about 4000 bbls/day additional fluid disposal capacity for the field.

A slurry fracture injection project application was submitted to the EPA under the project XL program, and a subsequent application was submitted to the California Department of Oil and Gas under the Class II injection program.

South Ellwood Field Slurry Fracture Injection

The South Ellwood field is located offshore of the California coast, west of the City of Santa Barbara. The field was drilled and produced using the Platform Holly, which is located in 221 ft of water. The field was discovered in 1961 and first put into production in 1967. Initial production started with the Rincon Formation, and has produced over 8.3 million barrels of oil. The majority of production in the field has come from the overlying Monterey Formation. The Monterey Formation has produced over 49 MMBO sweet oil and 36 BCF sour natural gas (Venoco Internal Report). Oil and gas production is continuing, with 21 wells currently active in Leases 3120 and 3242. Venoco plans to drill two additional production wells from the Platform Holly in 2001. Disposal of drilling mud and drill cuttings by Slurry Fracture Injection (SFI) is proposed to minimize environmental impact.

The generalized stratigraphy of the South Ellwood Field area consists of the Pliocene to Recent Santa Barbara, Pico, and Repetto Formations; the upper Miocene Sisquoc Formation, the middle Miocene Monterey Formation, the lower Miocene Rincon Formation, the Vaqueros and Sespe Formations of Oligocene age, the Coldwater, the Cozy Dell, Matilija Formations and the Anita Shale of Eocene age on top of Cretaceous Jalama Formation and basement. Figures 71 and 72 present generalized stratigraphic columns and type logs for Blocks 3120 and 3242 respectively.

We have evaluated five formations with respect to the appropriate geologic criteria for successful SFI. These are the Monterey, Rincon, Vasqueros, Sespe and Coldwater Formations. The Monterey and the Rincon Formations as the primary target horizons for injection. There are no wells completed into the Vasqueros, Sespe and Coldwater Formations, and they are relatively deep, therefore these lower formations are more costly alternatives for SFI operations.

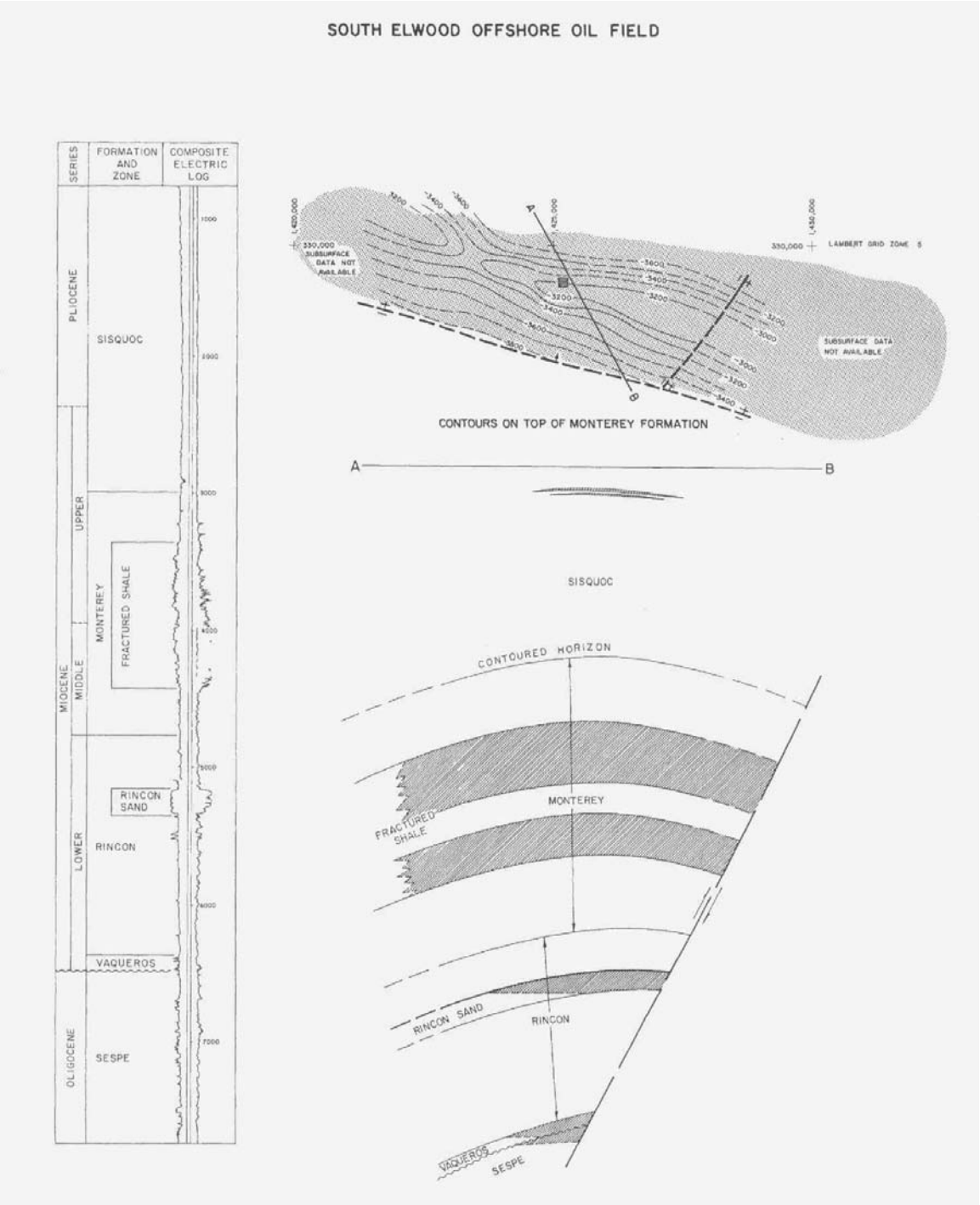

Figure 71. Geologic Map – Top Monterey Formation, Cross Section and Composite Electric Log for South Ellwood Field

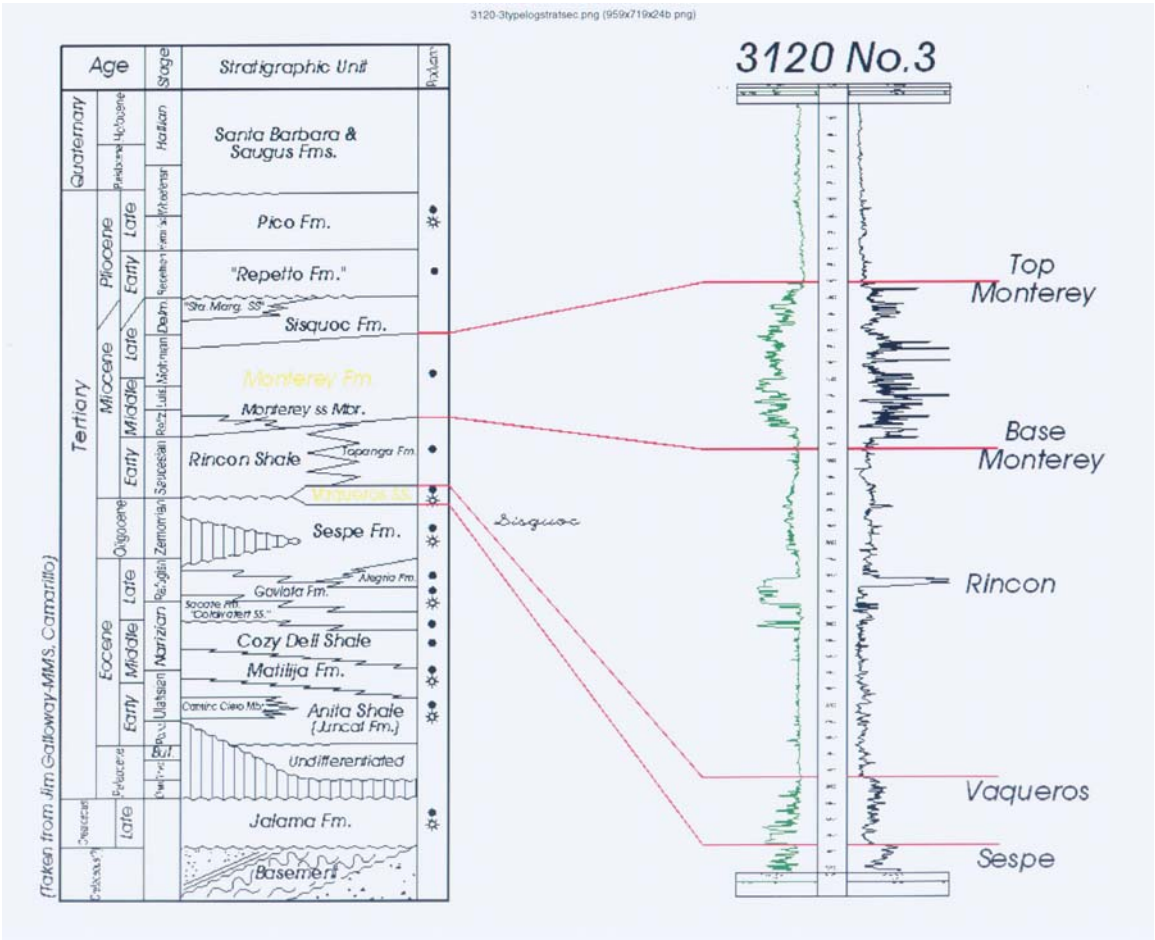

Figure 72. Type stratigraphic section and type log for South Ellwood Block 3120

The Rincon and Monterey Formations are identified as primary potential disposal targets. The best target is the Rincon Formation. The Rincon is underpressured (623psi). Low formation pressure provides reduced fracturing pressures, and a natural pressure sink and containment zone for Slurry Fracture Injection operations. The Rincon Formation is a well sorted turbidite sandstone with siltstone and shale interbeds. The interbedded nature of the turbidites provides good impermeable cap rock for the SFI project. Average porosity of the sand unit is 29% while permeability is about 150 millidarcy.

Field evidence from previous projects indicates that solids injection can create a fracture and dilation process zone extending up to 1000 ft from the well with an aspect ration of about 2 to 1 in the direction of maximum stress. Multiple injections create multiple fractures at varying orientation and an extensive dilation zone. About 2% to 5% of the available porosity compacts and accepts solids. Assuming an average 150 ft sand thickness, a single well completed within the Rincon Formation can handle in excess of several hundred thousand barrels of injected waste (much more than needed for this project).

A second potential target is the Monterey Formation, a fractured siliceous formation about 1000 ft thick. Average porosity is about 20%, but it is not interconnected, so that matrix permeability is very low (on the order of a few millidarcies or less). Taking into account fractures common in the Monterey, bulk permeability increases to about 50md. This is on the low end conditions necessary for quick leakoff and limited fracture growth during SFI operations. Since the anticipated volumes for waste injection are

relatively small (mud and cuttings from two wells), a fractured interval of the Monterey might be viable for waste injection, but with some risk.

There are no wells completed into the deeper Vasqueros, Sespe and the Coldwater Formations. Hence for economic reason, these three formations are not viable candidates for slurry injection.

In summary, the stratigraphy and previous oil production operations in the South Ellywood Field indicate favorable conditions for use of SFI as a waste disposal technique. We recommend permitting the Rincon interval for injection.

Terralog also analyzed historical completion practices throughout the field, with particular attention to cement coverage over potential injection intervals. Thirty wells are present at the Platform Holly. Many of these wells were re-drilled one or more times to access new production horizons. Twenty-one wells are currently producing oil or gas. Two wells are currently being used as gas injection wells. The remaining seven wells are shut-in.

Of the seven non-producing wells, Well 3120-04 is the best suited for SFI operations. The advantages of using this well are:

1. It has existing perforations in the Rincon formation.
2. The Rincon formation is composed of thick sands of high permeability (~150 md) and high porosity (29%) which are best suited for SFI.
3. No other active wells are present in this zone aside from gas injection well 3120-05.
4. Perforations are present in the Sisquoc, Monterey and Rincon formations, but a tubing and packer can be set so that cuttings are injected into the Rincon only.

The disadvantage of using this well is that it will need to be recompleted prior to SFI to remove the current tubing and electric submersible pump (ESP).

No cement bond log could be found for this well, but casing cement was placed in the Sisquoc, Monterey & Rincon zones (Table 3). Two cement squeezes were also performed to improve cement bond in the Sisquoc (3190 ft) and Rincon shales (5400 ft). The existing cement should be in sufficient condition for a small volume SFI project.

Our geologic and well review and analysis to date supports the following conclusions and recommendations:

1. The Rincon sand is the most suitable target for slurry fracture injection of the drilling wastes. It is a 150 ft thick sand of high porosity (29%) and fair permeability (155 md). It is overlaid by Rincon and Monterey shales of about 700 ft thickness, which will provide good containment of the injected wastes. It is also underpressured due to oil and gas production, which will aid fracturing and containment processes.
2. Because the anticipated waste volume is relatively small, the Monterey formation may also be used for small volumes of cuttings disposal if necessary, but with some risks. The Monterey consists of thinly interbedded layers of fractured chert, porcelanites, silceous shale, dolomites, and mudstones. Matrix permeability is only on the order 0.1 to 1md, and even taking into account fractures bulk permeability of this zone is only in the range of 2 to 50 md. Low permeability inhibits fluid leakoff after fracture injection, and results in long-thin fractures rather than thick fracture and dialation zones within permeable sands. The containment ability of the upper Monterey is not well known, and hydraulic fractures may enter the Sisquoc formation.
3. The best well for cuttings injection is Well 3120-04, assuming it is recompleted to inject materials into the Rincon formation. This will require a tubing and packer assembly set to

5720 ft depth to isolate the Rincon perforations from the Monterey perforation. Current perforations within the Monterey formation can either be isolated with an uphole packer, squeezed, or left open and used for monitoring (subject to approval by the Division of Oil and Gas).

A second option is to inject cuttings into Well 3242-17. This well has existing perforations in the M1 Monterey zone. Unfortunately, there is a fault immediately adjacent to the perforations, which may permit upward movement of injected materials. If this option is pursued, the Monterey and Sisquoc formations should be permitted for cuttings disposal.

A Class II injection permit was prepared for both wells 3120-4 and 3242-17 on behalf of Venoco Inc in August, 2001.

Aliso Canyon Field Slurry Fracture Injection

The Aliso Canyon Field is a multi-zone reservoir with commercial oil and gas production from five producing intervals (Aliso, Porter, Del Aliso, Sesnon and Frew) varying from 4,000 to 8,000 ft. in average depth. This field is a southeasterly plunging anticline with structural closure on the south and east, fault closure on the north and west. The Santa Susana fault on the north has a vertical displacement of about 5,000 feet and a horizontal displacement of about 2-3 miles. The Santa Susana fault thrusts Miocene sediments over Pliocene strata and dips from 15 to 80°. A structure map and cross section for the field is presented in Figure 73.

The uppermost producing zone, the Aliso formation is Upper Pliocene age and comprises of poorly sorted, medium to coarse-grained sands with occasional pebbles. This clastic package is approximately 650 to 700 feet thick with average net sand thickness of about 100 feet (DOGGR, 1991). The formation is divided into numerous sand intervals, A1-A42, some with their own oil/water contacts. Porter #27 was the first well completed in the Aliso formation with initial production at 510 barrel per day of 16.5°API oil. Present average production per well has dropped to 30 barrels of oil per day.

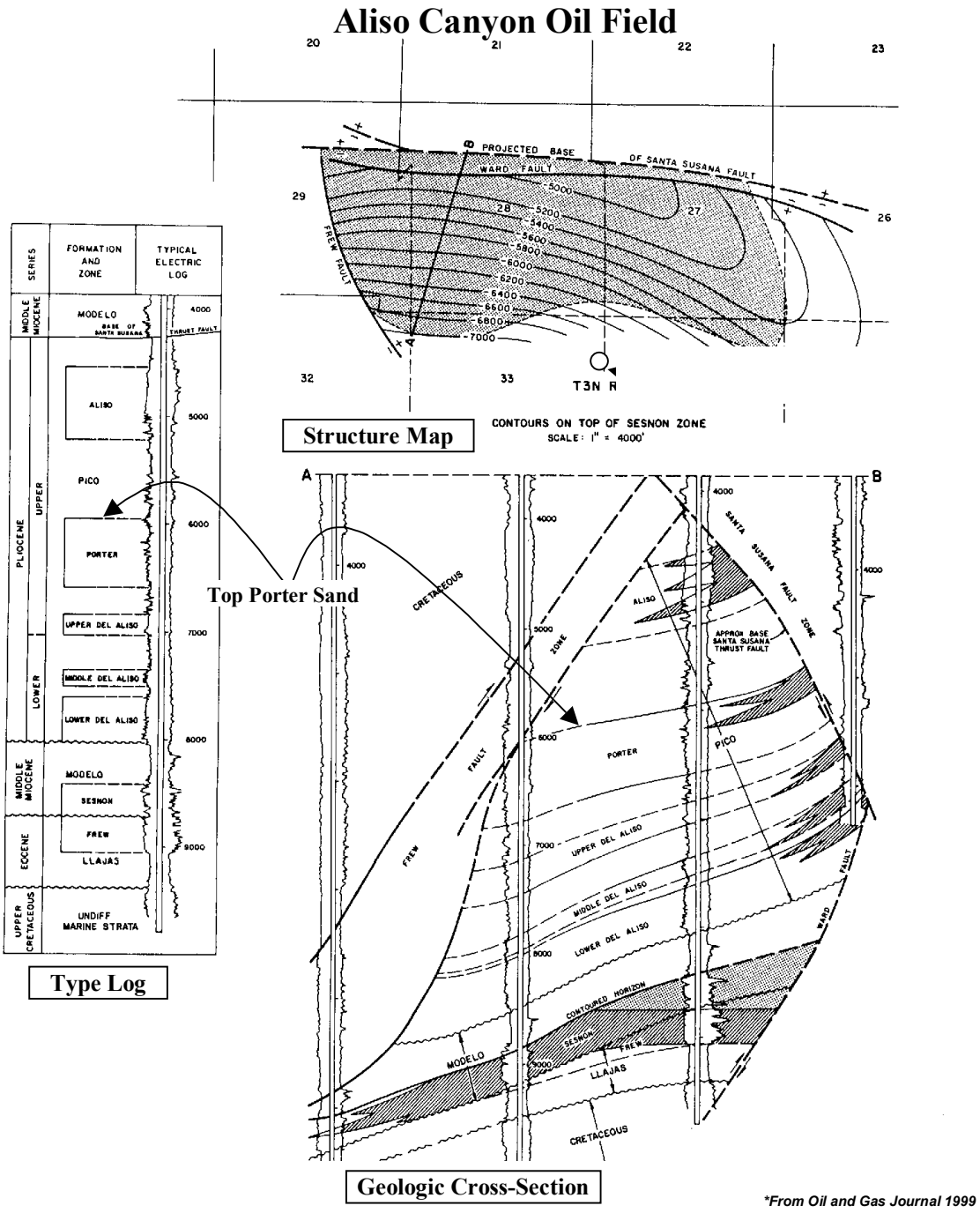

Figure 73. Geologic structure map and cross section of the Aliso Canyon Field

Our geologic review evaluated the potential suitability of the Aliso and Porter formations. We estimate solids injection capacity for these formations, taking into account net thickness, porosity, and permeability. Our well review also included an analysis of historical completion practices throughout the field, with particular attention to cement coverage over potential injection intervals.

We evaluated and compared the relative advantages and disadvantages of using one or more of the existing water disposal wells or idle production wells in the field and the alternative of drilling one or more new wells for solids injection. Finally, we evaluated the costs to modify an existing well or drill a new well in the area, the capital costs for an appropriately sized slurry fracture injection system, and operating costs for a range of waste material volumes. Our review and analysis to date supports the following conclusions and recommendations:

1. Both the Aliso and Porter formations are sufficiently porous and thick to accommodate in excess of 250,000 yd^3 of waste solids per well, assuming the wells are spaced at least 2000 feet apart. Slurry injection rates into these formations can anticipated to be as high as 300 cu-yds/day of solids and about 5000 bbls/day of water per well.
2. The Porter formation is highly depleted, providing a good pressure sink and containment mechanism. The formation thickness ranges from 600 to 800 feet, and is capped by an impermeable shale interval of at least 300 feet in thickness. The average permeability is on the order of 500md and the porosity ranges from about 23% to 30%. Typical depths, however, are on the order of 6000 to 7000 ft. This would increase pressure and horsepower requirements for slurry fracture injection in comparison to shallower targets.
3. The Aliso formation is also depleted, providing another pressure sink and good containment zone. The gross interval thickness is about 600 feet and provides a good combination of interbedded shales (to act as vertical migration barriers) and high porosity sands (to act as pressure sinks inhibiting vertical migraiton). The formation depth lies from about 4000ft to 5000ft across the structure, sufficiently deep to be well isolated from near-surface fresh water yet not too deep to require excessive pumping pressure.
4. We recommend that existing well #43 be used for waste injection at this site. This currently abandoned well is situated downdip of the present oil/water contact and can be re-entered and completed for injection into the Pliocene Aliso formation at approximately 4800 ft depth.

A permit application for injection at Aliso Canyon has been prepared for the Department of Oil and Gas. We examined and provided casing diagrams for all wells within a ¼ mile radius of the proposed injection well. We identified wells to be used for monitoring, and described an appropriate operating plan. About 20,000 barrels of mud and cuttings has been proposed for injection into the Aliso formation over a period of about one month. Proposed monitoring tools include continuous down-hole pressure recording, daily pressure fall-off analysis, periodic temperature and tracer surveys at both the injection well and offset monitoring wells, and periodic step-rate tests.

THUMS LONG BEACH SFI OPERATIONS AND ANALYSIS

Field Overview

The Wilmington Oil Field in the Los Angeles Basin is the fourth largest oil field in the Contintental United States. It has an extensive history of oil production as well as a long history of successful high-volume oilfield waste injection (Hainey et al, 1997). The THUMS Long Beach Company, currently a subsidiary of Occidental Petroleum, operates the offshore portion of the Field. Since its inception in 1965, THUMS has produced more than 800 million barrels of 17.6 API gravity crude petroleum from more than 1000 wells. At peak production in July 1985, THUMS produced 110,000m barrels of oil per day (Berman and Clarke, 1987). Production is currently about 38,000 barrels per day.

In order to recover the large oil reserves (over 900 million oil in place) under the City of Long Beach and the adjacent tidelands, 4 offshore islands were built by THUMS in 1965 and 1966. The islands were named after the 4 astronauts who lost their lives in the U.S. Space program; Grissom, White, Chaffee and Freeman. These islands have a surface area of about 10 to 12 acres each. Slurry Fracture Injection Operations are conducted on one of these, Island Chafee, shown in Figure 74.

Figure 74. Offshore Island in Long Beach Harbor includes production wells and slurry injection operations.

Local Geology and Reservoir Characterization

The petroleum reservoirs of the Long Beach Unit are found within 5 fault blocks and 7 zones. These are the early Pliocene Tar and Ranger zones, and the late Miocene Upper Terminal, Lower Terminal, Union Pacific, Ford and 237 zones. About 5000 feet of upper Miocene Puente formation was deposited in a deep-water turbidite environment (Berman and Clarke, 1987). Episodes of folding resulted in emergence, erosion and non-deposition. Deformation continued until early Pliocene where about 1000 feet of Repetto formation were deposited in a shallow marine environment. By mid Pliocene time, the area was eroded to peneplanation; all subsequent layers (approximately 1400 feet of San Pedro and Pico formations) were deposited almost horizontal to the lower Pliocene unconformity.

Structural contours on the Top of the Ranger zone are presented in Figure 75. A stratigraphic Column for the Long Beach Unit is presented in Figure 76. A summary of reservoir and fluid properties is presented in Table 11.

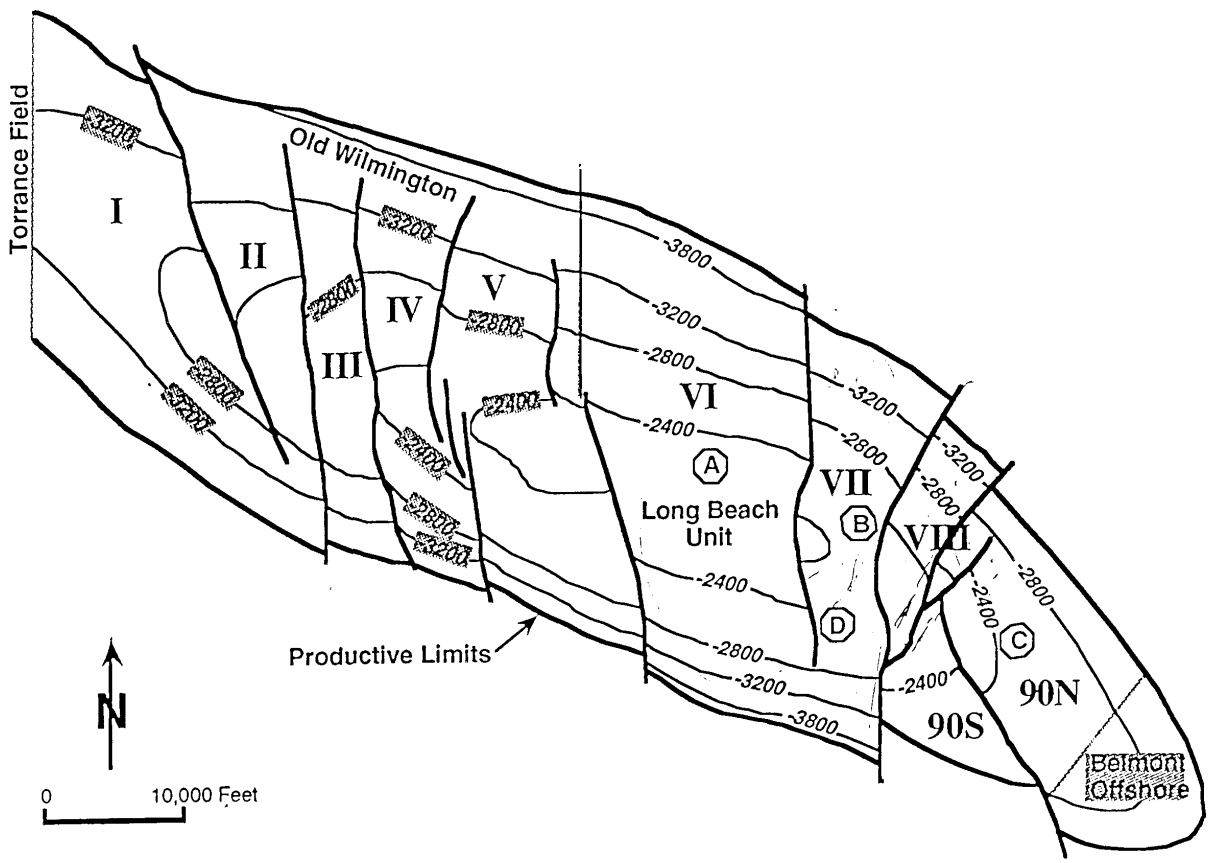

Figure 75. Top of Ranger zone structure map
(Norton and Otott., Jr., 1996)

AGE	Million Years	FM.	THICK (feet)	ZONE	LITH.	SUBZONES
Pleisto-cene	1.8	San Pedro	1400			
Upper Pliocene		Pico				JF,KF *Up Repetto unconf.*
Lower Pliocene	5.3	Repetto	500			
			150	Tar		So,S,T,U DU
			300	Upper Ranger		F1,F_0,F,H,X
Miocene / Pliocene		Puente	300	Lower Ranger		G,G4,G5,G6
			650	Upper Terminal		HX1,HX_0,HX,HXb,HXc,J,Y,Y4K,Z,WA
			600	Lower Terminal		AA,AB,AC,AD ADI
			900	Union Pacific		AE,AF,AI,AK1 AK,AL1,AM
			1200	Ford		AO,AO1,AR,AR1,AU,AU2.AV,AX,AY,AY1,AZ
			1200	237		BA,BB,BC
Middle Miocene	16.4	Monterey				
?		Catalina Schist				

Figure 76. Stratigraphic Column of the Long Beach Unit, Wilmington Oil Field (Norton and Otott., Jr. 1996, Clarke and Henderson, 1987, Plate 1)

Table 11. Reservoir and fluid properties

	Tar	Ranger	Upper Terminal	Lower Terminal	Union Pacific-Ford	237
Porosity (%)	28	25	26	23	18	10
Permeability (md)	280	230	280	220	27	5
Water resist. (ohm/m@75°F)	.27	.22	.22	.20	.23	.30
Initial water saturation	31	33	24	27	40	--
Initial FVF	1.01	1.085	1.056	1.092	1.24	1.54
Initial GOR (cf/bbl)	100	133	156	162	437	850
Initial oil gravity (°API)	12.5	15-20	19	20	28	35
Oil viscosity (Cp@100°F)	1380	30	32	12	1/05@278°F	1/05@278°F
Reservoir Temp. (°F)	106	145	170	189	200	270
Initial Press. (% hydrostatic)	60	76	64	90	100	100

(Berman and Clarke, 1987)

Local Stress Analysis

The stress orientation in the Long Beach Unit is assumed to be consistent with the Los Angeles Basin's regional stress orientation with a maximum horizontal stress in NE to NNW direction. High casing pressure and flow was discovered in one of the THUMS' monitoring well (C-130) approximately 1596 ft away from the injection well, with pressure fluctuations consistent with those of the disposal well (Hainey et al. 1997). After analysis, an induced fracture in the Lower Terminal, AD sand bearing N33.4°E was discovered. Previous estimates of induced fracture orientation (from ASR, DSA and borehole ellipticity) ranged similarly from N2.1°E to N25°E (Hainey et al., 1997). The observation is consistent with the Los Angeles Basin NE to NNW regional maximum horizontal direction deduced by Zoback and Zoback, 1980; Zoback, 1992; Hauksson, 1990; and Jones, 1988 (in Wilde and Stock, 1997).

Slurry Fracture Injection History

Each year the THUMS drilling program and production operations generate about 90,000 barrels of waste, most of which is disposed by slurry fracture injection operations on Island Chafee. Slurry injection of tank bottoms, drill cuttings and mud, fracture sands and oily waste started in 1994 (Hainey et al, 1997) and have operated continuously since then. Approximately 1.9 million barrels have been injected into the Lower Terminal AD, AC, and AB sands with a single well, C822I. Table 12 presents a summary of injection volumes into each formation through 2001. Table 13 presents a summary of injection well and slurry specifications.

Table 12. Total Volume Injected and Waste Composition

	AD Sand (bbls)	AC sands (bbls)	AB sands (bbls)
Drilled cuttings	29,436	56,237	87,422
Clay waste	85,403	314,064	585,689
Tank bottoms	37,307	210,054	337,652
Injection water	25,211	58,394	105,614
Waste water		38,172	1,870
Total injection	177,357	636,246	1,116,600

Table 13. C-822I Well and Slurry Specifications

Average Injection	20,000-25,000 bbls/mn
Rate of Fluid Injection	2.9-5.9 bbls/min
Surface Pressure	2,534-2,905 psi
Downhole Pressure	4,117-5,161 psi
Slurry Density	8.3-11.2 ppg
DOG approved gradient	0.94 psi/ft
Max. hole angle	27.5° at 2049 ft MD
Viscosity	70 – 90 s/qt
Yield Point	20 – 30 lbf/100 ft^2
Gel Strength	10 – 20 lbf/100 ft^2
Solid Content	18 – 25%

Approximately 20,000 to 25,000 barrels of slurry wastes are injected each month. Slurry wastes are transferred by boat from the four THUMS islands and Pier J (Figure 74), and also any waste locally generated by production operations on Island Chafee (Figure 77). The process starts with drill cuttings and other dry waste feeding into a shale shaker to remove any large debris. The dry waste is then dumped into the first of the two 50-barrel mixing tanks, with jets and agitators. The cuttings are slurrified by pumping 20 to 25 barrels of water into the mixing tank and broken down by continuously circulating until viscous slurry is obtained. The mixture is then transferred to the second 50-barrel tank for further shearing (Figure 78). When the slurry is near the target specifications listed in Table 3 below, the slurry is then transferred to a 200-barrel holding tank (Figure 79). The slurry is run over a final 10-mesh shale shaker before injecting down hole. The operation runs only in the daytime. The formation is allowed to relax and reduce pressure each evening before the next day of injection.

Figure 77. Drilling rigs on Island Chafee produce cuttings and mud waste requiring disposal.

Figure 78. Slurry processing system includes two 50 barrel tanks for shearing and slurrification.

Figure 79. 200 barrel holding tank for final mixing prior to injection.

DOE Research Project Description

In February 2002, THUMS and Terralog Technologies agreed to apply some of the analysis tools developed through this DOE project to new slurry fracture injection operations into the AA sands. New perforations were added over depth interval from 4670 to 4680 ft. The completion diagram for injection well C-8221 is presented in Figure 80. The project objectives were to evaluate potential changes in formation stiffness and permeability with episodic injection, and by taking such changes into account to accurately match injection pressures and subsequent fall-off behavior. Pinnacle Technologies provided analysis support for this effort, using the FracproPT simulation software.

C-822I Well Completion

The well completion for C-822 is summarized from Berman and Clarke (1987) and THUMS Internal Reports. C-822 was drilled in 1968 to a total depth of 7768 feet (measured depth). A 20" conductor pipe was driven to approximately 90 feet. An 18 5/8" hole was drilled to the base of brackish water sands at 1610 feet (measured depth) and cemented with 13 3/8" surface casing. The surface casing was cemented to the surface with 1400 sacks of cement. Then a 12 ¼" deviated hole was drilled to the top of the completion interval at 5370 feet (measured depth). An 8 5/8" production casing was cemented with drillable cement to the top of the completion interval. The completion interval was drilled with a 7 5/8" bit to 7768 feet total depth. A 6 5/8" slotted liner was hung from 5252 feet (measured depth) and completed in the AF to BA sands within the Union Pacific and Ford zones.

In September 1994, C-822 well was permitted as an injection disposal well (C-822I). The 6 5/8" liner was plugged with cement. The 8 5/8" casing was perforated for slurry injection. C-130 is the designated monitoring well as mandated by the Division of Oil and Gas. C-130 and C-822I are approximately 300 feet apart at the surface location and 1600 feet apart at the AD sand.

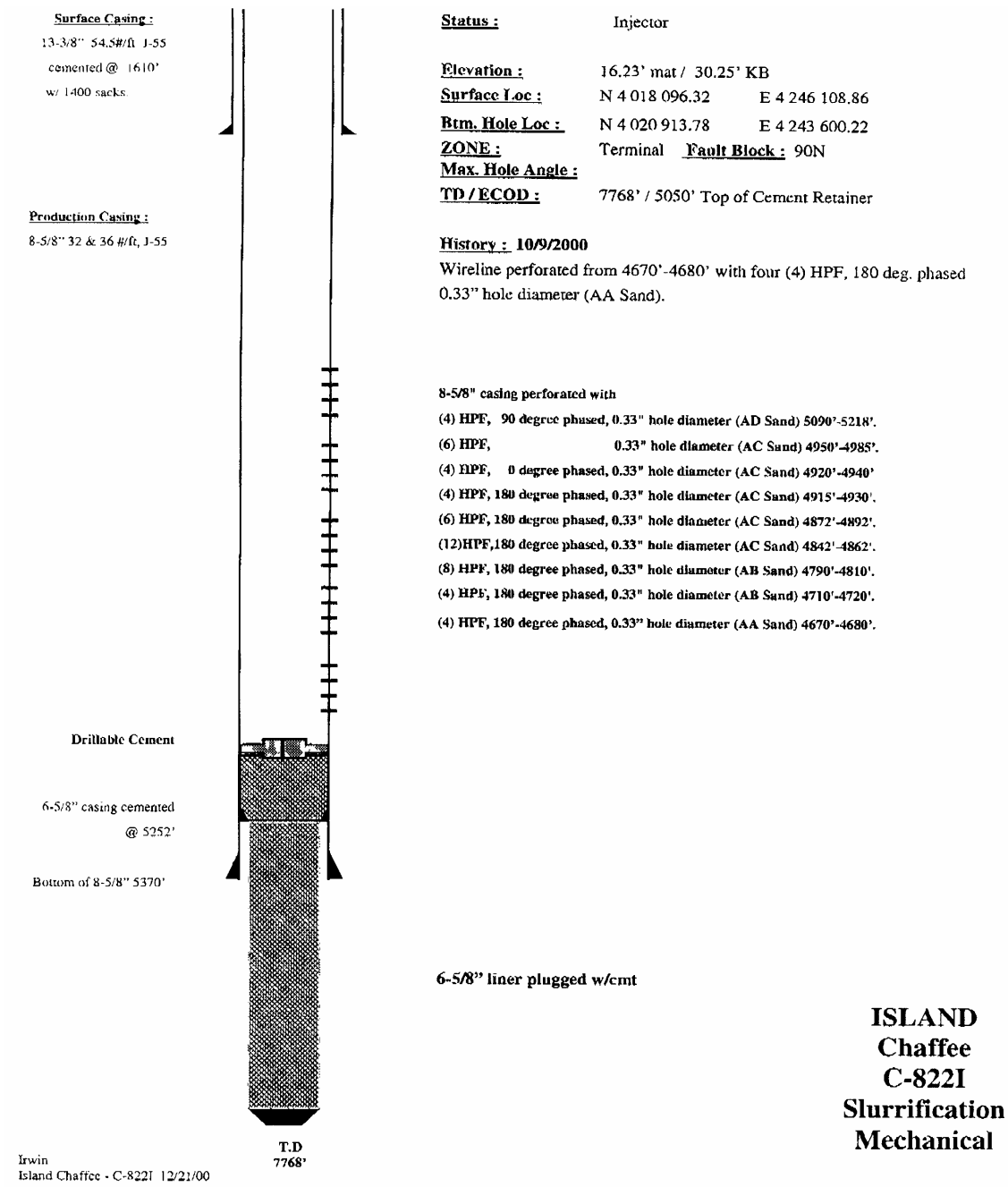

Figure 80. C-822I Well Completion Diagram

AA Sand SFI Operations

Terralog visited Island Chafee and analyzed injection in the AA sands over a two-week interval in February, 2002. Recorded data, as illustrated in Figure 81, included density, flowrate, tubing pressure, bottom-hole pressure, and annular pressure. Figures 82 and 83 present detailed treatment data for the period from February 18 to February 26.

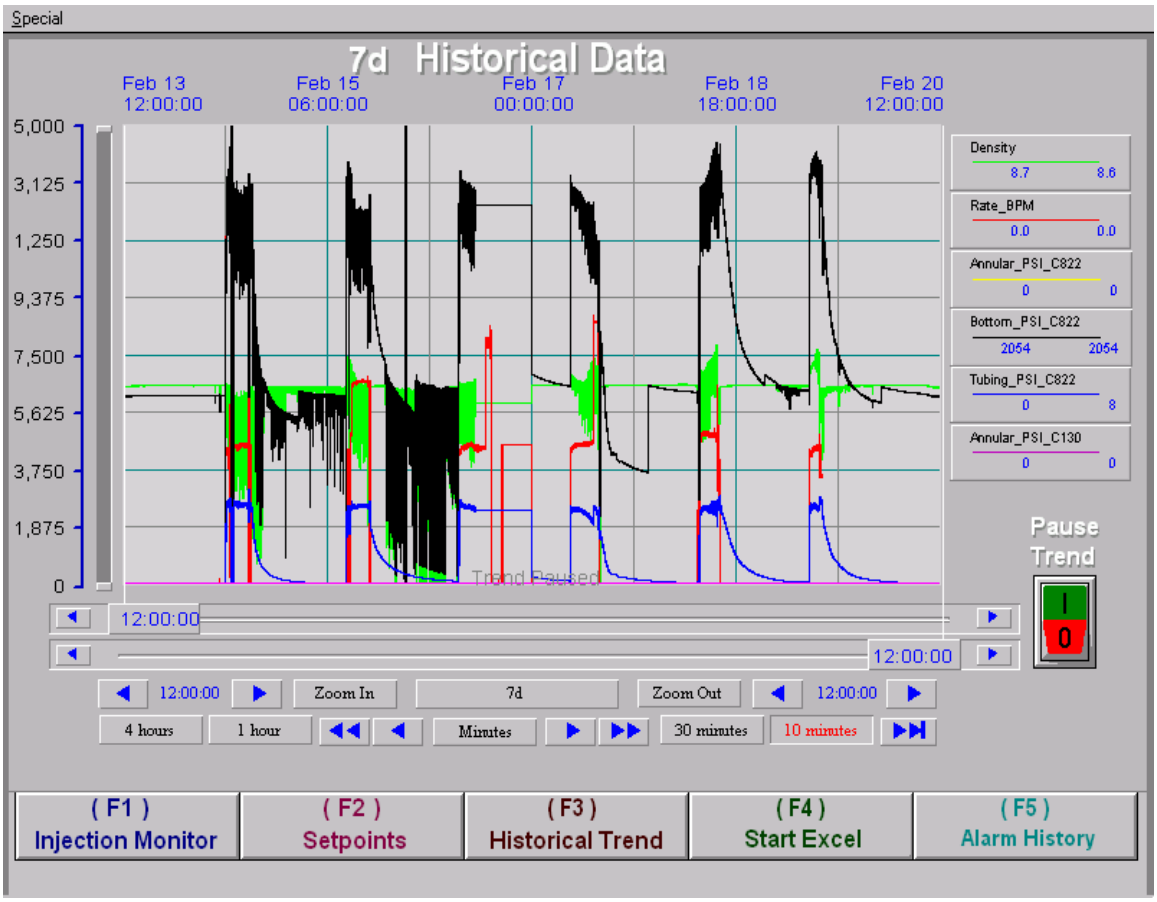

Figure 81. Injection monitoring software for THUMS SFI operations.

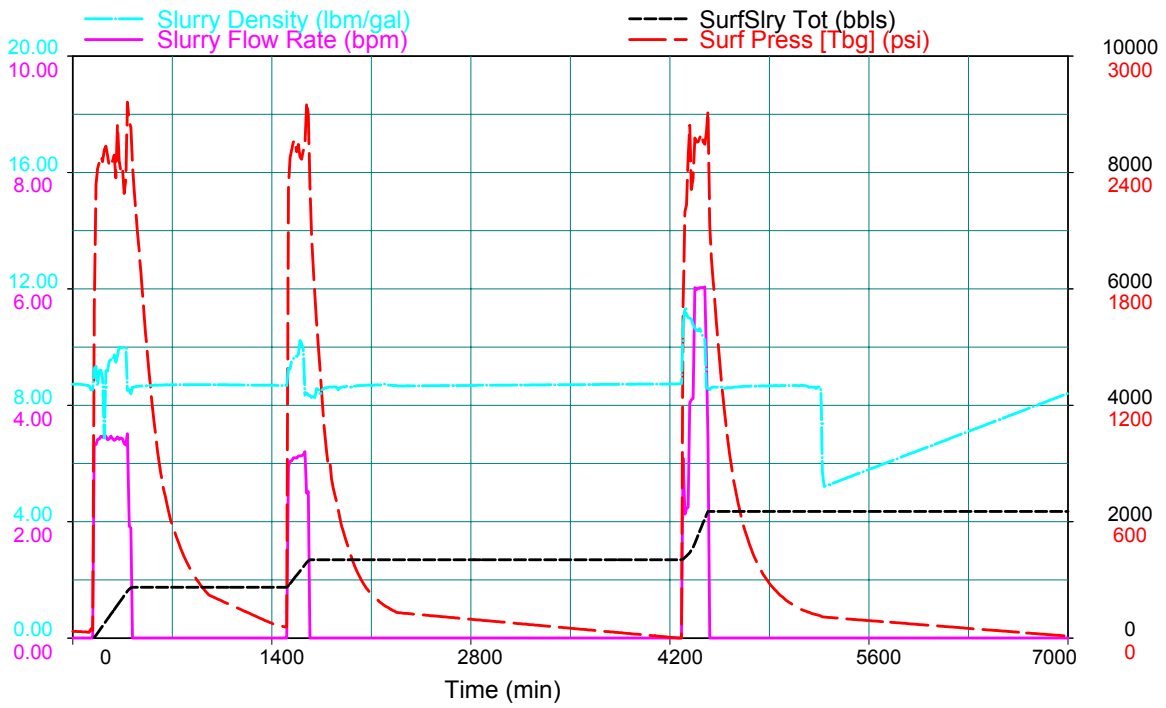

Figure 82: Treatment Data for February 18, 19 and 21, 2002.

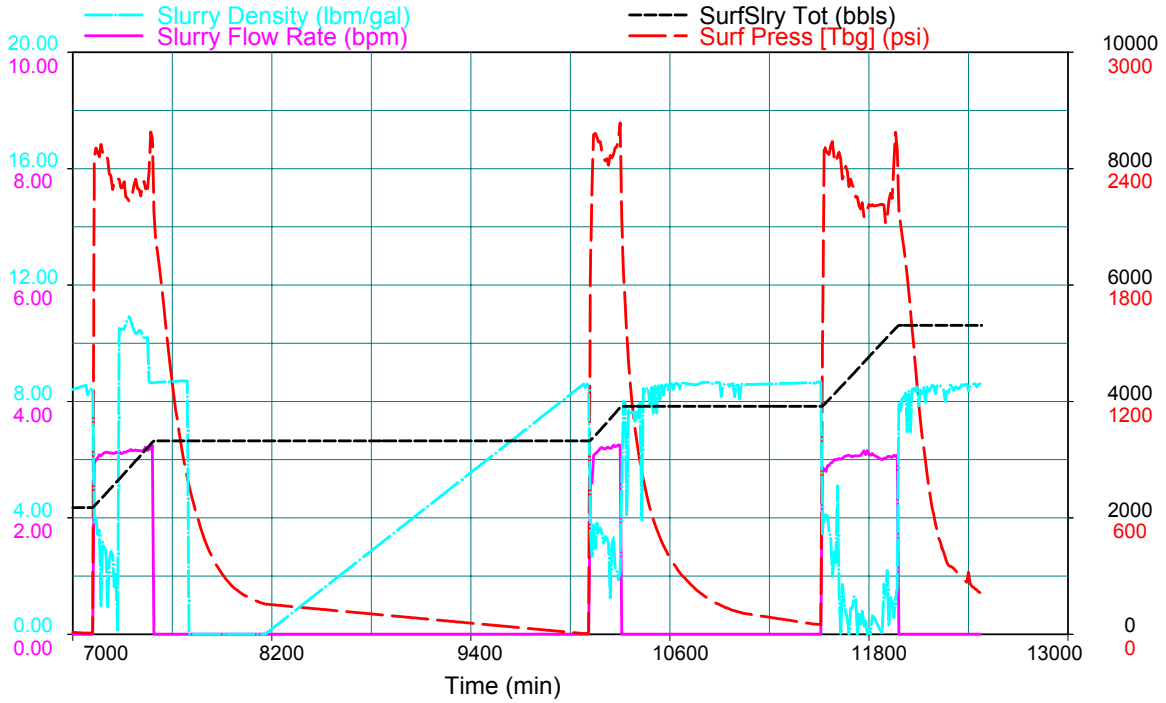

Figure 83: Treatment Data February 23, 25 and 26, 2002.

Determining fracture closure stress

The first and most critical analysis step in this project was to determine the fracture closure stress. Fracture closure stress is the single most important variable that should be measured for net pressure fracture treatment analysis, as the level of the net pressure p_{net} is directly determined from it through the following equation:

$$p_{net} = p_{surface} + p_{hydrostatic} - \Delta p_{friction} - \sigma_{closure} \ .$$

Fracture closure stress is generally measured by observation of a change in the slope in a pressure decline diagnostic plot, such as the pressure vs. square-root time plot or the G-function plot (which are available in FracproPT's minifrac analysis module). Table A provides an overview of all the results from fracture closure stress analysis in each injection, while closure stress measurements are shown in Figure 84.

.

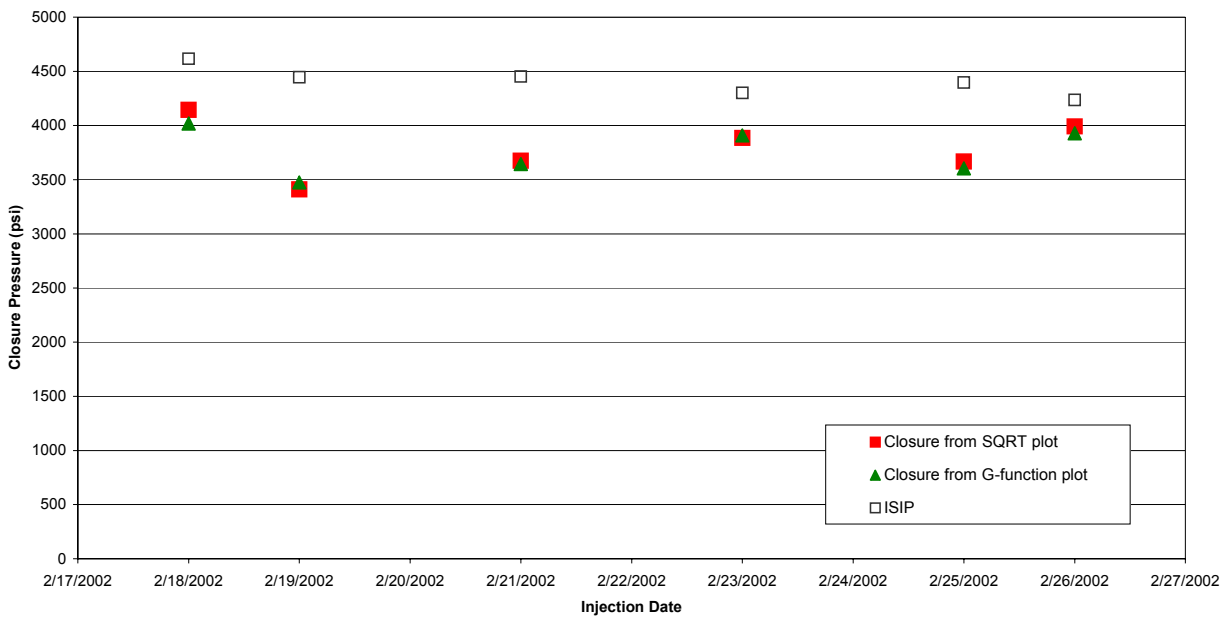

Figure 84: Closure stress measurements using different techniques for each injection.

It is clear from these closure stress estimates that they fall in a relatively wide range between about 3500 and 4100 psi, with an average closure stress gradient of 0.843 psi/ft. The individual closure stress estimates using different techniques are quite consistent, increasing our confidence in the closure stress value.

Figure 84 also shows the Instantaneous Shut-In Pressure (ISIP). The net fracturing pressure at the end of the treatment is equal to the difference between the ISIP and the closure stress. Therefore, there is also a relatively wide range in net pressures that we observe for subsequent injections.

Fracture growth behavior

Three different fracture growth scenarios were investigated to evaluate potential rock mechanical property changes over time with subsequent injections. Table 14 provides an overview of the different scenarios that were evaluated.

Table 14: THUMS SFI Fracture growth scenarios

	Sand Closure Gradient (psi/ft)	Matching Variables		
Scenario	**(psi/ft)**	**Permeability**	**Opening Fact.**	**Modulus**
1	0.843	x	x	
2	0.843	x		x
3	x	x		x

Two matching variables are used in each of the 3 scenarios. During net pressure matching, it is important to match both the level of the net pressure and the pressure decline slope following the injection. Matching the level of the net pressure is mainly controlled by changing the Young's modulus of the rock or the multiple fracture opening factor. The multiple fracture opening factor represents the level of fracture growth complexity using an "equivalent" number of fracture multiples, and assumes that multiple fractures open against each other to "compete" for fracture width. Matching the slope of the pressure decline is achieved by changing the leakoff multiplier, which is roughly proportional to the permeability squared.

Scenario 1 assumes a constant fracture closure stress of 3780 psi at 4484 ft depth (0.843 psi/ft). Figure 85 shows the fracture dimensions and matching parameters for this scenario, together with the net pressure and obtained fracture dimensions. Fracture length clearly increases with a decreasing leakoff multiplier as the fracture volume at the end of pumping will be higher for a lower leakoff. We are able to match the net pressure response for these injections, and obtain a fracture slurry efficiency of about 8-19% at the end of all injections (meaning that only 8-19% of fluid is still in the fracture at the end of pumping). By matching net pressure decline behavior, we obtain a fracture half-length of order 50 ft and a fracture height of about 100 ft. Note that fracture growth is assumed to be roughly radial, as we have assumed a constant closure stress gradient with depth.

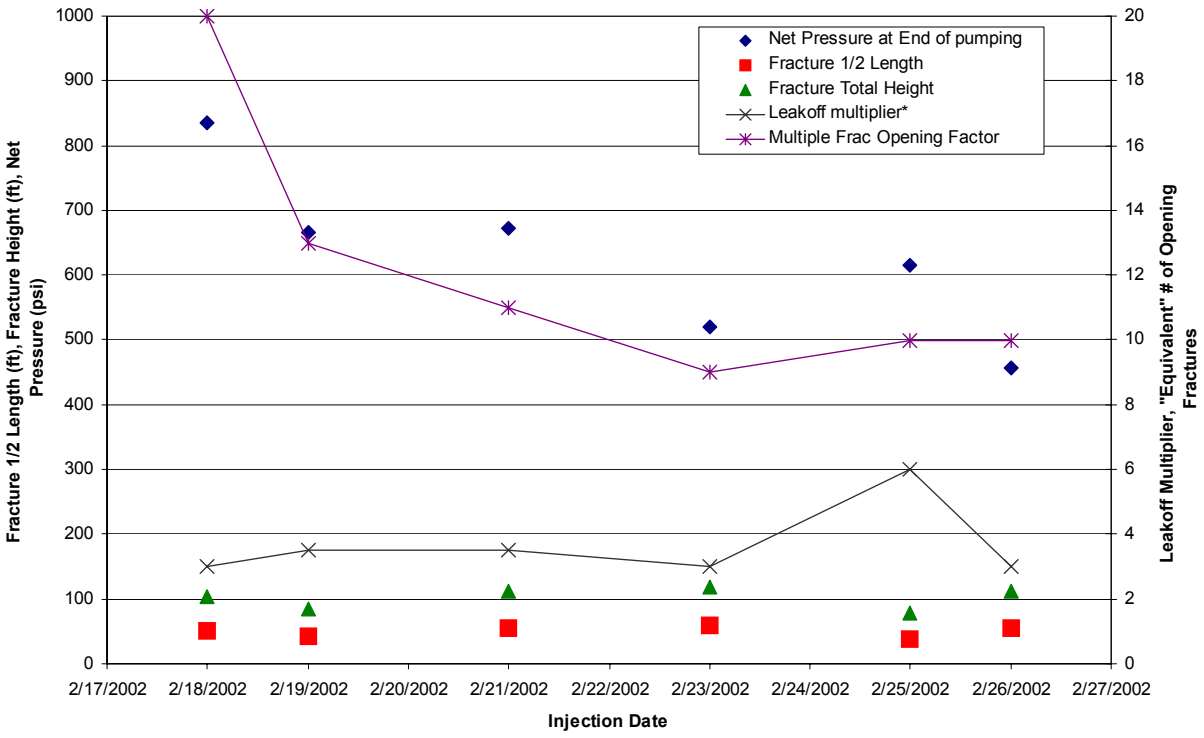

Figure 85: Fracture dimensions at the end of each injection for pressure matching scenario 1.

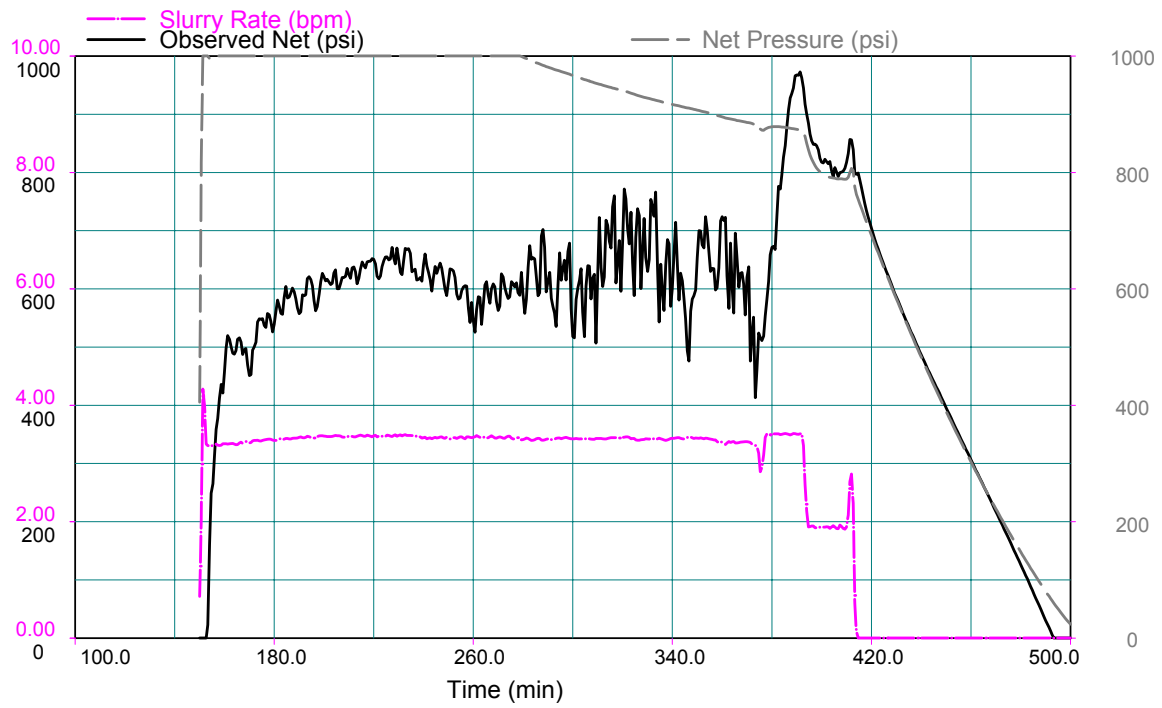

Figure 86. Net Pressure Match for Wilmington Field - C822I - 2/18/2002

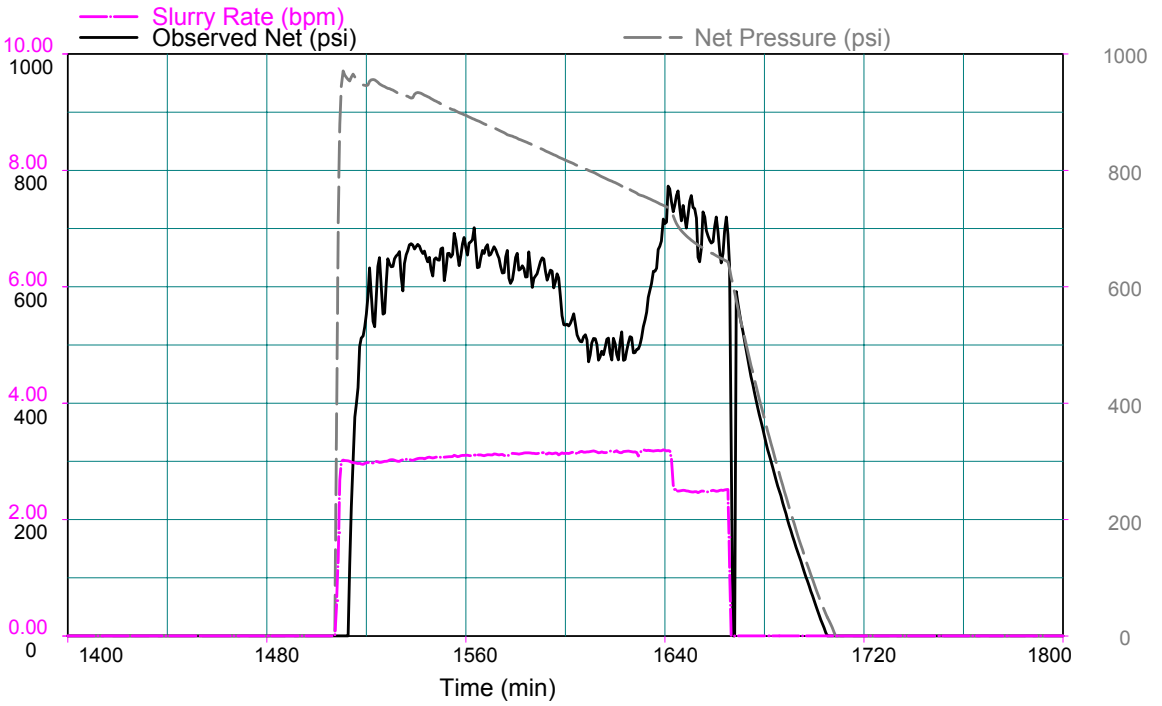

Figure 17. Net Pressure Match for Wilmington Field - C822I - 2/19/2002

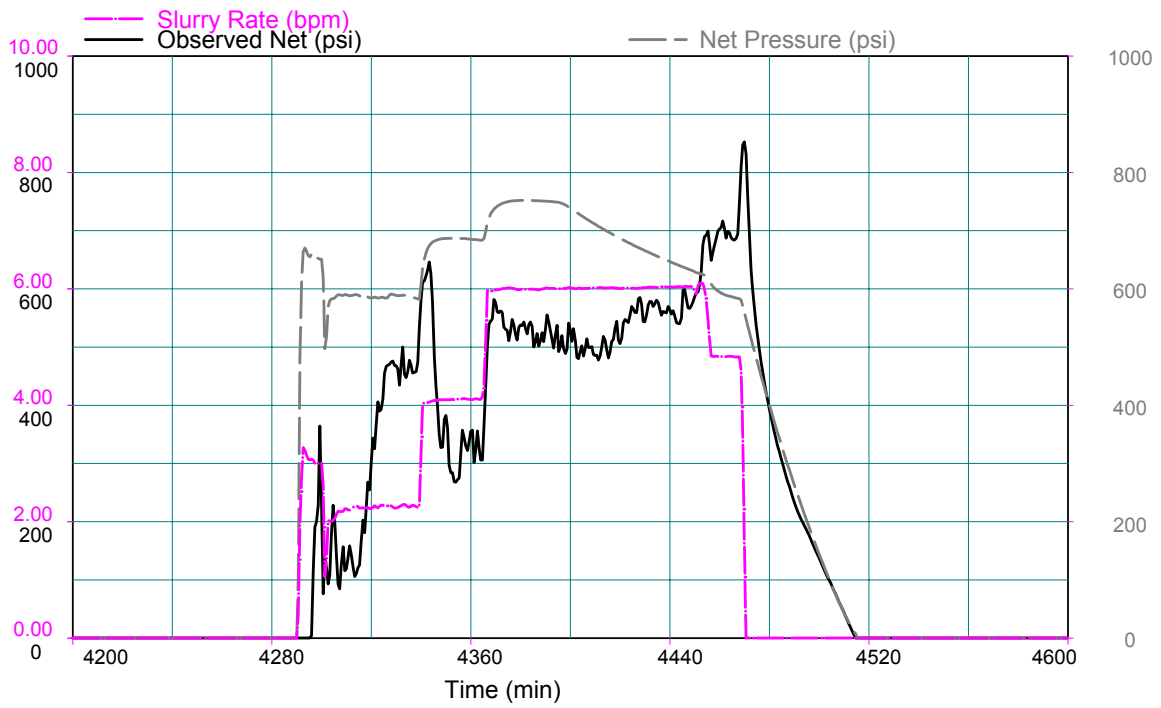

Figure 88. Net Pressure Match for Wilmington Field - C822I - 2/21/2002

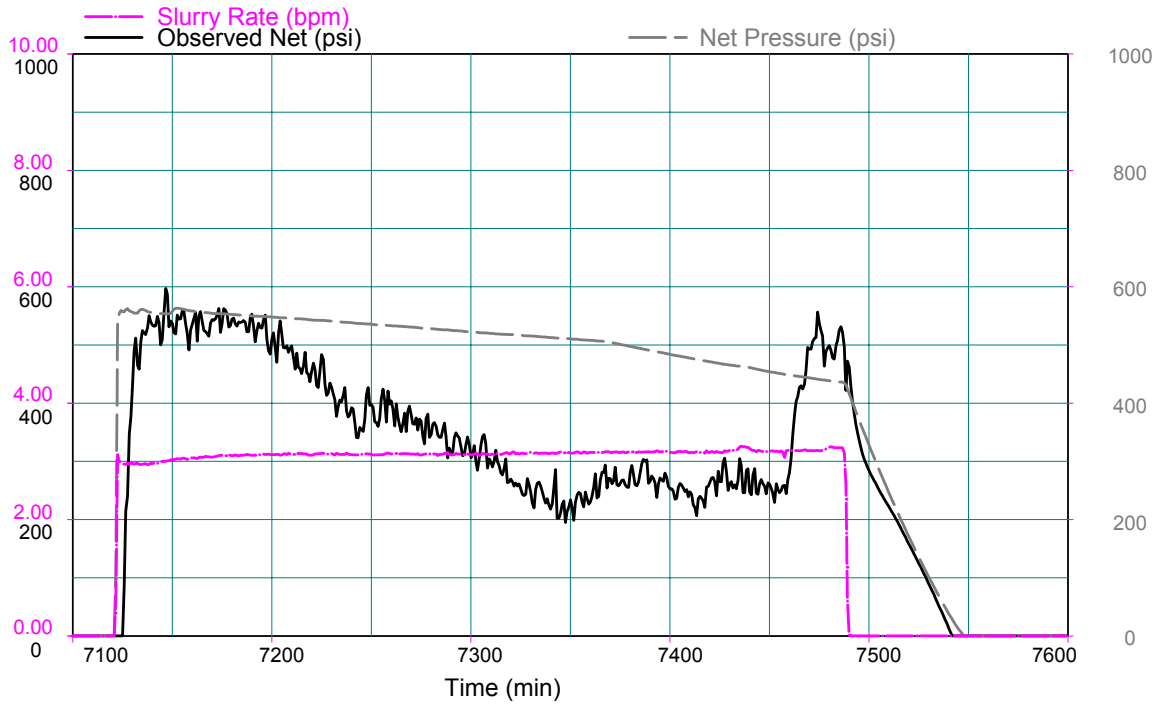

Figure 89. Net Pressure Match for Wilmington Field - C822I - 2/23/2002

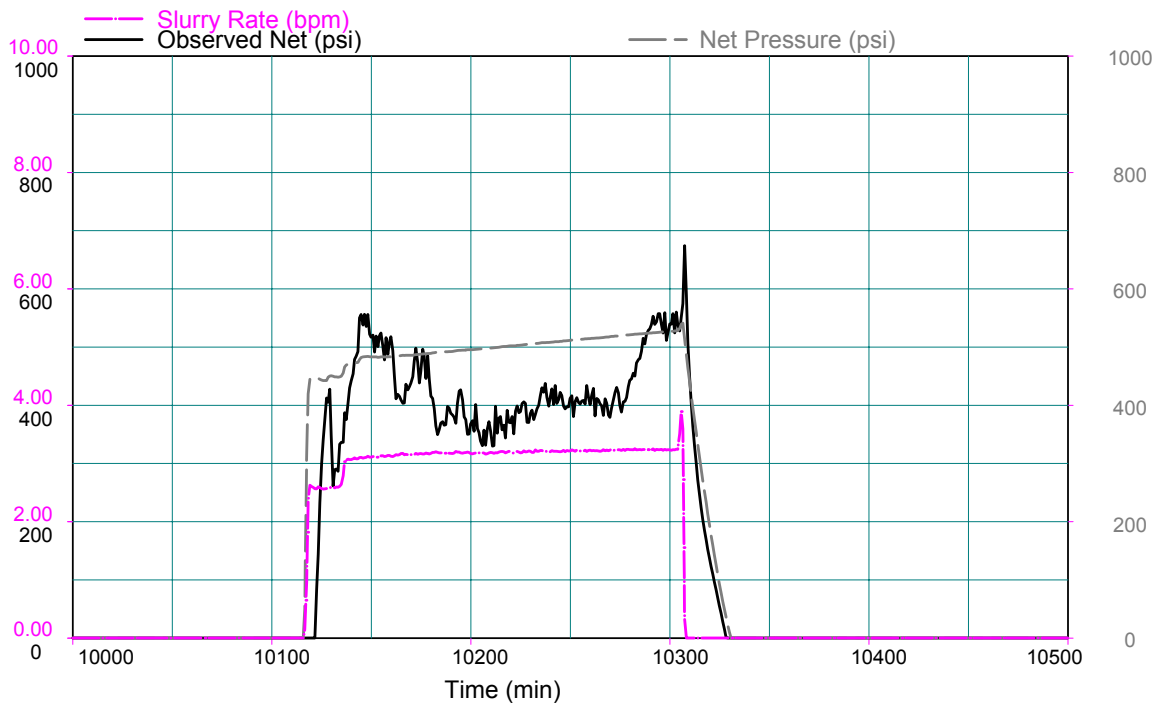

Figure 90. Net Pressure Match - Injection #5 for Wilmington Field - C822I - 2/25/2002

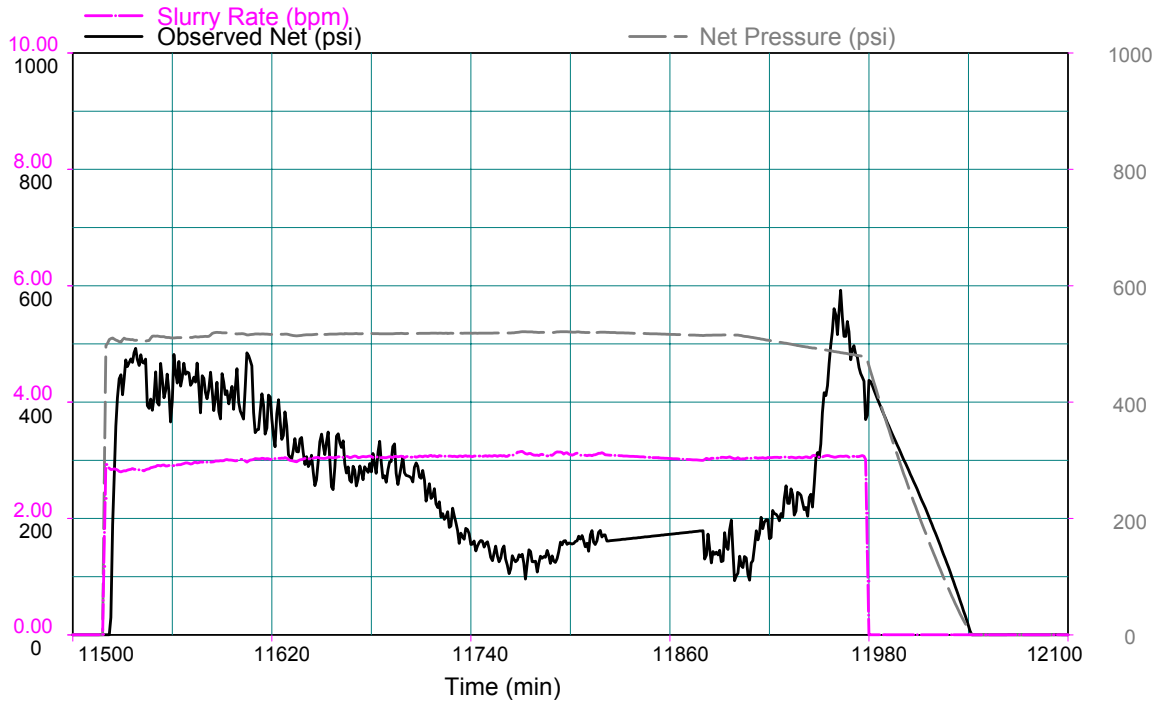

Figure 91. Net Pressure Match for Wilmington Field - C822I - 2/26/2002

Scenario 2 assumes the same fracture closure stress profile along the depth of the wellbore as in scenario 1, but the matching parameter for the level of the net pressure has been changed from the fracture opening factor (how many "equivalent" fractures are interfering with each other) to the Young's modulus. The idea for this modeling approach is that the injected waste could over time make the rock stiffer as the pore space/natural fractures fill. Figure 86 shows the fracture dimensions and matching parameters for this scenario, together with the net pressure at the end of the treatment and the final fracture dimensions. The Young's modulus appears to slightly decrease during subsequent injections, but a clear trend is not visible in the data.

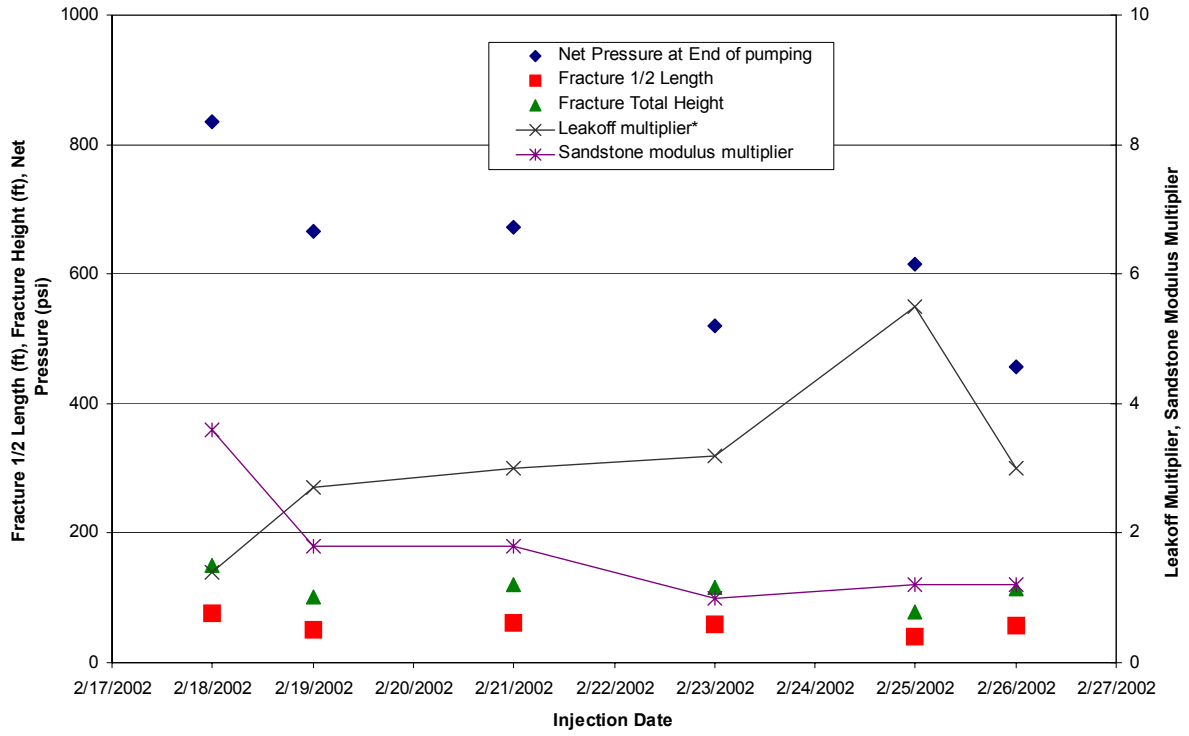

Figure 92: Fracture dimensions at the end of each injection for pressure matching scenario 2.

In scenario 3, we have assumed that the fracture closure stress changes with each individual injection, as the injected waste may gradually increase the fracture closure stress. Figure 93 shows the fracture dimensions and matching parameters for this scenario, and together with the net pressure at the end of the treatment and the obtained fracture dimensions. Similar to the previous scenario, the Young's modulus decreases with subsequent injections. The observed variability in the fracture closure stress may indicate that the fracture grows along a different azimuth and/or dip with each subsequent injection.

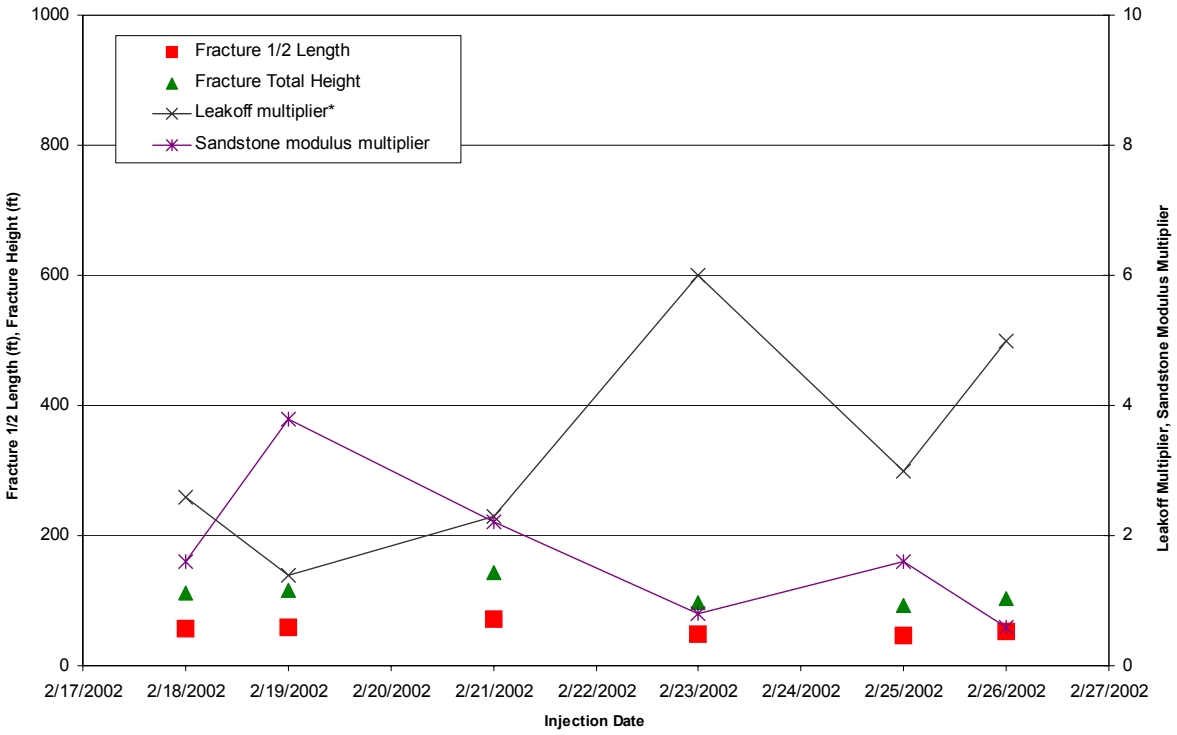

Figure 93: Fracture dimensions at the end of each injection for pressure matching scenario 3.

Injection Analysis Summary

- Fracture closure stress and ISIP vary considerably between injections, indicating that the fracture system is most likely growing along a different azimuth/dip with each subsequent injection. The average closure stress gradient of 0.843 psi/ft is somewhat higher than previously thought.
- Fracture slurry efficiencies are off order 8-19 % at the end of pumping, and created fracture half-length is of order 50 ft.
- The variable leak-off versus injection time/volume possibly also indicates that new fracture area was encountered at various times. This would be consistent with the disposal domain theory identified at the Mounds Drill Cutting Disposal Injection Experiment.

- The complexity of the fracture is generally reducing versus injection time/volume. This could be the result of the solids filling the natural fractures resulting in a more of a single fracture later in time (less complex fracture). However, a longer dataset needs to be studied to determine if this is a general trend.
- Accurate fracture closure stress determination is very critical for this analysis, and the pressure decline periods in this project allowed accurate closure identification. However, the closure stress should also be accurately determined at the beginning of a disposal project by performing both steprate injection test and fall-off test using moderate (~100 bbl) volumes slickwater. Once the disposal project has begun the closure stress should be determined periodically using these slickwater injections, preferably after injection has been shut down for an extended period of time (over the weekend).
- We can effectively match observed net pressure response using the FracproPT system by changing several rock mechanical parameters over time. We have used the formation permeability, Young's modulus, and fracture opening factor (fracture complexity) as matching parameters. For the most part, the general dimensions of the fracture were consistent regardless of the method used to match the net pressure.

CONCLUSIONS

The goals of this DOE project have been to: 1) assemble a comprehensive database of past waste injection operations; 2) evaluate empirical correlations between waste type, operating parameters, and formation response; 3) investigate improved modeling techniques for fracture growth and formation response; and 4) develop and apply operating guidelines to optimize daily operations and ultimate storage capacity of the target formation. Each of these research objectives have been accomplished, providing valuable new insights and practical information to improve large-scale waste injection operations in high porosity formations.

Successful project completion has provided a number of significant benefits to the oil and gas industry. Some of these benefits include:

1. Establishment and documentation of a comprehensive database of slurry fracture injection operations, and associated database query tools;
2. Identification of empirical trends (or lack thereof) between various operating parameters and formation response, for comparison with future injection operations;
3. Investigation, development, and documentation of improved slurry injection modeling techniques; and,
4. Establishment of design and operating guidelines to maintain waste containment in the target interval (environmental management), help control formation response and optimize operating parameters (operating cost management), and reduce risks for well damage or loss of long-term injectivity (asset management).

REFERENCES

Bathurst, R.J. and Rothenburg, L.: "Observations on Stress-Force-Fabric Relationships in Idealized Granular Media", *Mech. of Mat*. V. 9 (1990) pp. 65-80.

Bear, J. (1972): *Dynamics of Fluids in Porous Media.* Environmental Science Series, American Elsevier Pub. Co., New York. Reprinted Dover Publications, Inc, 1988.

Boone et al, (1999): Microseismic monitoring for fracturing in Colorado Shales above a thermal oil recovery operation, Proc. 37th US Rock Mech. Symp., Vail Colorado, 6-9 June, 1999, pp 1017-1024

Bruno, M.S., Bovberg, C.A. Meyer, R.F., (1996): Some influences of saturation and fluid flow on sand production: laboratory and discrete element model investigations. SPE Paper 36534, Proc. SPE Ann. Tech. Conf. And Exhibit, Denver, Colorado, 6-9 October, 1996.

Bruno, M.S.: "Micromechanics of Stress-Induced Permeability Anisotropy and Damage in Sedimentary Rock", *Mech. of Mat*. V. 18 (1994) pp. 31-48.

Carman, P.C. (1937): Fluid Flow through a Granular Bed. *Transaction Inst. Chem. Eng. London* v.15, p.150-156.

Carman, P.C. (1956): *Flow of Gases through Porous Media.* Butterworths. London.

Crockett, A.R., Okusu, N.M., Cleary, M.P. (1986): A complete integrated model for design and real-time analysis of hydraulic fracturing operations. Society of Petroleum Engineers, Dallas, Texas. SPE Paper 15069.

Cundall, P.A. and Strack, O.D.L.: "A Discrete Numerical Model for Granular Assemblies", *Geotechnique* V. 29 (1979) pp. 47-65.

Deresiewicz, H. (1958): Mechanics of Granular Matter. In: *Advances in Applied Mechanics*, H.L. Dryden et al. Eds. Vol. 5, 233-306, New York.

Flaman, C.: Determining *Fracture and Reservoir Properties From Slurry Fracture Injection Monitoring Data*, Master's Thesis, Waterloo, Ontario, 1998

Geertsma, J., deKlerk, F. (1969): A rapid method of predicting width and extent of hydraulically induced fractures. *Journal of Petroleum Technology*, December 1969, p.1571-1581.

Horne, R.N.: *Modern Well Test Analysis*, 2nd Edition, Petroway, Inc., Palo Alto, California, 1995

Howard, G.C., Fast, C.R. (1957): Optimum fluid characteristics for fracture extension. *Drilling and Production Practices API*, p.261-270. Appendix by R.D. Carter.

Itasca Consulting Group Inc. (1996): FLAC, Theory User Manual, Version 3.3. Itasca Consulting Group Inc., Minnesota.

Itasca Consulting Group Inc. (1999): PFC, Theory and Background, Version 2.0. Itasca Consulting Group Inc. Minnesota, USA.

Kozeny, J. (1927): Über kapillare Leitung des Wassers im Boden. *Sitzungsbericht*, Akademische Wissenschaft Wien, v.136, p.271-306.

Lee, J.: Well *Testing*, SPE Textbook Series, Volume 1, Society of Petroleum Engineers, Dallas, 1982

Moschovidis et al, (1999): The Mounds Drill Cuttings Injection Field Experiment, Proc. 37th US Rock Mech. Symp., Vail Colorado, 6-9 June, 1999, pp 1017-1024

Nordgren, R.P. (1972): Propagation of a vertical hydraulic fracture. *Society of Petroleum Engineers Journal*, August 1972, p.306-314.

Perkins, T.K., Kern, L.R. (1961): Widths of hydraulic fractures. *Journal of Petroleum Technology*, September 1961, p.937-949.

Pinnacle Technologies Inc. (2000): FracProPT Technical Description. FracProPT software, Version 10.0. San Francisco, California.

Schmidt, J.H., Friar, W.L., Bill, M.L., Cooper, G.D. (1999): Large-scale injection of North Slope drilling cuttings. SPE Paper 52738, 1999 SPE/EPA Exploration and Production Environmental Conference, Austin, Texas.

Swamee, K.P., and Jain, A.K.: "Explicit Equations for Pipe-Flow Problems", Journal of the Hydraulics Division, Proceedings of the American Society of Petroleum Engineers, Volume 102, No. HY5, May 1976

Taylor, D.W. (1948): *Fundamentals of Soil Mechanics*. John Wiley, New York.

Terralog Technologies Inc. (2000a): Development of Improved Oil Field Waste Injection Disposal Techniques, Topical Report #1: Database Assembly, January 1, 2000. DOE Contract DE-AC26-99BC15222

Terralog Technologies Inc. (2000b): Development of Improved Oil Field Waste Injection Disposal Techniques: Topical Report #2: Empirical Correlationss, June 15, 2000. DOE Contract DE-AC26-99BC15222

Terralog Technologies Inc. (2000c): Development of Improved Oil Field Waste Injection Disposal Techniques: Topical Report #3: Fracture Modelling and Diagnostic Investigations, October 31, 2000. DOE Contract DE-AC26-99BC15222

Terralog Technologies Inc. (2001): Development of Improved Oil Field Waste Injection Disposal Techniques, Technical Progress Report for the Period Ending March 06, 2001. DOE Contract DE-AC26-99BC15222

Terzaghi, K. (1943): *Theoretical Soil Mechanics.* John Wiley, New York.

Thiercelin, M.J., Jeffrey, R.G. and Ben-Naceur, K. (1987): The influence on fracture toughness on the geometry of hydraulic fracture. SPE Paper 16431, SPE/DOE Low Permeability Reservoir Symposium, Denver, Colorado.

Visser, J.H.M. (1998): *Extensile Hydraulic Fracturing of (Saturated) Porous Materials.* Ph.D. Dissertation, Technical University of Delft.